# UNIVERSITÀ DEGLI STUDI DI PADOVA

DIPARTIMENTO DI TECNICA E GESTIONE DEI SISTEMI INDUSTRIALI


COURSE ON PRODUCT'S INNOVATION ENGINEERING

MASTER THESIS

# Local approaches for predicting the failure of static structural foam characterized by different densities


RELATOR: CH.MO PROF. **FILIPPO BERTO**

STUDENT: **ALBERTO PICCOTIN**
ID NUMBER: **1081265**



ACADEMICAL YEAR: **2015/2016**

# Summary

In this essay will be treated the Strain Energy Density method on PUR foams made in different densities, a local approach to predict the static failure of the components. In literature are present studies about these foams and are showed the parameters that could be used for the SED method; the main goal is to define these parameters through different experimental tests and after to see the difference between the obtained values and the values defined in literature. The following step is to define the SED parameters through the obtained experimental results and apply the SED method on different notched specimens (blunt V notch components, U notched components, holed components and cracked components) made by different densities and see the dispersion of the data, dispersion means the difference between the experimental and theoretical fracture loads. All the configuration loads are in pure mode I except the cracked components that are tested under mode I, mode II and mixed mode II.

# INTRODUCTION

Polyurethane (PUR) foam materials are widely used as cores in sandwich composites, for packing and cushioning. They are made of interconnected networks of solid struts and cell walls incorporating voids with entrapped gas. The main characteristics of foams are lightweight, high porosity, high crushability, and good energy absorption capacity. In this last years these type of material are becoming very important for their properties of lightweight and good energy absorption capacity.

In this project the main purpose is to apply a local approach to predict the static failure. This local approach is called SED and is based on the strain energy density of the material; this local approach will be applied on different specimen's geometries made by different densities. At the beginning the SED method has been applied for welded components but can be extended to predict the failure in static condition for notched components. The SED method (and other methods that take part of MFLE) it's a part of the mechanic linear elastic fracture (MFLE), so it can be applied only on materials with a linear elastic behaviour, as ideally brittle materials ( ceramics, glasses and some polymers). These foams, under tensile loads, present no plasticity but show a non-linear behaviour so seems that it's not possible to apply the methods based on MFLE; the particularity of these foams is that the notched specimens has a quasi-linear elastic behaviour, so it's possible to apply the MFLE's methods.

Recently has been conducted study on this foams and it has been applied the TCD method, a point method based on the same theory of the SED method. In these studies are defined the parameters that could be used for the SED method. The main goal is to determine these parameters through a different way (through different experimental tests). It's very important to underline that the work will be made in this paper represents a different approach of the same problem and the expectation is that the parameters, that will be defined through experimental test, are not so far from the parameters already defined.

It's known that the parameters for calculate the SED depend fundamentally from the strength of the material ($\sigma_t$): in the previously studies, this $\sigma_t$ is defined in a certain way and it has wanted to demonstrate that with different tests, the parameters has the same order of magnitude.

The specimens investigated are notched geometries, with different types of notch. To evaluate if the parameters defined are reasonable or not, it will determined the theoretical fracture loads of these notched specimens (applying SED method) and after compared with the experimental fracture loads. The notched specimens investigated are blunt V notch components, U notched components and holed components under mode I load configuration while ASCB specimens under mode I, mode II and mixed mode I+II.

For the cracked cases will be proposed a personal approach to define the SED parameters under mode II and mixed mode I+II loads configuration.

To determine the SED parameters, it's necessary to know the mechanical properties of the materials; in this work it will be used the mechanical properties (as Young's modulus, Poisson's ratio, fracture toughness, etc..) determined in the precedent studies.

In the last chapter will be analysed some specimens with plasticization in a region of the components but not where the crack born and propagate (a non-linear behaviour), under compression loads, and the goal is to verify if the SED method could be applied and if the plasticity influences the results or not.

(In the Appendix has been applied the TCD method and to define the TCD's parameters has been used the tension determined through the experimental tests: it's reported only the main passages because the finite element models used are the same of the SED method).

TABLE OF CONTENTS

# CHAPTER 1 :Theoretical basis of SED approach

In this last years, the strain energy density (SED) method is becoming a very important method to predict the failure of a material. At the beginning this method is born for the welded joints and after it has been extended to the static case. The SED method takes part of the linear elastic mechanic fracture (MFLE), based on the linear elastic behaviour of the materials. The SED is a local approach used for notched components and is based on the energy determined by the strain in a finite volume (control volume) near the notch tip. The strain depends from the tensions in this volume so it's necessary to see how is the stresses behaviour near the notch tip.

After this theoretical background, it will be presented the definition of the SED method and the main formulation of the method's parameters for different notch's geometries.

## 1.1.Analitical frame

The deformation energy is a function linked to the stress states present in the material in three dimensions. It is therefore impossible to define an energy of deformation without clearly defined before what are the tensions in play and how their performance is linked to the notch and loading system .

Filippi [1] proposed an analytical method for the definition of stresses in notched components . With reference to the coordinate system shown in Fig. 1, the stress distribution in Mode I , the apex of a V-shaped notch , is given by:

$$\sigma_{ij} = a_1 r^{\lambda_1 - 1}\left[f_{ij}(\theta;\alpha) + \left(\frac{r}{r_0}\right)^{\mu_1-\lambda_1} g_{ij}(\theta;\alpha)\right] \qquad [1]$$

Where the parameter $a_1$ can be expressed as a function of the stress intensity factor $K_I^V$ , in the case of a V-notch not connected, when and where $\lambda_1 > \mu_1$.

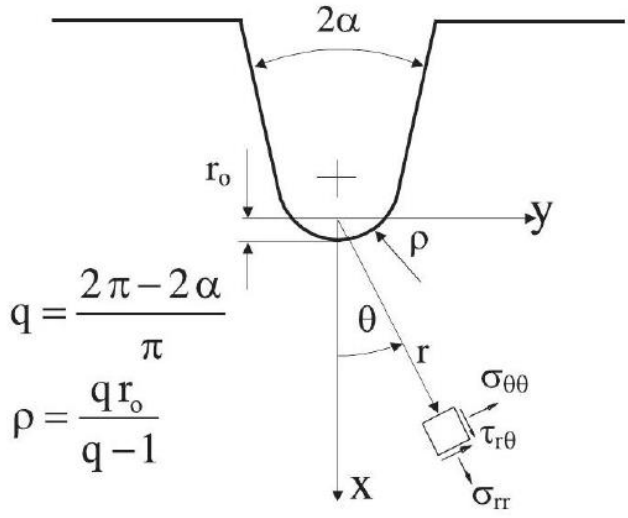


***Fig. 1.*** *Polar coordinate system and relative parameters.*

In the eq. (1), indicates the distance from the apex of the notch of the origin of the polar coordinate system and depends on the notch fillet radius and the opening angle ,Fig. 1 , in accordance with the equation:

$$r_0 = \rho\frac{(\pi - 2\alpha)}{(2\pi - 2\alpha)} = \rho\frac{(q-1)}{q} \qquad [2]$$

The distance $r_0$ is maximum for $2\alpha = 0$ , resulting $r_0 = \rho/2$ , and decreases with the increase of the angle of opening up to a value of $r_0 = 0$ for an angle $2\alpha = \pi$ . The parameter q varies according to the angle $2\alpha$ and has a maximum value $q = 2$ for $2\alpha = 0$ and a minimum value for $q = 1$ and $2\alpha = \pi$.

$$q = \frac{(2\pi - 2\alpha)}{\pi} \qquad [3]$$

The angular functions $f_{ij}(\theta;\alpha)$ and $g_{ij}(\theta;\alpha)$ are defined in function of William's parameter $\lambda_1$ , e in a less way from the parameter $\mu_1$ [1]. Eq. (3) and (4) reports the formulas to calculate these two functions, in a vector form that contains the three components θθ, rr and rθ.

$$\begin{Bmatrix} f_{\theta\theta} \\ f_{rr} \\ f_{r\theta} \end{Bmatrix} = \frac{1}{1+\lambda_1+\chi_{b1}(1-\lambda_1)}\left[\begin{Bmatrix} (1+\lambda_1)\cos(1-\lambda_1)\,\theta \\ (3-\lambda_1)\cos(1-\lambda_1)\,\theta \\ (1-\lambda_1)\sin(1-\lambda_1)\,\theta \end{Bmatrix} + \chi_{b1}(1-\lambda_1)\begin{Bmatrix} \cos(1+\lambda_1)\theta \\ -\cos(1+\lambda_1)\theta \\ \sin(1+\lambda_1)\theta \end{Bmatrix}\right] \quad [4]$$

$$\begin{Bmatrix} g_{\theta\theta} \\ g_{rr} \\ g_{r\theta} \end{Bmatrix} = \frac{q}{4(q-1)[1+\lambda_1+\chi_{b1}(1-\lambda_1)}\left[\chi_{d1}\begin{Bmatrix} (1+\mu_1)\cos(1-\mu_1)\theta \\ (3-\mu_1)\cos(1-\mu_1)\theta \\ (1-\mu_1)\sin(1-\mu_1)\theta \end{Bmatrix} + \chi_{c1}(1-\lambda_1)\begin{Bmatrix} \cos(1+\mu_1)\theta \\ -\cos(1+\mu_1)\theta \\ \sin(1+\mu_1)\theta \end{Bmatrix}\right] \quad [5]$$

The value of the parameters regarding the Filippi's formulation, has been summarized in table, where they depend from the opening angle 2α, as seen in Table 1.

| $2\alpha$ [rad] | q | $\lambda_1$ | $\mu_1$ | $\chi_{b1}$ | $\chi_{c1}$ | $\chi_{d1}$ | $\tilde{\omega}_1$ | $F(2\alpha)$ |
|---|---|---|---|---|---|---|---|---|
| 0 | 2.0000 | 0.5 | -0.5 | 1 | 4 | 0 | 1 | 0.7850 |
| $\pi/6$ | 1.8333 | 0.5014 | -0.4561 | 1.0707 | 3.7907 | 0.0632 | 1.034 | 0.6917 |
| $\pi/4$ | 1.7500 | 0.5050 | -0.4319 | 1.1656 | 3.5721 | 0.0828 | 1.014 | 0.6692 |
| $\pi/3$ | 1.6667 | 0.5122 | -0.4057 | 1.3123 | 3.2832 | 0.0960 | 0.970 | 0.6620 |
| $\pi/2$ | 1.5000 | 0.5448 | -0.3449 | 1.8414 | 2.5057 | 0.1046 | 0.810 | 0.7049 |
| $2\pi/3$ | 1.3334 | 0.6157 | -0.2678 | 3.0027 | 1.5150 | 0.0871 | 0.570 | 0.8779 |
| $3\pi/4$ | 1.2500 | 0.6736 | -0.2198 | 4.1530 | 0.9933 | 0.0673 | 0.432 | 1.0717 |
| $5\pi/6$ | 1.1667 | 0.7520 | -0.1624 | 6.3617 | 0.5137 | 0.0413 | 0.288 | 1.4417 |

***Table1 .*** *Parameters for the stress distributions.*

In plane strain conditions, the functions $f_{ij}(\theta)$ and $g_{ij}(\theta)$ can be expressed as a function of the Poisson's ratio v.

$$f_{zz}(\theta) = \nu\left(f_{\theta\theta}(\theta) + f_{rr}(\theta)\right) \quad [6]$$

$$g_{zz}(\theta) = \nu\left(g_{\theta\theta}(\theta) + g_{rr}(\theta)\right) \quad [7]$$

In plane stress conditions, these two values go to zero.

## 1.2.The SED method

The SED approach is based on the idea that under prevailing tensile stresses failure occurs when the strain energy density averaged over a given control volume reaches a critical value:

$$\bar{W} = W_c \quad [8]$$

where $W_c$ depends on the material. If the material behaviour is ideally brittle, then $W_c$ can be evaluated by using simply the conventional ultimate tensile strength $\sigma_t$, so:

$$W_c = \sigma_t^2 / 2E \quad [9]$$

In principle $W_c$ as determined from uniaxial tests cannot be considered independent on the loading mode. Under compression, for example, the critical value of $W_c$ is surely different from the critical value under tension.

Often unnotched specimens exhibit a non-linear behaviour whereas the behaviour of notched specimens remains linear. Under these circumstances the stress $\sigma_t$ should be substituted by “the maximum normal stress existing at the edge at the moment preceding the cracking”, where it is also recommended to use tensile specimens with large semi-circular notches to have a full notch sensitivity.

### 1.2.1.Sharp V notch, under pure mode I

The $a_1$ parameter in eq. (1), can be linked to stress intensity factor in mode I through the following equation:

$$a_1 = \frac{K_I^V}{\sqrt{2\pi}} \qquad [10]$$

Where the value of $K_I^V$ has defined by Gross and Mendelson [5] as:

$$K_I^V = \sqrt{2\pi} \lim_{r\to 0}[\sigma_\theta(r,0)] r^{1-\lambda_1} \qquad [11]$$

For sharp V notches, the value of $r_0$ , eq. (2), is equal to zero because the centre of the polar coordinate system is coincident with the notch tip and the components linked to the term μ is null.

In plane strain condition is possible to define the strain energy density in mode I as a Filippi's equations, as made by Lazzarin and Berto [6]:

$$W_I(r,0) = \frac{1}{2E}\frac{(K_I^V)^2}{2\pi r^{2(1-\lambda_1)}}[f_{\theta\theta}^2 + f_{rr}^2 + f_{zz}^2 - 2\nu(f_{\theta\theta}f_{rr} + f_{\theta\theta}f_{zz} + f_{rr}f_{zz}) + 2(1+\nu)f_{r\theta}^2] \qquad [12]$$

Known the equation for the determination of the total strain energy density, it's necessary to define the area where this strain energy density should be calculated. This control area has radius $R_c$ . This area is defined through the two free edges of the crack, oriented of an angle equal to γ respects to the notch bisector and the control radius $R_c$ , as seen in Fig. 2.

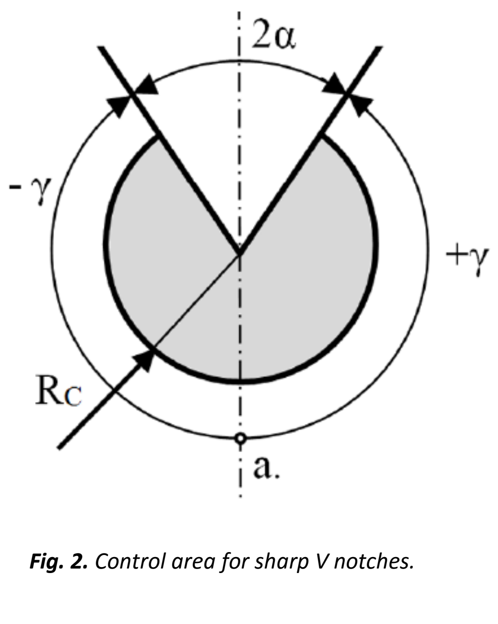


***Fig. 2.*** *Control area for sharp V notches.*

$$A = \int_0^{R_c} \int_{-\gamma}^{+\gamma} r\, dr\, d\theta = R_c^2 \gamma \quad [13]$$

So, the total strain energy $E_I$ inside the control area, is possible to define integrating eq. (12) in the control area, eq. (14).

$$E_I = \int W_I dA = \int_0^{R_c} \int_{-\gamma}^{+\gamma} W_I(r,\theta) r\, dr\, d\theta = \frac{1}{E} \frac{I_1(\gamma)}{4\lambda_1} (K_I^V)^2 R_c^{2\lambda_1} \quad [14]$$

Where the $I_1(\gamma)$ is obtained integrating the stress components reported in eq. (12) ,respects to opening angle ± γ.

$$I_I(\gamma) = \frac{1}{2\pi} \int_{-\gamma}^{+\gamma} [f_{\theta\theta}^2 + f_{rr}^2 + f_{zz}^2 - 2\nu(f_{\theta\theta} f_{rr} + f_{\theta\theta} f_{zz} + f_{rr} f_{zz}) + 2(1+\nu) f_{r\theta}^2] d\theta \quad [15]$$

$I_1(\gamma)$ is a function depending from:

- The geometry through the opening angle 2α, in fact γ = π – α.
- The material, through the Poisson's ratio.

The value of $I_1$ different typology of sharp notch and different material is showed in Table 2.

| ***2α* (degrees)** | ***γ/π* rad** | ***λ₁*** | ***$I_I$* pl. strain** ν=0.10 | ν=0.15 | ν=0.2 | ν=0.25 | ν=0.3 | ν=0.35 | ν=0.4 | ***$I_I$* pl. stress** ν=0.3 |
|---|---|---|---|---|---|---|---|---|---|---|
| 0 | 1 | 0.50 | 1.1550 | 1.0925 | 1.0200 | 0.9375 | 0.8450 | 0.7425 | 0.6300 | 1.0250 |
| 15 | 23/24 | 0.50 | 1.1497 | 1.0880 | 1.0162 | 0.9346 | 0.8431 | 0.7416 | 0.6303 | 1.0216 |
| 30 | 11/12 | 0.50 | 1.1335 | 1.0738 | 1.0044 | 0.9254 | 0.8366 | 0.7382 | 0.6301 | 1.0108 |
| 45 | 7/8 | 0.50 | 1.1063 | 1.0499 | 0.9841 | 0.9090 | 0.8247 | 0.7311 | 0.6282 | 0.9918 |
| 60 | 5/6 | 0.51 | 1.0678 | 1.0156 | 0.9547 | 0.8850 | 0.8066 | 0.7194 | 0.6235 | 0.9642 |
| 90 | 3/4 | 0.54 | 0.9582 | 0.9173 | 0.8690 | 0.8134 | 0.7504 | 0.6801 | 0.6024 | 0.8826 |
| 120 | 2/3 | 0.61 | 0.8137 | 0.7859 | 0.7524 | 0.7134 | 0.6687 | 0.6184 | 0.5624 | 0.7701 |
| 135 | 5/8 | 0.67 | 0.7343 | 0.7129 | 0.6867 | 0.6558 | 0.6201 | 0.5796 | 0.5344 | 0.7058 |
| 150 | 7/12 | 0.75 | 0.6536 | 0.6380 | 0.6186 | 0.5952 | 0.5678 | 0.5366 | 0.5013 | 0.6386 |

***Table 2.*** *Values of $I_1$ parameter for different material and different sharp notch.*

From eq. (13) and (14), it's calculated the value of the average strain energy density as a function of the control area:

$$\overline{W_I} = \frac{E_I}{A_C} = \frac{I_1}{4E\lambda_1\gamma}\left(\frac{K_I^V}{R_c^{1-\lambda_1}}\right)^2 \qquad [16]$$

The SED method assumes that the failure of the material occurs when the average value of the strain energy density ($\overline{W_I}$) , defined in a control volume near the notch tip, reach the critical value $W_c$ .

If the material has an ideally brittle behavior, the value of the critical energy density can be defined as:

$$W_c = \frac{\sigma_{uts}^2}{2E} \qquad [17]$$

In the case where the specimens have not a linear behavior or for notched specimens, Seweryn [8] impose the substitution of the $\sigma_{uts}$ with maximum tension existing at the notch tip in the moment that preceding the crack; this tension is determined through experimental tests on specimens with semi-circular notch under tensile load.
From eq. (18) is possible to calculate the value of the control radius $R_c$ as a function of the material parameters $K_I^V$ and $W_c$ , that bring the material to the failure's condition.

$$R_c = \left[\frac{I_1(K_I^V)^2}{4E\lambda_1\gamma W_c}\right]^{1/[2(1-\lambda_1)} \qquad [18]$$

Eq. (18) is valid for all types of notch with opening angle different from zero.

### 1.2.2. Sharp V notch under mixed mode I+II

As for the mode I is possible to define the strain energy density when the load's configuration is in mode II. From eq. (12) for mode I configuration, is possible to explicit the function respects to the components of mode II:

$$W_{II}(r,0) = \frac{1}{2E}\frac{(K_{II}^V)^2}{2\pi r^{2(1-\lambda_2)}}[f_{\theta\theta}^2 + f_{rr}^2 + f_{zz}^2 - 2\nu(f_{\theta\theta}f_{rr} + f_{\theta\theta}f_{zz} + f_{rr}f_{zz}) + 2(1+\nu)f_{r\theta}^2] \qquad [19]$$

This equation depends from the stress terms of Filippi (eq. (4)) and from the terms regarding mode II of Williams solution.

In presence of mix mode I+II, the total strain energy density $W_{total}$ is given by the sum of relative terms in mode I $W_I$ and in mode II $W_{II}$ , and of a component relative to the mutual action of the two modes $W_{I+II}$ .

The value of the mutual component $W_{I+II}$ is given by the linear combination of the terms relative to mode I and mode II:

$$w_{I+II} = \frac{1}{E}\frac{K_I^V K_{II}^v}{r^{(2-\lambda_1-\lambda_2)}}\left[f_{\theta\theta}^I f_{\theta\theta}^{II} + f_{rr}^I f_{rr}^{II} + f_{zz}^I f_{zz}^{II} - v\left(f_{\theta\theta}^I f_{rr}^{II} + f_{\theta\theta}^I f_{zz}^{II} + f_{zz}^I f_{zz}^{II} + f_{rr}^I f_{zz}^{II} + f_{zz}^I f_{\theta\theta}^{II} + f_{zz}^I f_{rr}^{II}\right) + 2(1+v)f_{r\theta}^I f_{r\theta}^{II}\right] \qquad [20]$$

So the total strain energy is given by the integration of the $W_i$ terms in the control area:

$$E_t = \int W_I + W_{II} + W_{I+II}\, dA = \int_0^{R_c}\int_{-\gamma}^{+\gamma} W_I(r,\theta)\cdot W_{II}(r,\theta)\cdot W_{I+II}(r,\theta) r\, dr\, d\theta \qquad [21]$$

In the case that the control area $A_c$ is symmetric respects to the notch bisector, Fig. 2., the mutual component $W_{I+II}$ is null. In this case, the strain energy in mix mode is easily given by the sum of the two terms:

$$E_{I+II} = E_t(W_I, W_{II}) = \frac{1}{E}\left(\frac{I_1(\gamma)}{4\lambda_1}\cdot(K_I^V)^2\cdot R_c^{2\lambda_1} + \frac{I_2(\gamma)}{4\lambda_2}\cdot(K_{II}^V)^2\cdot R_c^{2\lambda_2}\right) \qquad [21]$$

Where the value of $I_{II}(\gamma)$ depends from the components in mode II:

$$I_{II}(\gamma) = \frac{1}{2\pi}\int_{-\gamma}^{+\gamma}[f_{\theta\theta}^2 + f_{rr}^2 + f_{zz}^2 - 2\nu(f_{\theta\theta}f_{rr} + f_{\theta\theta}f_{zz} + f_{rr}f_{zz}) + 2(1+\nu)f_{r\theta}^2]_{II}\, d\theta \qquad [22]$$

So it's possible to calculate the average value of strain energy density in mixed mode I+II dividing the value of the total strain energy by the control area:

$$\overline{W_{I+II}} = \frac{E_{I+II}}{A_C} = \frac{I_1}{4E\lambda_1\gamma}\left(\frac{K_I^V}{R_c^{1-\lambda_1}}\right)^2 + \frac{I_2}{4E\lambda_2\gamma}\left(\frac{K_{II}^V}{R_c^{1-\lambda_2}}\right)^2 \qquad [23]$$

As for mode I, the failure occurs when the average value of strain energy density is greater than the critical value $W_c$ .

In the case that the control area is rotated by an angle β > 0 respects to the notch bisector, this one is asymmetric so the mutual energy component $W_{I+II}$ should be took in account for the determination of the strain energy density.

### 1.2.3Blunt notch

Berto and Lazzarin [2] and following Radajand and Wormwald [3], presented a re-formulation of strain energy density criteria based on a control volume. Following are showed the most important concept about the SED method for blunt notches with brittle behaviour.

At the beginning Lazzarin and Zambardi [4] have proposed a local approach of SED for sharp V notch under mix mode I+II load configuration. The analytical development is referred to a plane system and considers a circular sector as a control volume, with centre near the notch tip. (as it possible to see in Fig. 3.).

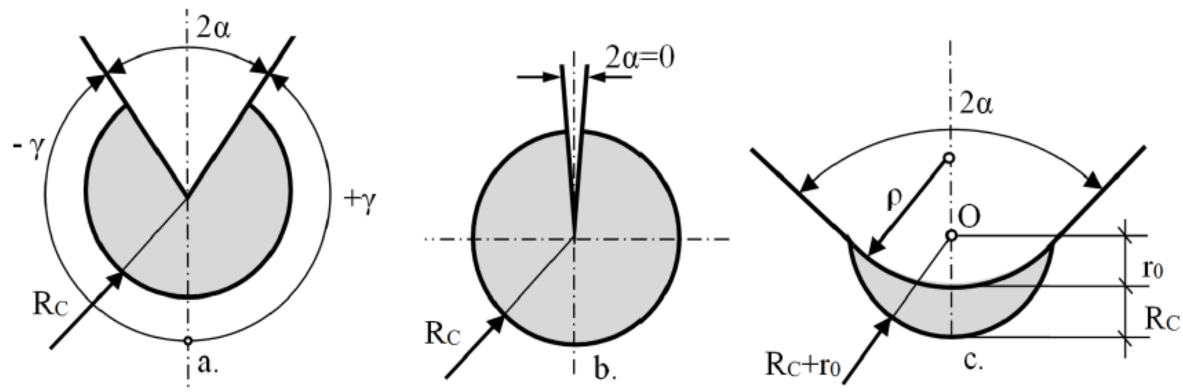


***Fig. 3.*** *Shape of control volume for different type of notch: a) sharp V notch case, b) crack case and c) blunt notch case.*

The main assumption is that the material is isotropic and has a linear elastic behavior.

The radius of the control volume $R_c$ ( or control area in plane case), for how it can be found the critical $W_c$ , is considered a material's parameter, independent from the opening angle of the notch. This value is calculated from the value of the fracture toughness and under plane strain conditions can be express as:

$$Rc = \frac{(1+v)(5-8v)}{4\pi}\left(\frac{K_{Ic}}{\sigma_t}\right)^2 \qquad plane\ strain \qquad [24]$$

While under plane stress conditions:

$$Rc = \frac{(5-3v)}{4\pi}\left(\frac{K_{Ic}}{\sigma_t}\right)^2 \qquad plane\ stress \qquad [25]$$

Following Lazzarin and Berto extend the local SED approach to sharp V notch, blunt V notch and U notch. The analytical development are made in case of tensile load (mode I) using the stress distribution at the notch tip proposed by Filippi and considering an isotropic material with linear elastic behavior.

For rounded V notch, has been introduced a control volume with radius given by the sum of two different radii, $r_0 + R_c$ . The lower limit for the radius of the control volume is represented by the curvature radius while the upper limit is represented by the sum of these two radii.

The $r_0$ length represents the distance between the origin of the polar system (used to express the tensions field) and the notch tip, showed at the beginning of the chapter (Fig. 4.).

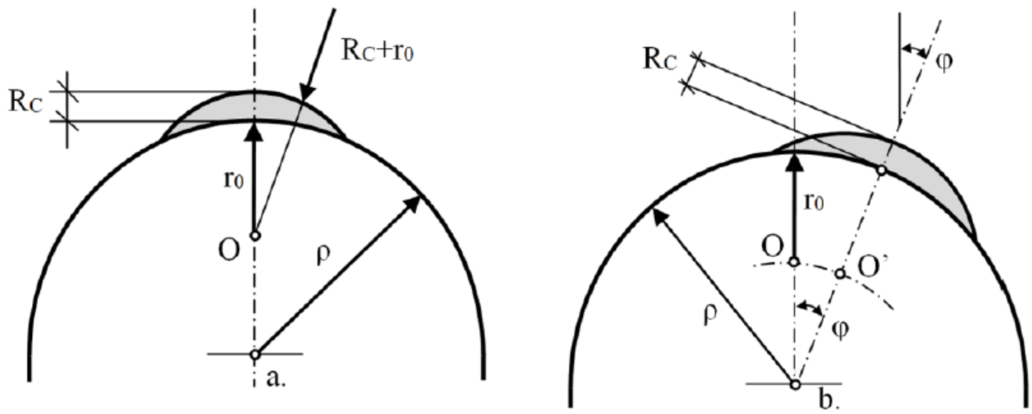


***Fig. 4.*** *Control volume for U notch, under mode I a) and under mixed mode b).*

For mode I, Lazzarin and Berto obtained a form to express the SED:

$$\overline{W_1} = F_{(2\alpha)} \cdot H_{(2\alpha, R_c/\rho)} \cdot \frac{\sigma_{max}^2}{E} \quad [26]$$

where $\sigma_{max}$ is the maximum tension in the notch.

The values of the functions F(2α) and H(2α, $R_c/\rho$) are exhibit in tables, where they are reported for different values of 2α, $R_c/\rho$ and the Poisson's ratio (Table 3).

| 2α (rad) | $R_0/\rho$ | *H* ν=0.3 | ν=0.35 | ν=0.4 | 2α (rad) | $R_0/\rho$ | *H* ν=0.3 | ν=0.35 | ν=0.4 |
|---|---|---|---|---|---|---|---|---|---|
| 0 | 0.01 | 0.563 | 0.5432 | 0.5194 | π/2 | 0.01 | 0.6290 | 0.6063 | 0.5801 |
| | 0.05 | 0.508 | 0.4884 | 0.4652 | | 0.05 | 0.5627 | 0.5415 | 0.5172 |
| | 0.1 | 0.451 | 0.4322 | 0.4099 | | 0.1 | 0.4955 | 0.4759 | 0.4535 |
| | 0.3 | 0.306 | 0.2902 | 0.2713 | | 0.3 | 0.3296 | 0.3144 | 0.2972 |
| | 0.5 | 0.227 | 0.2135 | 0.1976 | | 0.5 | 0.2361 | 0.2246 | 0.2115 |
| | 1 | 0.131 | 0.1217 | 0.1110 | | 1 | 0.1328 | 0.1256 | 0.1174 |
| π/6 | 0.01 | 0.639 | 0.6162 | 0.5894 | 2π/3 | 0.01 | 0.5017 | 0.4836 | 0.4628 |
| | 0.05 | 0.576 | 0.5537 | 0.5280 | | 0.05 | 0.4465 | 0.4298 | 0.4106 |
| | 0.1 | 0.510 | 0.4894 | 0.4651 | | 0.1 | 0.3920 | 0.3767 | 0.3591 |
| | 0.3 | 0.343 | 0.3264 | 0.3066 | | 0.3 | 0.2578 | 0.2467 | 0.2339 |
| | 0.5 | 0.253 | 0.2386 | 0.2223 | | 0.5 | 0.1851 | 0.1769 | 0.1676 |
| | 1 | 0.142 | 0.1333 | 0.1226 | | 1 | 0.1135 | 0.1079 | 0.1015 |
| π/3 | 0.01 | 0.667 | 0.6436 | 0.6157 | 3π/4 | 0.01 | 0.4114 | 0.3966 | 0.3795 |
| | 0.05 | 0.599 | 0.5769 | 0.5506 | | 0.05 | 0.3652 | 0.3516 | 0.3359 |
| | 0.1 | 0.530 | 0.5087 | 0.4842 | | 0.1 | 0.3206 | 0.3082 | 0.2938 |
| | 0.3 | 0.354 | 0.3372 | 0.3179 | | 0.3 | 0.2082 | 0.1997 | 0.1900 |
| | 0.5 | 0.259 | 0.2457 | 0.2301 | | 0.5 | 0.1572 | 0.1504 | 0.1427 |
| | 1 | 0.143 | 0.1349 | 0.1252 | | 1 | 0.1037 | 0.0988 | 0.0932 |

***Table 3.*** *Values of H parameter for Blunted V notched shapes, depending from the opening angle and from the material's property (Poisson's ratio).*

Under mode I+II conditions, the maximum principal tension $\sigma_{max}$ is located in in one point at the border of the notch, rotated with a φ angle respects to the notch bisector, Fig. 4. Gomez assumes that the control volume has centre in this point, without any shape's change of this one. This hypothesis determines that the control volume rotates of an angle fi near the origin of the curvature radius ρ. Also, the angle fi indicates the point where the crack starts to propagate, with normal direction to the maximum principal tension on the border of the notch.

| $R_0/\rho$ | H | | | | |
|---|---|---|---|---|---|
| | $\nu$=0.1 | $\nu$=0.15 | $\nu$=0.2 | $\nu$=0.25 | $\nu$=0.3 |
| 0.0005 | 0.6294 | 0.6215 | 0.6104 | 0.5960 | 0.5785 |
| 0.001 | 0.6286 | 0.6207 | 0.6095 | 0.5952 | 0.5777 |
| 0.005 | 0.6225 | 0.6145 | 0.6033 | 0.5889 | 0.5714 |
| 0.01 | 0.6149 | 0.6068 | 0.5956 | 0.5813 | 0.5638 |
| 0.05 | 0.5599 | 0.5515 | 0.5401 | 0.5258 | 0.5086 |
| 0.1 | 0.5028 | 0.4942 | 0.4828 | 0.4687 | 0.4518 |
| 0.3 | 0.3528 | 0.3445 | 0.3341 | 0.3216 | 0.3069 |
| 0.5 | 0.2672 | 0.2599 | 0.2508 | 0.2401 | 0.2276 |
| 1 | 0.1590 | 0.1537 | 0.1473 | 0.1399 | 0.1314 |

***Table 4.*** *H values for U notched specimens.*

# CHAPTER 2: PUR foams and properties

Polyurethane (PUR) foam materials are widely used as cores in sandwich composites, for packing and cushioning. They are made of interconnected networks of solid struts and cell walls incorporating voids with entrapped gas. The main characteristics of foams are lightweight, high porosity, high crushability, and good energy absorption capacity.

Polyurethane (PUR) materials represent a class of organic units joined by urethane links. They can be manufactured in a wide range of densities:

- At low densities (30–200 kg/m$^3$) they are rigid foams having a close cell cellular structure. The main applications of PUR foams are: high-resilience seating, rigid foam insulation panels, microcellular foam seals and gaskets, high durable elastomeric wheels and tires, automotive suspension bushings.
- At higher densities (>200 kg/m$^3$) they show a porous solid structure, and are used for fixtures and gauges, master and copy models, draw die moulds, hard parts for electronic instruments.

Mechanical properties of these materials are directly related to the mechanical property of solid materials used for manufacturing, by the geometry of cellular structure and the relative density. Cellular and porous materials have a crushable behaviour in compression, being able to absorb considerable amount of energy due to plateau and densification regions. However, in tensile they have a linear elastic behaviour up to fracture and a brittle failure. So they can be treated as brittle materials.
The mechanical properties of the foams depend directly from the density, so for this reason following are showed the mechanical properties and the way how these properties are determined.

## 2.1.Study of microstructure and density of the foams

Polyurethane materials of five different densities (100, 145, 300, 708 and 1218 kg/m$^3$) manufactured by Necumer GmbH – Germany, under commercial designation Necuron 100, 160, 301, 651 and 1020, were experimentally investigated. At low densities 100 and 145 kg/m$^3$ the materials have a rigid closed cellular structure, while the PUR materials of higher densities show a porous solid structure (300 and 708 kg/m$^3$), approaching the solid polyurethane material for the highest density 1218 kg/m$^3$. A QUANTA™ FEG 250 SEM was used to investigate the microstructures of the materials (at 1000x magnification), Fig. 1. The cell diameter and wall thickness were determined by statistical analysis and are presented in Table 1, together with the density of PUR materials obtained experimentally according with ASTM D1622-08, using cubic specimens of 15 x 15 x 15 mm, an electronic balance Sartorius LA230S for weighting and a digital calliper Mytotoyo for dimension determination.

In Fig. 1. is showed the microstructure of the materials, where the dimensions of the cell change with the density. Increasing the density, the cell's diameter and the cell's thickness decrease.

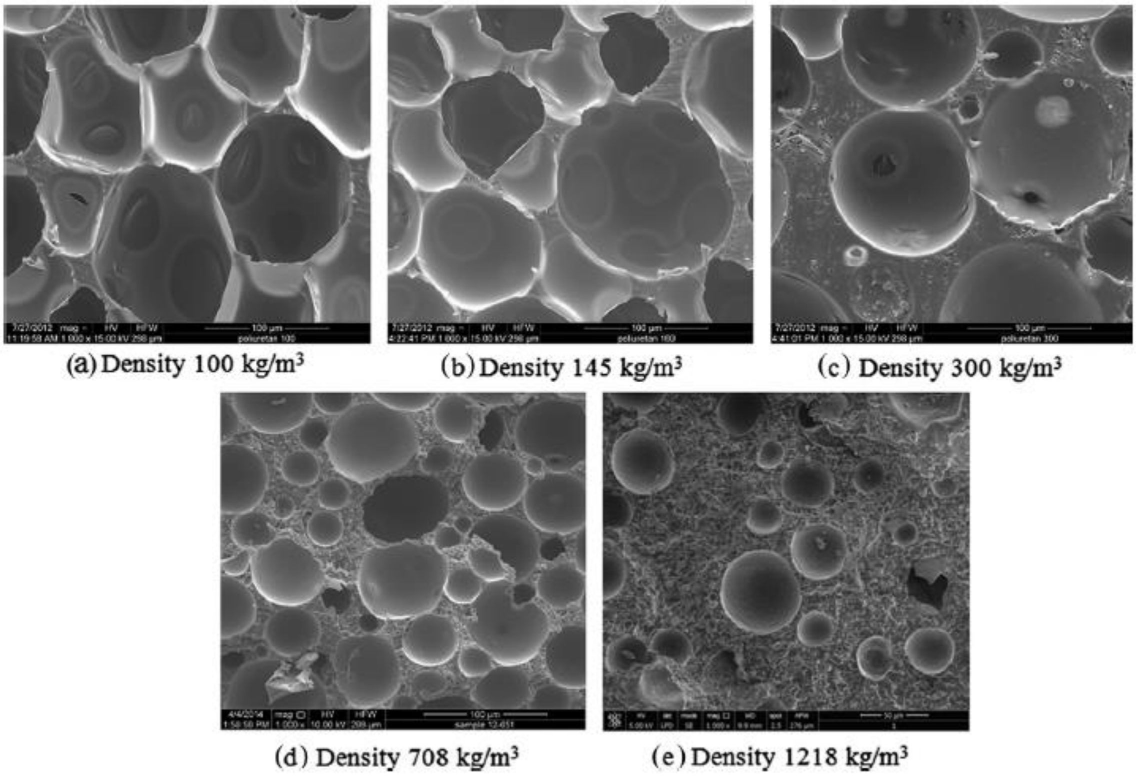


***Fig. 1.** Microstructures of PUR foams materials (at 1000X magnification) at different densities.*

| Foam | 100 | 160 | 301 | 651 | 1020 |
|---|---|---|---|---|---|
| **Cell length [µm]** | *104.5 ± 9.4* | *83.8 ± 9.6* | *68.5 ± 33.9* | *49.1 ± 30.2* | *22.6 ± 10.0* |
| **Cell wall thickness[µm]** | *2.9 - 5.8* | *5.1 - 13.1* | *3.8 - 21.8* | *4.7 - 37.6* | *12.3 -72.5* |
| **Density [Kg/m$^3$]** | *100.35 ± 0.25* | *145.53 ± 0.22* | *300.28 ±1.38* | *708.8 ±3.45* | *1218 ± 6.76* |

***Table 1.** Microstructure dimensions for the different foam density values examined.*

From these tests is very important to underline that Necuron 300 shows a very scattered data, as it possible to see in Fig. 2.

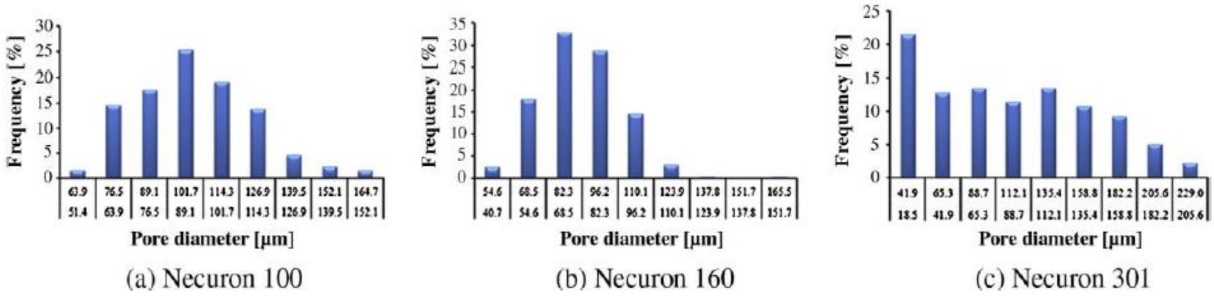


***Fig. 2.*** *Statistical analysis of the cell dimensions.*

## 2.2.Elastic properties

The elastic properties Young modulus and Poisson ratio were determined by Impulse Excitation Technique and are summarized in Table 2. Tensile strength was determined on dog bone specimens according with a gage length of 50 mm and a cross section in the calibrated zone with 10 mm width and 4 mm thickness, according to EN ISO 527.

| Necuron | 100 | 160 | 300 | 651 | 1020 |
|---|---|---|---|---|---|
| **Young's Modulus [MPa]** | *30.18 ± 1.75* | *66.89 ±1.07* | *281.39 ±2.92* | *1250 ± 15.0* | *3340 ± 7.1* |
| **Poisson's ratio [-]** | *0.285* | *0.285* | *0.302* | *0.302* | *0.343* |
| **Tensile strength [MPa]** | *1.16 ± 0.024* | *1.87 ± 0.036* | *3.86 ± 0.092* | *17.40 ± 0.32* | *49.75 ± 0.18* |

***Table 2.*** *Mechanical properties of the foams.*

In Fig. 3. and Fig. 4. is reported the characteristic curves of the materials and the load-displacement curves see from the tensile machine.

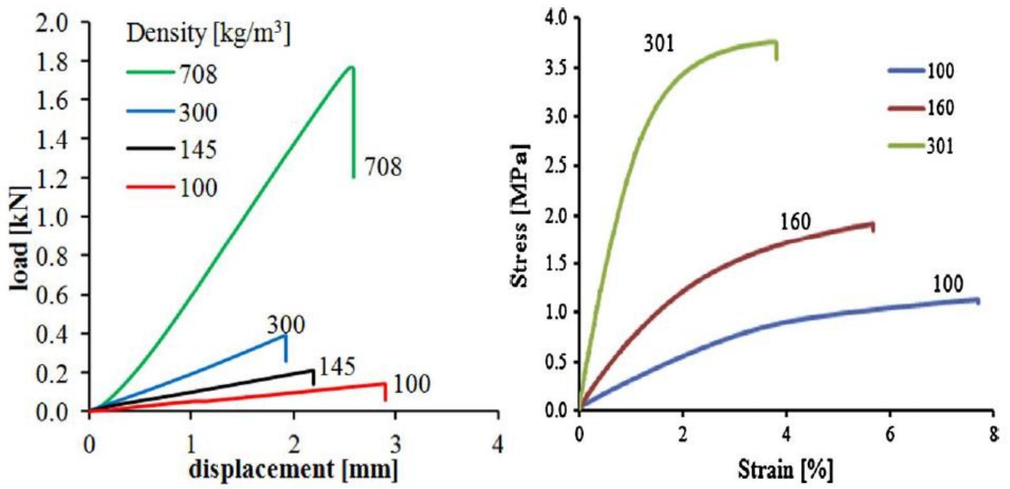


***Fig. 3.*** *Graphs of the characteristic curve for Necuron 100,160 and 301 (on the right) and load-displacement curves during a tensile test for Necuron 100, 160, 300 and 651.*

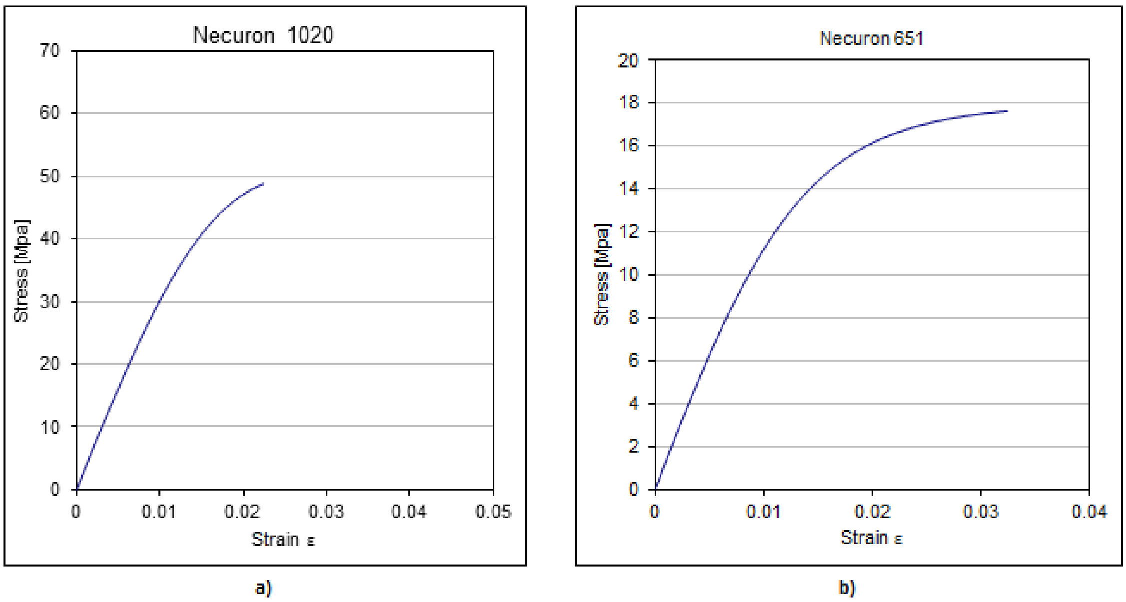


***Fig. 4.*** *Characteristic curve for Necuron 1020 a) and Necuron 651 b).*

It's possible to see that with the increasing of the density increase the maximum tensile strength but decrease the maximum displacement: this means that the capability of the material to absorb the energy during the deformation decrease with the increasing of the mechanical properties.

## 2.3.Fracture toughness

Two types of specimens were adopted for estimating the fracture toughness of PUR foams. The three point bend tests were performed on a 5 kN Zwick Proline testing machine, Fig. 5. The SENB specimens were cut in the two main directions, Fig. 6, and loaded with 2 mm/min. The load–displacement curve was recorded and the maximum force $P_{max}$ was used for calculation of fracture toughness (eq. (1)):

$$K_{Ic} = \frac{3P_{max}S}{2BW^2}\sqrt{\pi a} f(a/W) \quad (MPa \ mm^{0.5}) \qquad [1]$$

where $P_{max}$ is the maximum load in Newton, B and W are specimen dimensions in millimetre. The function f(a/W) is given by eq. (2):

$$f(a/W) = 1.122 - 140(a/W) + 7.33(a/W)^2 - 13.08(a/W)^3 + 14.0(a/W)^4 \quad [2]$$

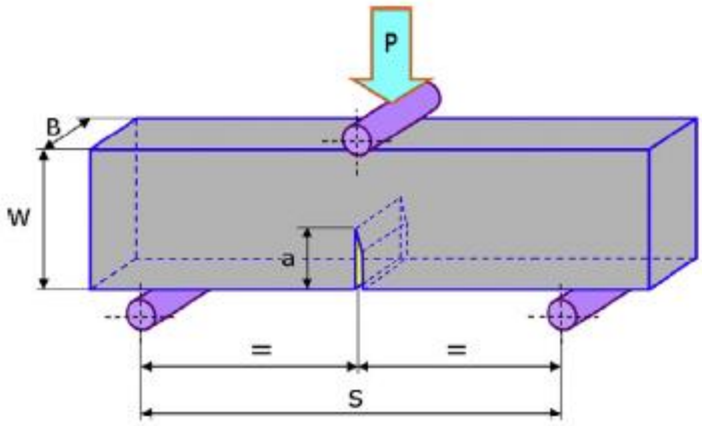


***Fig. 6.*** *SENB specimen.*

Evaluation of fracture toughness under mixed mode was carried out on Asymmetric Semi-Circular Bend (ASCB) specimens, Fig. 7. This ASCB specimen with radius R, which contains an edge crack of length a oriented normal to the specimen edge, loaded with a three point bend fixture, was proved to give a wide range of mixed modes, from pure mode I ($S_1$ = $S_2$), mixed modes I and II ($S_1$ – $S_2$), to pure mode II, only by changing the position of one support [22–24]. The considered geometry of the specimen has: R = 40 mm, a = 20 mm, t = 10 mm, $S_1$ = 30 mm and $S_2$ = 30, 12, 8, 6, 4, 2.66 mm. The Stress Intensity Factors (SIFs) of the ASCB specimen are expressed in the form (eq. (3)):


***Fig. 5.*** *Three points bend test.*

$$K_i = \frac{P_{max}}{2Rt}\sqrt{\pi a}Y_i(a/R\,, S_1/R\,, S_2/R) \qquad i = I, II \qquad [3]$$

Where the non-dimensional SIFs Yi(a/R, $S_1$/R, $S_2$/R) were determined by finite element analysis (eq (4)) for a/R = 0.5 and $S_1$/R = 0.75:

$$Y_I(S_2/R) = 6.235(S_2/R)^3 - 15.069(S_2/R)^2 + 17.229(S_2/R) - 1.062 \qquad [4]$$

$$Y_{II}(S_2/R) = 1.884(S_2/R)^5 - 7.309(S_2/R)^4 + 5.037(S_2/R)^3 + 2.77(S_2/R)^2 - 5.075(S_2/R) + 1.983 \qquad [5]$$

The tests were performed on a Zwick/Roell 5 kN testing machine at room temperature with a loading rate of 2 mm/min, except of the studies investigating the effect of loading rate. Fig. 7b presents a picture with the ASCB specimen in the bending fixture. For each position of support S2 four specimens were tested.

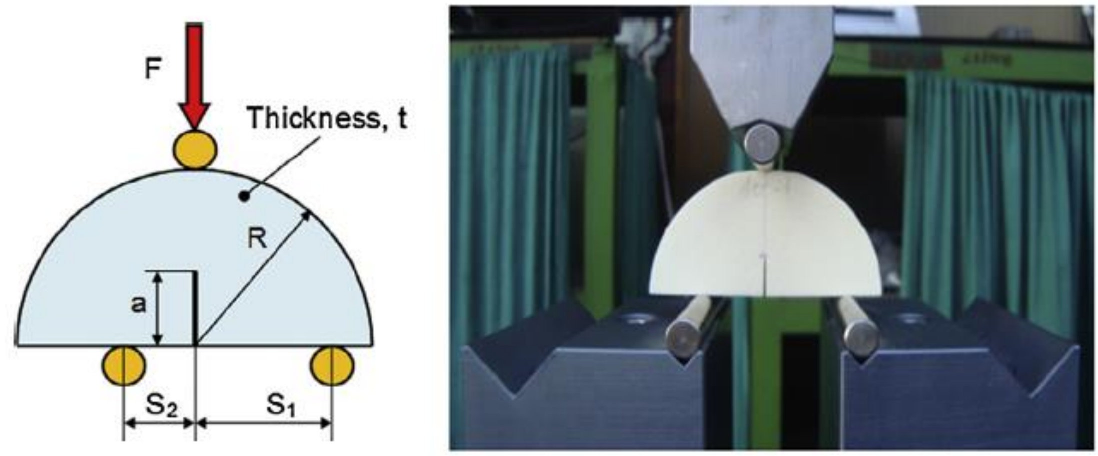


a) b)

***Fig. 7.*** *ASCB specimen a) and the test Set-up for this one b).*

## 2.4.Summarise of mechanical properties

The materials studied in the landmark sponges are produced by Necumer GmbH, a German company specializing in the production of polymeric materials . In particular have been considered five materials , commercially designated as NECURON 100, 160, 301, 651 and 1020. The mechanical properties of these materials are presented in Table 3 and make reference to the tests previously discussed.

| Necuron | 100 | 160 | 300 | 651 | 1020 |
|---|---|---|---|---|---|
| **Density [Kg/$m^3$]** | *100* | *145* | *300* | *708* | *1218* |
| **Poisson [-]** | *0.285* | *0.285* | *0.302* | *0.302* | *0.343* |
| **Tensile strength [MPa]** | *1.16 ±0.24* | *1.87 ± 0.036* | *3.86 ± 0.092* | *17.40 ± 0.32* | *49.75 ± 0.18* |
| **Fracture toughness in mode I[ MPa*$mm^{0.5}$]** | *0.087 ±0.003* | *0.131 ± 0.003* | *0.372 ±0.014* | *1.253 ± 0.026* | *2.86 ± 0.11* |
| **Fracture toughness in mode II MPa*$mm^{0.5}$]** | *0.05 ± 0.002* | *0.079 ± 0.004* | *0.374 ±0.013* | *1.376 ± 0.047* | *2.424 ± 0.135* |

These are the value of the mechanical properties that will be used in all the analysis.

# CHAPTER 3: Experimental tests

The SED approach is based on the idea that under prevailing tensile stresses failure occurs when the strain energy density averaged over a given control volume reaches a critical value, $\overline{W} = W_c$ , where $W_c$ depends on the material. If the material behaviour is ideally brittle, then $W_c$ can be evaluated by using simply the conventional ultimate tensile strength $\sigma_t$, so that $W_c = \sigma_t^2 / 2E$ . In principle $W_c$ as determined from uniaxial tests cannot be considered independent on the loading mode. Under compression, for example, the critical value of $W_c$ is surely different from the critical value under tension.

The critical value $W_c$ can be evaluated using the ultimate tensile strength in the case that the material is ideally brittle (as for example materials like ceramics, some glasses, some polymers, etc. etc.. ). If the material has a perfect brittle behaviour, the critical value $W_c$ is the area below of the characteristics curve of the material. If the material is perfectly brittle, the area is a triangle and this area can be determined knowing the ultimate tensile stress and the Young's modulus, Fig. 1.

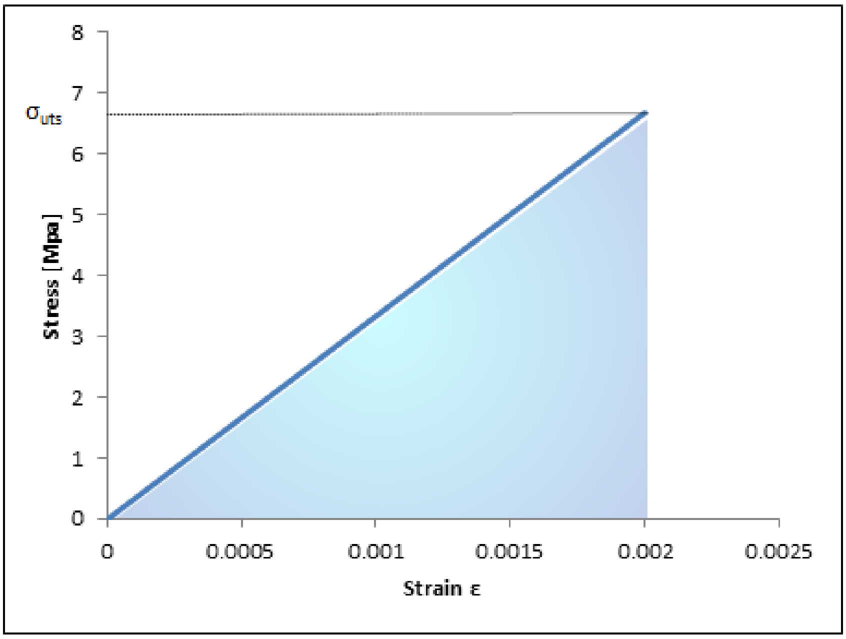


***Fig. 1.*** *The blue line represent the characteristic curve of a ideally brittle materials, the shadow area represent the strain energy density.*

The area is equal to:

$$A = \frac{1}{2} * \sigma_t * \varepsilon \quad [1]$$

In the case of elastic linear tract, is valid the following relation:

$$\sigma = E * \varepsilon \qquad [2]$$

So, the equation (1) become:

$$A = \frac{1}{2} * \frac{\sigma_{uts}^2}{E} \qquad [3]$$

In the case of the PUR foams, the characteristics curves of the different densities are the following:

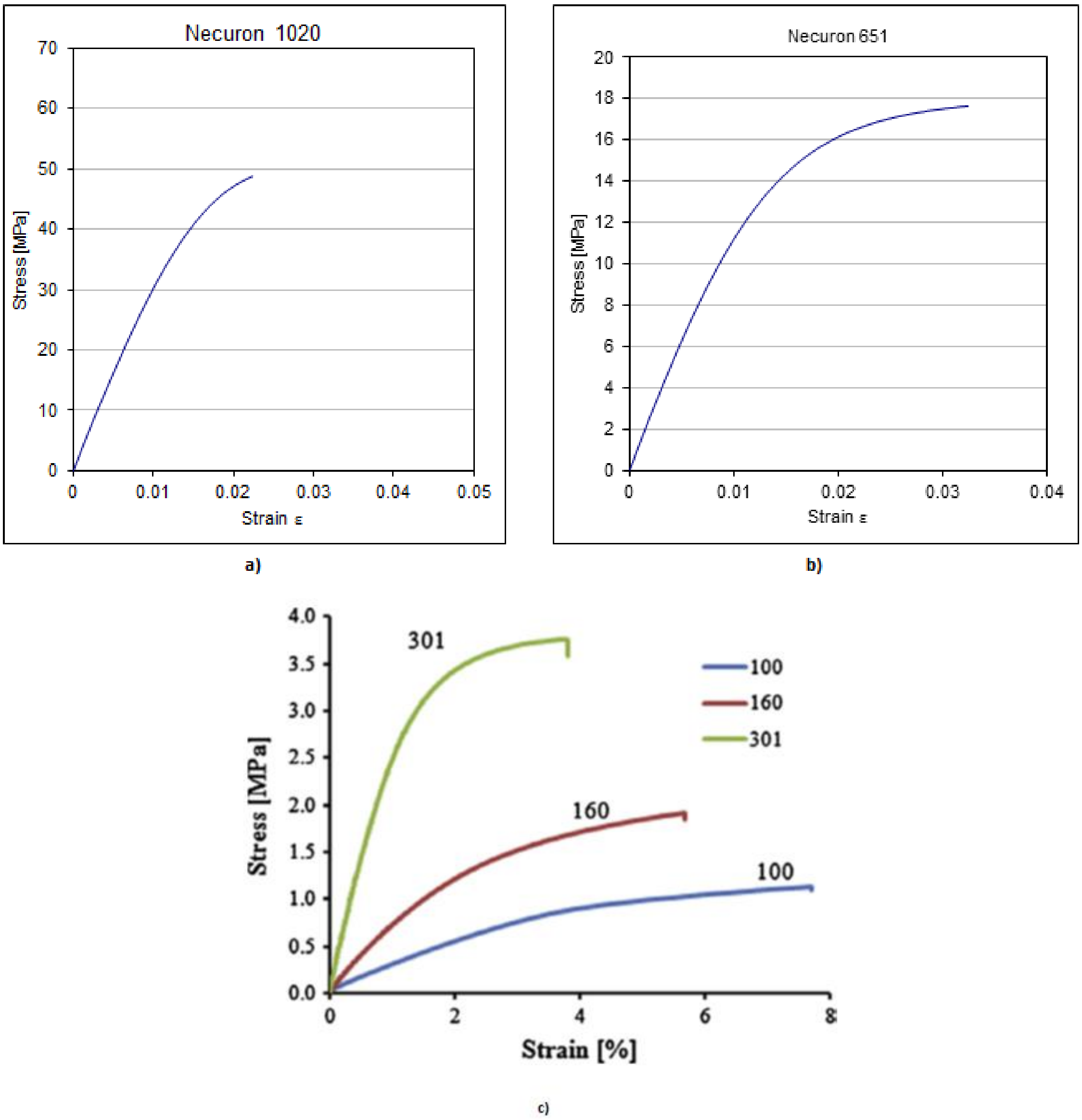


***Fig. 2.*** *Characteristics curve of the material, Necuron 1020 a), Necuron 651 b) , Necuron 300 ,160 and 100 c).*

From the characteristics curves of Necuron 651, 300, 160 and 100, the Young's modulus changes in relation with the applied stress and this trend increases with the decreasing of the density. Necuron 1020 presents a characteristic curve that is very near to a line, and this is

demonstrate by the fact that the Young's modulus calculate in the last tract of the curve moves away only by the 5 % from the average modulus, while for the lower densities the Young's modulus moves away more than 20 %.
It's possible to see that the material show a non-ideally brittle behaviour so for this reason is not possible to use the ultimate tensile strength to define the critical energy density. It's important to underline that all the unnotched materials don't show any plastic phenomenon.
All the tests made on these foams show that the notched materials has a quasi-ideally brittle behaviour: this is possible to see from the load-displacement curves, as it shown below.

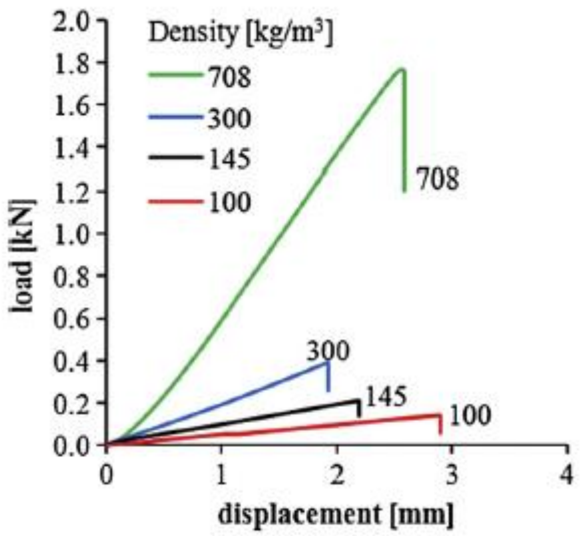


***Fig. 3.*** *Typical load–displacement curves in tensile for notched specimens.*

It's possible to notice that the behaviour of the notched material is very closed to a ideally brittle material's behaviour; the behaviour of the materials are linear and Young's modulus remain more or less the same.
As seen previously, to define the critical energy density is not possible to use the ultimate tensile strength. In the paper "A review of the volume-based strain energy density approach applied to V-notches and welded structures" di Berto F. e Lazzarin P. [2]. , the authors say:
*"The SED approach is based on the idea that under tensile stresses failure occurs when $W = W_c$, where the critical value $W_c$ obviously varies from material to material. If the material behaviour is ideally brittle, then $W_c$ can be evaluated by using simply the conventional ultimate tensile strength $\sigma_t$, so that $W_c = \sigma_t^2 / 2E$. Often unnotched specimens exhibit a non-linear behaviour whereas the behaviour of notched specimens remains linear.*

*Under these circumstances the stress $\sigma_t$ should be substituted by ''the maximum normal stress existing at the edge at the moment preceding the cracking", where it is also recommended to use tensile specimens with semi-circular notches."*

In this extract the authors say that it's possible to define the SED parameters, $R_c$ and $W_c$ , using the tension $\sigma_t$ , where $\sigma_t$ is the tension at the notch tip preceding the crack, defined in a plate with bland curvature radius, under tensile load.

With this $\sigma_t$ , $W_c$ and $R_c$ are determined through the following formulas:

$$Wc = \frac{\sigma_t^2}{2E} \qquad [4]$$

$$Rc = \left[\frac{I_1 * K_{1c}^2}{4 * \lambda_1 * (\pi - \alpha) * E * Wc}\right]^{\frac{1}{(2-2\lambda_1)}} \qquad [5]$$

All the parameters are known except $\sigma_t$ : knowing this tension, the SED parameters can be defined. The idea at the basis is to produce specimens with a bland curvature radius and test these ones under tensile load; the tensile machine gives back the fracture loads of the components. Applying the fracture load to a finite element model, is possible to discover the stress presents at the notch tip in the moment that preceding the crack.

In the following paragraphs are showed the procedure and the results obtained from the experimental tests.

### 3.1.Experimental tests

The procedure followed to determine this tension is the following:

1. Definition of the specimen's notched geometry, with a bland curvature radius.
2. Produce the specimens and measurements of the all dimensions.
3. Test the specimens under tensile load and discover the loads that preceding the crack, for each density.
4. Create a 2 D finite element model, apply the fracture loads and determine the stress $\sigma_t$ at the notch tip through a linear-elastic analysis.

The specimens are made for each density except the highest density, Necuron 1020, this because for this one the characteristic curve, in the first approximation, it's very closed to the ideal characteristic curve so it's possible use directly the ultimate tensile strength $\sigma_{uts}$ .

The tests are made on the following specimens:

1. Necuron 651: density 708 kg/m$^3$
2. Necuron 301 :density 300 kg/m$^3$
3. Necuron 160: density 145 kg/m$^3$
4. Necuron 100: density 100 kg/m$^3$

As says before, the first step is to define an appropriate geometry.

### 3.1.1.Definition of geometry and dimensions

For this kind of test, it has been choose a plate with a U notch, where the curvature radius is very bland. It has been chosen a U notch to have a full notch sensitivity.

The geometry and the nominal dimensions choose are the following:

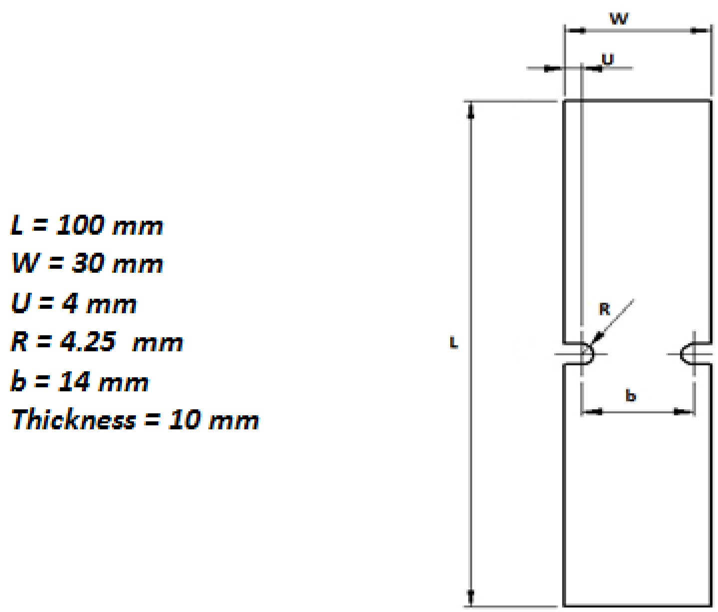


***Fig. 4***. *Geometry and dimensions of the U notched specimens with a bland curvature radius.*

With a curvature radius equal to 4 mm, in theory, is guaranteed the full notch sensitivity. The geometry is the same for each densities but what changes is the real dimensions.

### 3.1.2.Specimens dimensions

The specimens have been produced in the laboratory.

Previous are reported the nominal dimensions: it's known that the real dimensions of the produced specimens are different from the nominal dimensions. For each density has been produced many specimens but have been tested only a few of these ones.

It's important to underline that it's hard to cut the PUR foams specimens with low density, so only the best specimens has been choose.

All the dimensions are measured through a calliper, Mitutoyo digital calliper; for each specimens have been made four measurements for each dimensions: in the following table are exhibit the mean value for each dimension (Table 1.1).

***Necuron 100***

| N° Specimen | L [mm] | W [mm] | Thickness [mm] | b [mm] | D (2*R) [mm] | Notch depth [mm] |
|---|---|---|---|---|---|---|
| 1 | *100.01* | *30.51* | *9.75* | *14.98* | *9.39* | *7.63* |
| 2 | *100.13* | *30.6* | *9.8* | *15.17* | *8.86* | *7.41* |
| 3 | *100.25* | *30.53* | *9.87* | *14.96* | *8.61* | *7.72* |
| 4 | *100.12* | *30.36* | *11.01* | *14.69* | *8.66* | *6.58* |
| 5 | *100.12* | *30.51* | *10.78* | *15.68* | *8.88* | *6.79* |
| 6 | *100.27* | *30.61* | *9.71* | *14.96* | *8.42* | *7.84* |
| 7 | *100* | *30.36* | *9.75* | *14.8* | *8.4* | *7.61* |
| 8 | *100.21* | *30.69* | *9.73* | *14.8* | *8.2* | *7.78* |
| 9 | *100.08* | *30.66* | *10.8* | *14.87* | *8.6* | *7.55* |
| 10 | *100.02* | *30.61* | *9.85* | *15.57* | *9.1* | *7.37* |
| 11 | *100.04* | *30.53* | *9.67* | *14.8* | *9.23* | *7.77* |
| 12 | *100.1* | *30.59* | *10.64* | *15.08* | *8.72* | *7.62* |
| 13 | *100.3* | *30.82* | *9.6* | *15.64* | *9.01* | *7.43* |
| 14 | *100.1* | *30.56* | *9.66* | *14.4* | *9.08* | *7.61* |
| 15 | *99.68* | *30.23* | *9.68* | *14.63* | *9.7* | *7.44* |
| 16 | *99.87* | *30.55* | *9.71* | *14.37* | *9.56* | *7.77* |

**Table 1.1** *Measurements of all the specimens Necuron 100.*

For Necuron 100 are available sixteen specimens: every specimen presents some imperfection generated during the production; for the test have been choose the best six specimens. The specimens choose are: specimens n° ***3,6,7,8,9,12*** (Fig. 5).

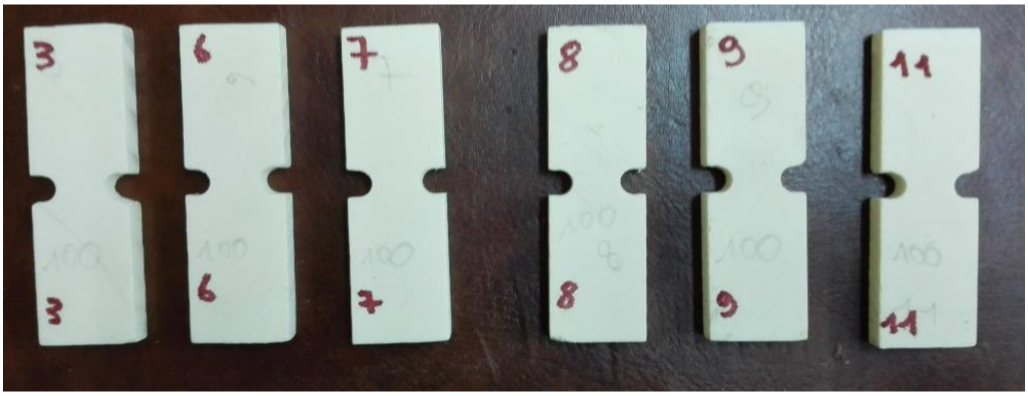


***Fig. 5.*** *Choose specimens for Necuron 100.*

The dimensions of the finite element model are the mean values defined only through the tested specimens. The mean values are:

| N° Specimen | L [mm] | W [mm] | Thickness [mm] | b [mm] | D (2*R) [mm] | Notch depth [mm] |
|---|---|---|---|---|---|---|
| 3 | *100.25* | *30.53* | *9.87* | *14.96* | *8.61* | *7.72* |
| 6 | *100.27* | *30.61* | *9.71* | *14.96* | *8.42* | *7.84* |
| 7 | *100* | *30.36* | *9.75* | *14.8* | *8.4* | *7.61* |
| 8 | *100.21* | *30.69* | *9.73* | *14.8* | *8.2* | *7.78* |
| 9 | *100.08* | *30.66* | *10.8* | *14.87* | *8.6* | *7.55* |
| 11 | *100.04* | *30.53* | *9.67* | *14.8* | *9.23* | *7.77* |
| **Average** | ***100.14*** | ***30.56*** | ***9.92*** | ***14.87*** | ***8.58*** | ***7.71*** |

**Table 1.2** *Measurements of choose specimens Necuron 100.*

The average values represent the value that will be used for the finite element model.
The same procedure has been done for the specimens of the other densities so following are reported only the table with the measurements of all the specimens, the image and the values of the choose specimens.

**Necuron 160**

For Necuron 160 are available sixteen specimens: every specimen presents some imperfection generated during the production; for the test have been chosen the best six specimens. The specimens choose are: specimens n° ***1,5,6,10,11,14***.

| N° Specimen | L [mm] | W [mm] | Thickness [mm] | b [mm] | D [mm] | Notch depth [mm] |
|---|---|---|---|---|---|---|
| 1 | *100.06* | *30.62* | *9.71* | *15.87* | *8.46* | *7.2* |
| 2 | *100.28* | *30.96* | *9.68* | *15.43* | *9.51* | *7.74* |
| 3 | *99.7* | *30.83* | *9.52* | *15.81* | *9.48* | *7.22* |
| 4 | *100.12* | *30.72* | *9.69* | *15.25* | *8.63* | *7.6* |
| 5 | *100.09* | *30.82* | *9.8* | *15.29* | *8.7* | *7.46* |
| 6 | *100.18* | *30.85* | *9.95* | *15.52* | *8.78* | *7.71* |
| 7 | *100.02* | *30.83* | *9.31* | *15.52* | *8.29* | *7.53* |
| 8 | *99.52* | *30.85* | *9.74* | *16.3* | *8.79* | *7.42* |
| 9 | *100.15* | *30.92* | *9.7* | *15.59* | *9.13* | *7.9* |
| 10 | *99.92* | *30.65* | *9.82* | *15.75* | *8.64* | *7.45* |
| 11 | *100.1* | *30.78* | *9.68* | *15.44* | *8.6* | *7.6* |
| 12 | *98.48* | *30.64* | *9.77* | *15.5* | *8.62* | *7.66* |
| 13 | *100.25* | *30.71* | *9.69* | *15.84* | *8.76* | *7.5* |
| 14 | *100.1* | *30.65* | *9.65* | *15.28* | *8.08* | *7.6* |
| 15 | *100.06* | *30.59* | *10.03* | *15.24* | *8.88* | *7.54* |
| 16 | *100.27* | *30.86* | *9.62* | *15.27* | *8.6* | *7.62* |

**Table 2.1** *Measurements of all the specimens Necuron 160.*

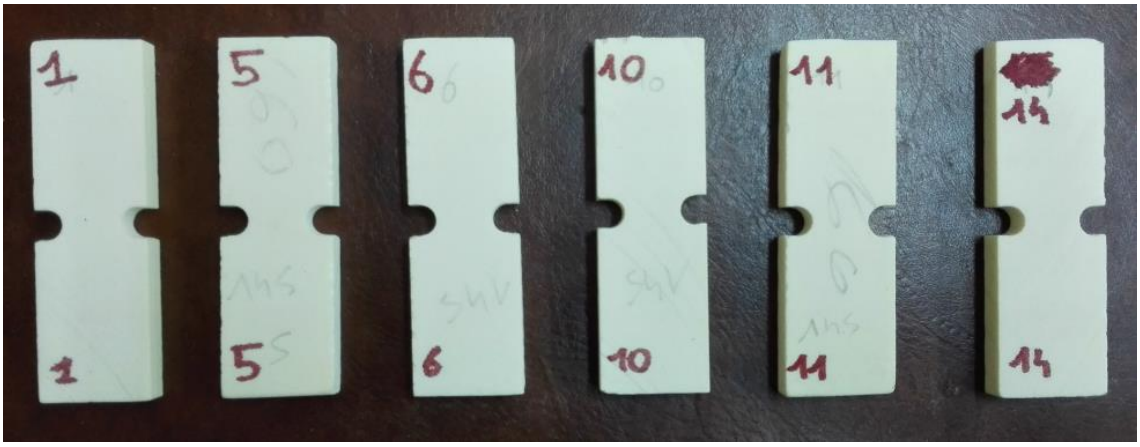


***Fig. 6.*** *Choose specimens for Necuron 160.*

| N° Specimen | L [mm] | W [mm] | Thickness [mm] | b [mm] | D [mm] | Notch depth [mm] |
|---|---|---|---|---|---|---|
| 1 | *100.06* | *30.62* | *9.71* | *15.87* | *8.46* | *7.2* |
| 5 | *100.09* | *30.82* | *9.8* | *15.29* | *8.7* | *7.46* |
| 6 | *100.18* | *30.85* | *9.95* | *15.52* | *8.78* | *7.71* |
| 10 | *99.92* | *30.65* | *9.82* | *15.75* | *8.64* | *7.45* |
| 11 | *100.1* | *30.78* | *9.68* | *15.44* | *8.6* | *7.6* |
| 14 | *100.1* | *30.65* | *9.65* | *15.28* | *8.08* | *7.6* |
| **Average** | ***100.08*** | ***30.73*** | ***9.77*** | ***15.53*** | ***8.54*** | ***7.50*** |

**Table 2.2** *Measurements choose specimens Necuron 160.*

**Necuron 300**

| N° Specimen | L [mm] | W [mm] | Thickness [mm] | b [mm] | D [mm] | Notch depth [mm] |
|---|---|---|---|---|---|---|
| 1 | *100.42* | *30.54* | *9.61* | *14.81* | *8.73* | *7.76* |
| 2 | *100.15* | *29.65* | *9.92* | *14.11* | *8.76* | *7.73* |
| 3 | *100.04* | *30.53* | *10.07* | *14.65* | *8.71* | *7.89* |
| 4 | *99.91* | *29.94* | *9.78* | *14.22* | *9.17* | *7.61* |
| 5 | *100.14* | *30.64* | *10.15* | *14.65* | *8.81* | *7.93* |
| 6 | *99.94* | *30.62* | *9.55* | *15.57* | *8.52* | *7.84* |
| 7 | *99.93* | *29.67* | *9.52* | *13.55* | *8.89* | *7.87* |
| 8 | *100.02* | *29.65* | *10.06* | *14.88* | *9.4* | *7.3* |

**Table3.1** *Measurements of all the specimens Necuron 300.*

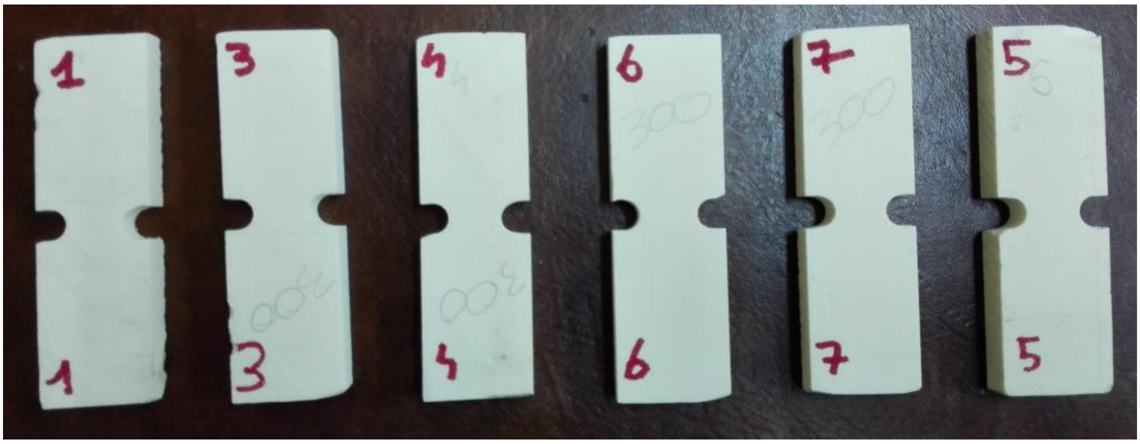


***Fig. 7.*** *Choose specimens for Necuron 300.*

| N° Specimen | L [mm] | W [mm] | Thickness [mm] | b [mm] | D [mm] | Notch depth [mm] |
|---|---|---|---|---|---|---|
| 1 | *100.42* | *30.54* | *9.61* | *14.81* | *8.73* | *7.76* |
| 3 | *100.04* | *30.53* | *10.07* | *14.65* | *8.71* | *7.89* |
| 4 | *99.91* | *29.94* | *9.78* | *14.22* | *9.17* | *7.61* |
| 5 | *100.14* | *30.64* | *10.15* | *14.65* | *8.81* | *7.93* |
| 6 | *99.94* | *30.62* | *9.55* | *15.57* | *8.52* | *7.84* |
| 7 | *99.93* | *29.67* | *9.52* | *13.55* | *8.89* | *7.87* |
| **Average** | ***100.06*** | ***30.32*** | ***9.78*** | ***14.58*** | ***8.81*** | ***7.80*** |

**Table 3.2** *Measurements of choose specimens Necuron 300.*

For  Necuron 300 are available eight specimens: every specimen presents some imperfection generated during the production; for the test have been choose the best six specimens. The specimens choose are: specimens n° ***1,3,4,5,6,7***.

**Necuron 651**

| N° Specimen | L [mm] | W [mm] | Thickness [mm] | b [mm] | D  [mm] | Notch depth [mm] |
|---|---|---|---|---|---|---|
| 1 | *100.32* | *30.21* | *10.45* | *15.75* | *8.71* | *7.33* |
| 2 | *100.33* | *29.95* | *10.42* | *16.24* | *8.37* | *7.1* |
| 3 | *100.31* | *30.37* | *10.42* | *15.17* | *9.4* | *7.88* |
| 4 | *100.2* | *30.14* | *10.43* | *15.77* | *8.22* | *7.51* |
| 5 | *100.41* | *30.52* | *10.42* | *15.43* | *9.33* | *7.68* |
| 6 | *100.25* | *30.61* | *10.4* | *16.16* | *8.56* | *7.3* |
| **Average** | ***100.26*** | ***30.23*** | ***10.42*** | ***16.06*** | ***8.38*** | ***7.30*** |

**Table 4** *Measurements of choose specimens Necuron 651.*

For  Necuron 651 the specimens available in the laboratory are equal to six; five over six specimens are tested.

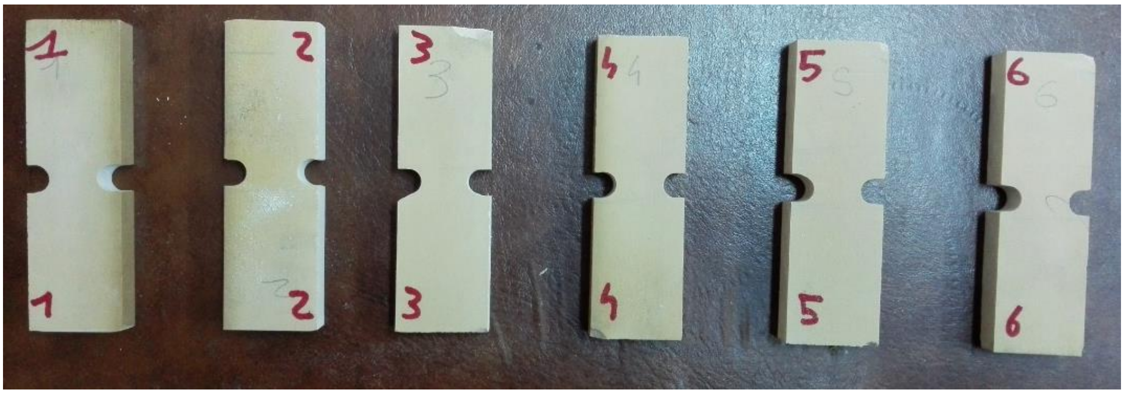


***Fig. 8.*** *Choose specimens for Necuron 651.*

### 3.1.3.Experimental results

Specimens are tested using a Zwick/Roell Z005 testing machine with a maximum force of 5 kN, under displacement control with a loading rate of 30 mm/min at room temperature. The machine can give the recorded load-displacement curve for each test. At least five tests were performed for each notch geometry.


***Fig. 9.*** *The Zwick/Roell Z005 tensile machine (on the left ) and a zoom of the fixture with the specimens (on the right).*

During the tests it has used an high speed camera to see in “slow motion” the behaviour of the specimens during the failure moment; through this camera is possible to study better how the material reach the failure.

***Fig. 10.*** *High speed camera positioned in front of the specimen.*

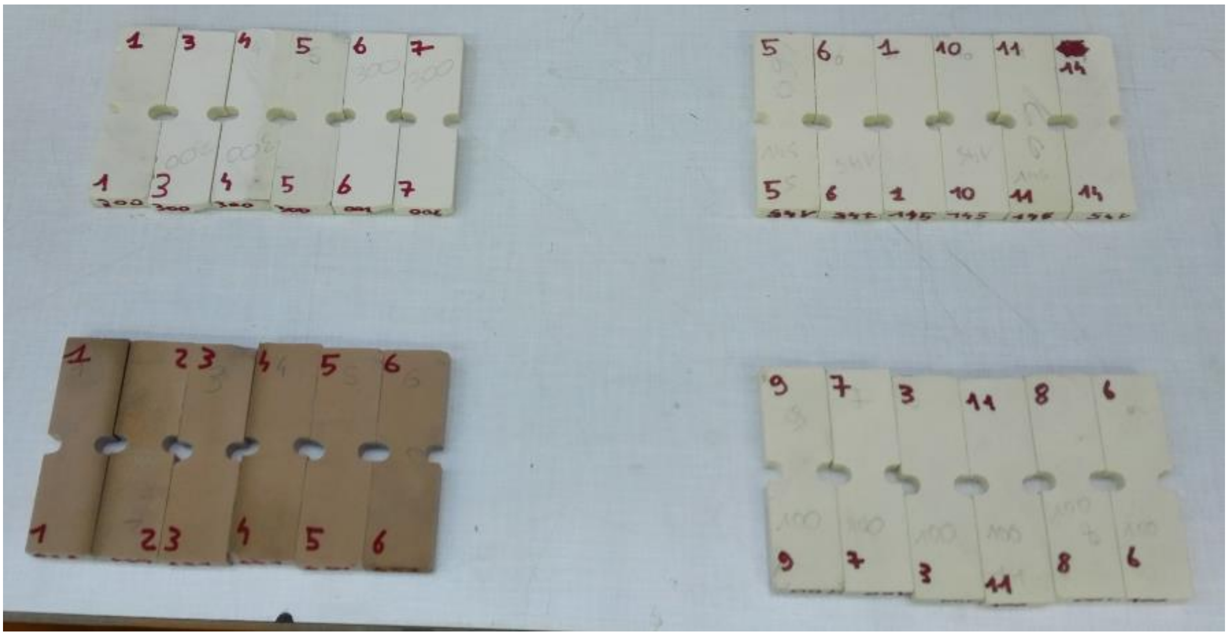

***Fig. 11.*** *Image of the tested specimens.*

The recorded load–displacement curves were linear, without any significant non-linearity, and the fracture occurred suddenly, indicating a brittle behaviour. Following are showed the experimental loads obtained from the tensile  test; near the results are reported the image of the specimen at the end of the test. It's possible to see that the crack starts at the notch tip and propagated along the notch bisector, as predicted by the theory.

**Necuron 100**

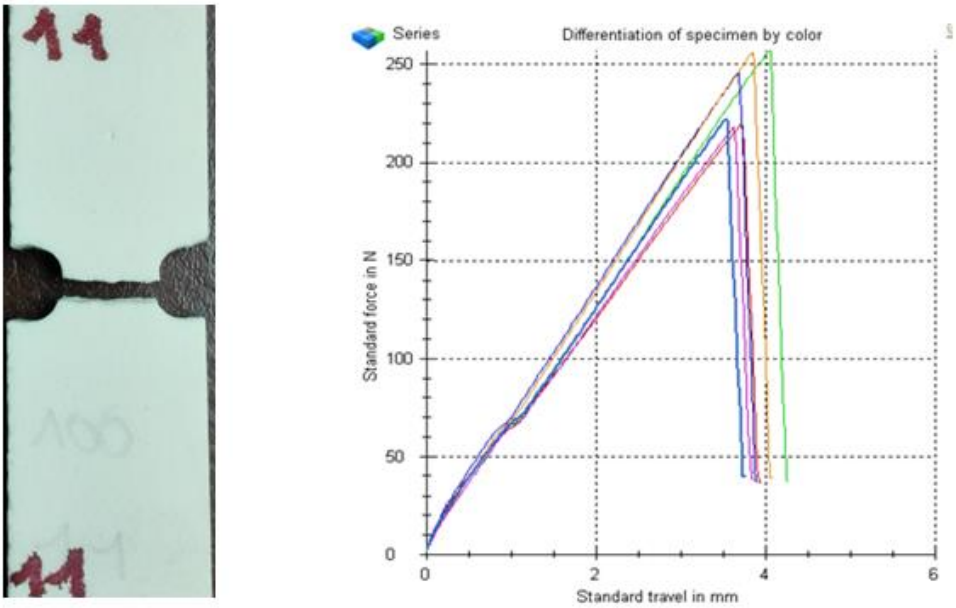


***Fig. 12.*** *On the left is showed the crack path while on the right the load-displacement curves of each test.*

It's possible to see that the load-displacement curve it's linear until the failure; the failure is suddenly ( Fig. 12 ). Through the high speed camera it has been seen that there are no plastic zone. This is possible to see in Fig. 13, where the two parts put together form the original body with the same dimensions. In Fig. 14 is showed the failure's surface.

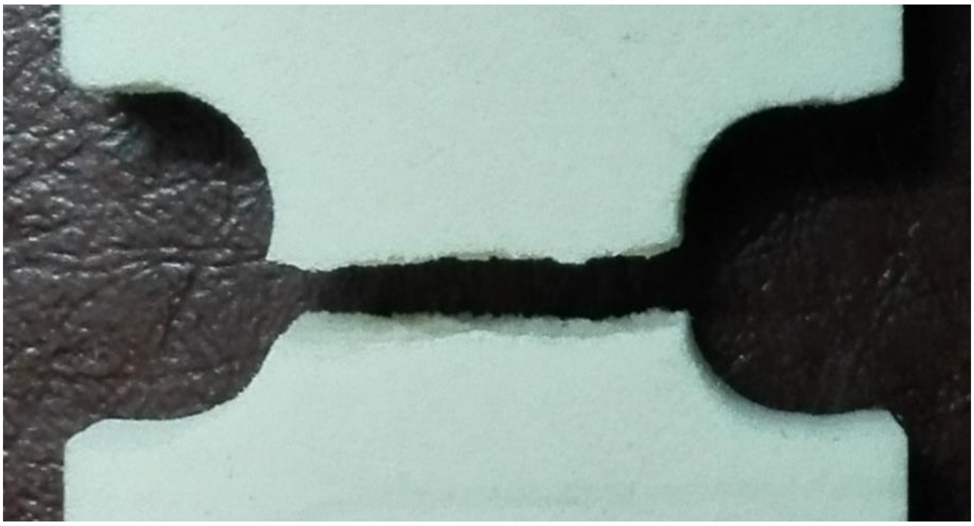

***Fig. 13.*** *Failure's zone of the specimens.*

***Fig. 14.*** *Surface's failure.*

Each other density shows the same behaviour of Necuron 100, so the same consideration made previous are valid. In the Table 5 are presented the fracture loads.

| NECURON 100 | |
|---|---|
| **N° specimen** | **Load [N]** |
| **3** | *220* |
| **6** | *257* |
| **7** | *246* |
| **8** | *256* |
| **9** | *222* |
| **11** | *218* |

**Table 5** *Experimental loads Necuron 100.*

The loads are very near each other, the dispersion is very low.

**Necuron 160**


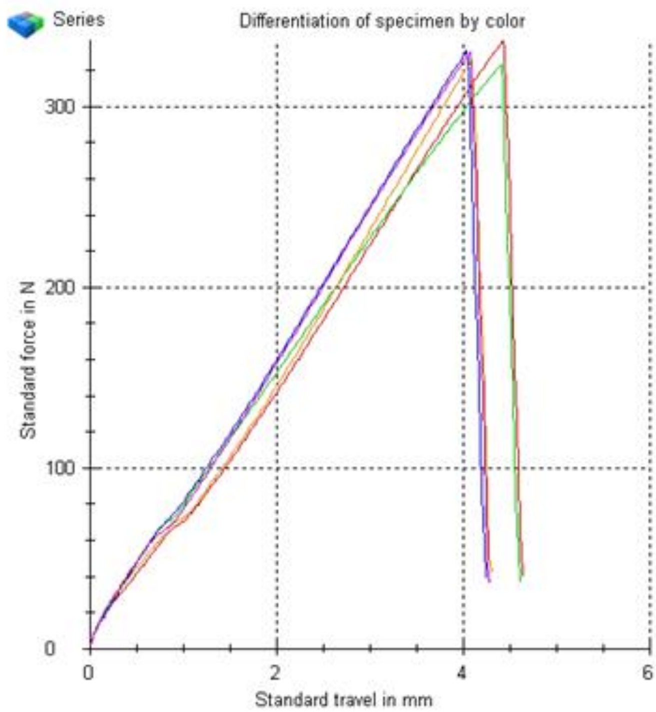


***Fig. 15.*** *On the left is showed the crack path while on the right the load-displacement curves of each test.*

| NECURON 160 | |
|---|---|
| N° specimen | Load [N] |
| 1 | *336* |
| 5 | *323* |
| 6 | *330* |
| 10 | *326* |
| 11 | *330* |

**Table 6** *Experimental loads Necuron 160.*

### Necuron 300

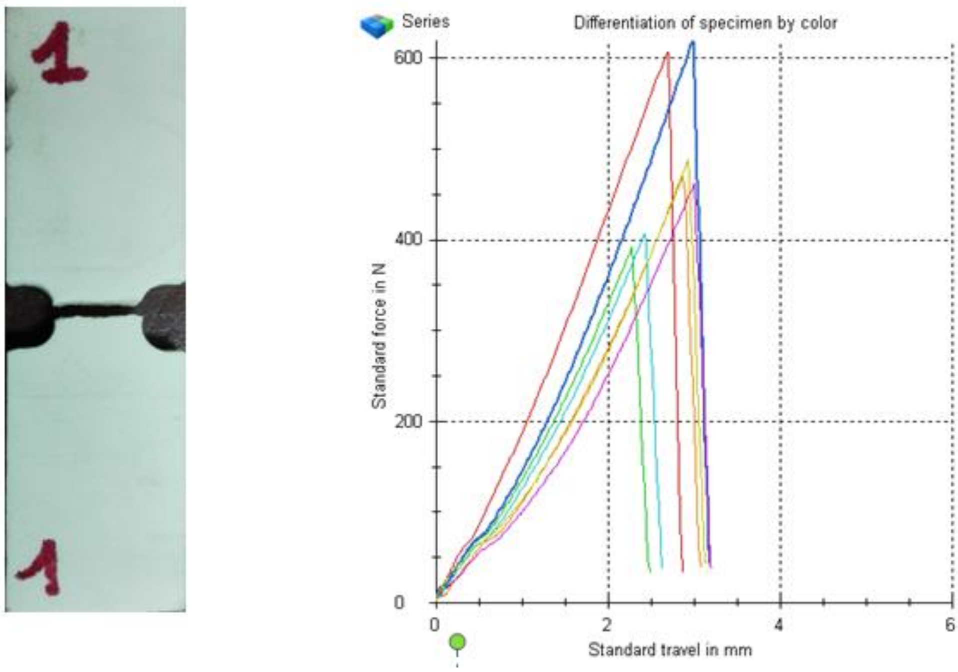


***Fig. 15.*** *On the left is showed the crack path while on the right the load-displacement curves of each test.*

| NECURON 300 | |
|---|---|
| N° specimen | Load [N] |
| 1 | *392* |
| 3 | *620* |
| 4 | *782* |
| 5 | *470* |
| 6 | *462* |
| 7 | *406* |
| 2 | *606* |
| 8 | *488* |

**Table 7** *Experimental loads Necuron 300.*

In all the tests made on Necuron 300, the results are very scattered, as it seen from Fig. 15, where some loads are very different in comparison with the others fracture loads. Necuron 300 has showed this behaviour in all the entire tests, with all the geometry tested.

**Necuron 651**

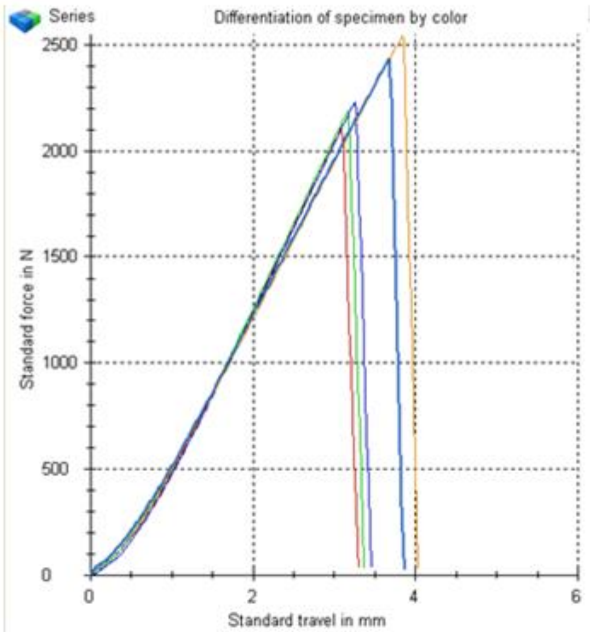


***Fig. 16.*** *On the left is showed the crack path while on the right the load-displacement curves of each test.*

| NECURON 651 | |
|---|---|
| **N° specimen** | **Load [N]** |
| **1** | *2110* |
| **2** | *2180* |
| **4** | *2230* |
| **5** | *2430* |
| **6** | *2540* |

**Table 8** *Experimental loads Necuron 651.*

Except Necuron 300, for all the other densities the loads are not so scattered.

### 3.1.4.Finite element analysis

It's important to underline that every specimens has its dimensions: in this case to define a unique model for each density, it is taking in account of the mean value (the average of the specimens tested) of each dimension.
These are the mean dimensions for each density:

| Density [Kg/m$^3$] | L [mm] | W [mm] | Thickness [mm] | b [mm] | D [mm] | Notch depth [mm] |
|---|---|---|---|---|---|---|
| **100** | *100.1* | *30.5* | *9.9* | *14.85* | *8.5* | *7.82* |
| **145** | *100.07* | *30.7* | *9.75* | *15.5* | *8.5* | *7.6* |
| **300** | *100* | *30.3* | *9.8* | *14.5* | *8.8* | *7.8* |
| **708** | *100.2* | *30.2* | *10.4* | *16* | *8.4* | *7.1* |

**Table 9** *Mean value of each dimension.*

For the analysis it has been used Ansys Multiphysics 14.5 software, an Enginsoft product. The analysis is linear elastic so the material data required are only the Young's modulus and the Poisson's ratio. The model created is a 2 D model, generated using a plane element with eight nodes (***PLANE 183***); the load is applied under plane strain conditions. In this case the purpose is to determine the first principal tension at the notch tip so use plane stress conditions produce the same results to use the plane strain conditions.
The geometry presents two axes of symmetry so it's possible to modelling only a quarter of the plate; the symmetry conditions have applied to horizontal line at the bottom of the model and to all vertical lines (on the right side) in front of the notch tip.

To determine with precision the first principal tension at the notch tip, the mesh plays a fundamental role: in fact more the mesh is refined near the notch tip, more the tension will be accurate. So it's necessary to create a very refined mesh near the notch (Fig. 18a) tip while far from the notch tip is possible to have a non-refined mesh ( Fig. 18b ).

It's been a 2D model and the load is applied as a pressure on line: to get this pressure on line just divide the load for area of the section (W*thickness), where W and the thickness are taken from the table of the mean value of the dimensions ( Table 1.2, Table 2.2, Table 3.2 and Table 4).
The load used for each density is the mean value; the mean value are exhibit in Table 9.

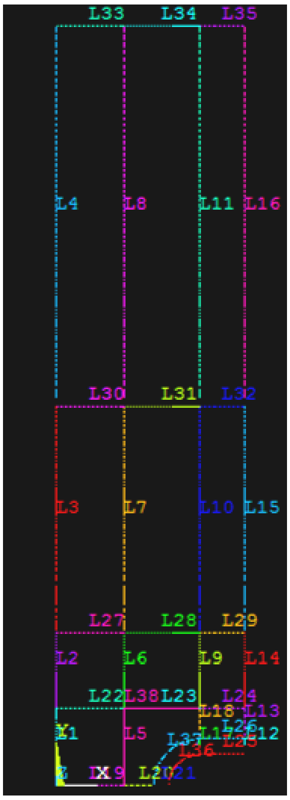


***Fig. 17.*** *Modelled geometry.*

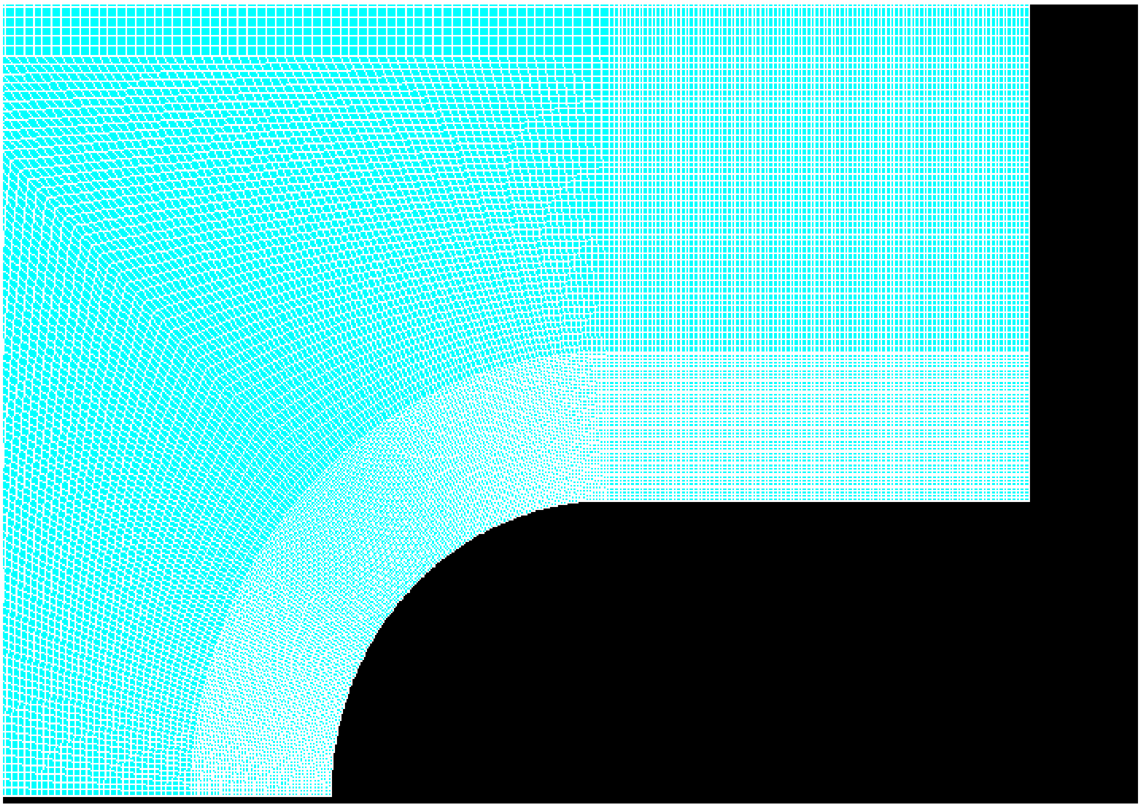

***Fig. 18.*** *A non-refined mesh  distant from the notch tip, refined mesh near the notch tip.*

To determine the stress $\sigma_t$ is necessary to plot the first principal tension, that in this case (at the notch tip) is the same of the stress $\sigma_y$ (the tension along the vertical axes).

In Fig. 19 is showed the tension's distribution along the geometry.

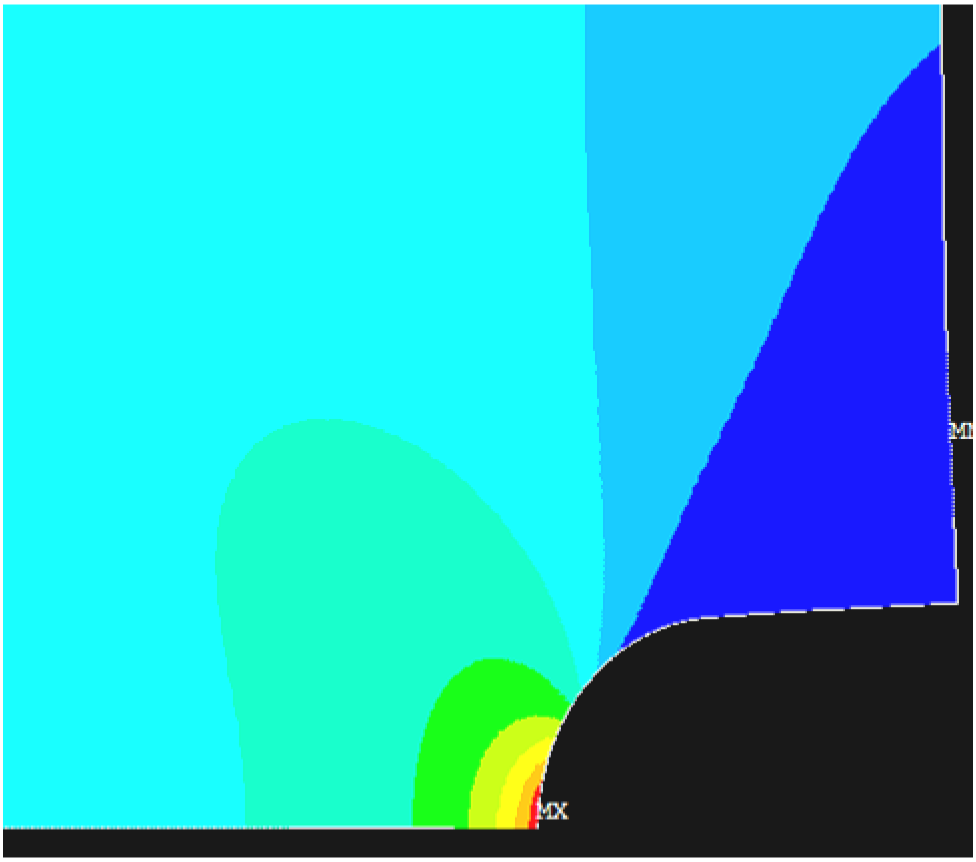


***Fig. 19.*** *Tension's distribution along the notch tip.*

In Table 10 are presented the stress at the notch tip for each density.

| Density [Kg/m$^3$] | $\sigma_t$ [MPa] |
|---|---|
| **100** | *3.19* |
| **145** | *4.39* |
| **300** | *7.13* |
| **708** | *28.31* |

**Table 10** *Value of stress at the notch tip.*

For Necuron 300 and Necuron 651, the stress $\sigma_t$ is calculated excluding the loads that are very different from the others. For example, for Necuron 300, three experimental loads over seven are very higher than the others four so in the first approximation these loads are excluded. The same procedure is made for Necuron 651, where two loads over five are distant in comparison with the others three values. So in Table 11 are reported the new mean load value and the respective stress at the notch tip calculated excluding the upper loads ( loads that are more distant in comparison with the others).

| Density [Kg/m$^3$] | Load [N] | $\sigma_t$ [MPa] |
|---|---|---|
| **300** | *443.6* | *6.06* |
| **708** | *2173.4* | *26.79* |

**Table 11** *Value of the mean load and the stress at the notch tip excluding the upper loads.*

### 3.2.Results and comments

In the paper "***Application of TCD for brittle fracture of notched PUR materials***" of R. Negru, L. Marsavina [7], is applied the TCD method on the same specimens taking that will be study in the next chapters. The TCD method (is a point method) is based on the same theory that is under the base of the SED method.
The Point Method says that the failure occurs when the stress, at an certain distance from the notch tip and along the direction where the normal stress is maximum, reaches a critical value called inherent strength or $\sigma_0$ ; the distance from the notch tip is called critical distance or L/2, where L is called characteristics length. The inherent strength and the characteristic length are a material's parameters so they depend only from the material, the geometry doesn't influence this parameters.
If the behaviour of the material is ideally brittle, the inherent strength is equal to the stress failure $\sigma_{failure}$ . For these foams , the experimental results show that the inherent strength is higher than the failure stress.
Characteristic length L under static loading could be evaluated on the basis of linear elastic fracture mechanics:

$$L = \frac{1}{\pi}\left(\frac{K_{IC}}{\sigma_o}\right)^2 \qquad [7]$$

An alternative procedure applied to determine the material parameters L and $\sigma_0$, requires the experimental determination of strength for two components with different notched geometries.

Then plotting on the same axes the two distributions of maximum normal stress $\sigma_n$, corresponding to the experimentally determined failure loads versus the distance from the notch tip r, the intersection point of the two distributions provides the values of the material parameters L/2 and $\sigma_0$.

In the precedent studies [7], is possible to find the characteristics length and inherent stress for the PUR foams: it's necessary to underline that these two parameters are different in case of pure mode I, pure mode II and mixed mode.

In this situation, the load configuration for all the specimens is pure mode I, so the parameters are:

| Density of PUR foams | 100 | 145 | 300 | 708 |
|---|---|---|---|---|
| $\sigma_{failure}$ as inherent stress [MPa] | *2.17* | *3.12* | *5.56* | *23.14* |
| $\sigma_{failure}$ as $\sigma_t$ [MPa] | *3.19* | *4.39* | *6.06* | *26.79* |

***Table 12.*** *Comparison between experimental stress failure and stress failure determined for TCD method.*

The failure stresses found through the experimental test in the previous paragraphs are not so far from the inherent stress determined experimentally in the paper aforementioned; for the lower densities the stresses differ from 1 MPa ( 30 %) while for the upper densities the differences are lower.

Someone could propose to use the characteristics length and the inherent stress determined in the work aforementioned; the purpose of this paper is to try to define the SED parameters through another way; through this different way it's possible to see that the inherent stress (that is in theory the stress that when this one is reached the failure occurs) determined is very closed to the value determined by R. Negru , L. Marsavina [7].

For this in the following chapter it has been made *the assumption that these stresses represent the parameters through which is possible to calculate the material's parameters*, as the control radius $R_c$ and the critical energy density $W_c$.

As already mentioned, the stress $\sigma_t$ is equivalent to the ultimate tensile strength for notched materials so, in theory, this stress should be less than the ultimate tensile strength for unnotched material: it's possible to see that this is not true. It has been said this because the stress $\sigma_t$ doesn't represent the real ultimate tensile strength but represents a fictitious ultimate tensile strength values that can permit to define the SED parameters.

# CHAPTER 4: Apply of SED method

In the previous chapter it has been determined the stress $\sigma_t$ at the notch tip for each density through experimental tests. From the theory, knowing $\sigma_t$ it's possible to define the value of the critical energy density $W_c$ and the radius of the control volume $R_c$ . The main purpose is to determine, in a first moment, these parameters and after try to apply the SED (using these parameters) on specimens with different geometries made by different densities.
From the literature, it's known that the parameters can be defined as:

$$W_c = \frac{\sigma_t^2}{2E} \qquad [1]$$

$$Rc = \left[\frac{I_1 * K_{1c}^2}{4 * \lambda_1 * (\pi - \alpha) * E * Wc}\right]^{\frac{1}{(2-2\lambda_1)}} \qquad [2]$$

In this case the densities of the specimens under study are:

1. Necuron 651: density 708 Kg/m$^3$
2. Necuron 301 :density 300 Kg/m$^3$
3. Necuron 160: density 145 Kg/m$^3$
4. Necuron 100: density 100 Kg/m$^3$

In particular, the geometries investigated are :

- Plate with symmetric Rounded V-Notch under tensile load of different densities
- Plate with symmetric U-Notch under tensile load of different densities
- Plate with circular hole under tensile load of different densities
- Plate with circular hole with different radii and for one density, under tensile load

In this situation, the load configurations are of pure mode I. As it seen from the chapter one, for the blunt V notch the control volume is centred in the tip of the crack while for the others cases (as rounded V notch, U notch and holed components) the origin of the control volume doesn't correspond with the notch tip. In Fig. 1 is possible to see the various configuration.

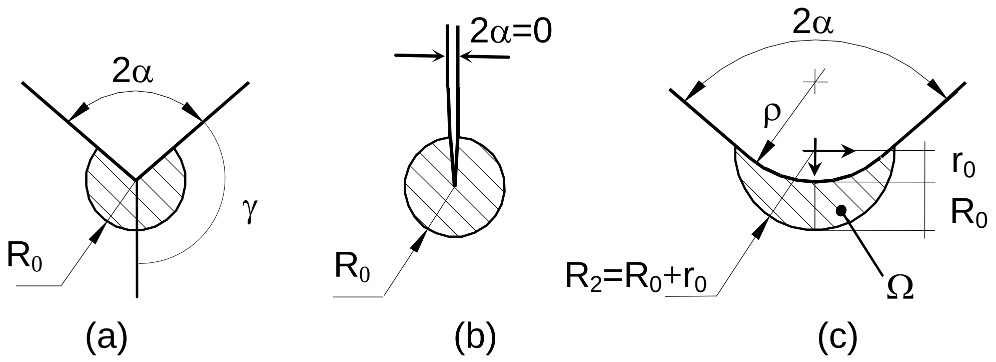


***Fig. 1. .*** *Critical volume (area) for sharp V-notch (a), crack (b) and blunt V-notch (c) under mode I loading.*

For rounded V notch (and U notch, that is the particular case when 2α =0° ) $r_0$ represent the distance between the notch tip and the centre of the control volume; $r_0$ can be defined as:

$$r_0 = \frac{q-1}{q}\rho \qquad [3]$$

Where ρ is the curvature radius of the notch and q is defined as:

$$q = \frac{2\pi - 2\alpha}{\pi} \qquad [4]$$

Knowing the geometry and the material parameter $R_c$ , the radius of the control volume $R_2$ is:

$$R_2 = R_c + r_0 \qquad [5]$$

Previously are exhibit in a few passages all the formulas that will be used in the next paragraphs.

The way to proceed is the following:

1. Show the geometries and the respective experimental fracture loads.
2. Define of the parameters $R_c$ , $W_c$ and $R_2$ , for each density.
3. Construction of the Ansys model and determine the predicted load through the parameters calculated in the precedent step.
4. Show the obtained results.

The idea at the basis of everything is to find the load that determine the $W_c$ calculated with the $\sigma_t$ for each geometries and after to compare with the experimental load and to see the dispersion of the data.

## 4.1.Geometry, dimensions and experimental fracture loads

For each geometry it's calculated the parameter q and $r_0$ . For all the geometries the thickness is equal to 10 mm. In Fig. 2 are showed the specimens geometry.

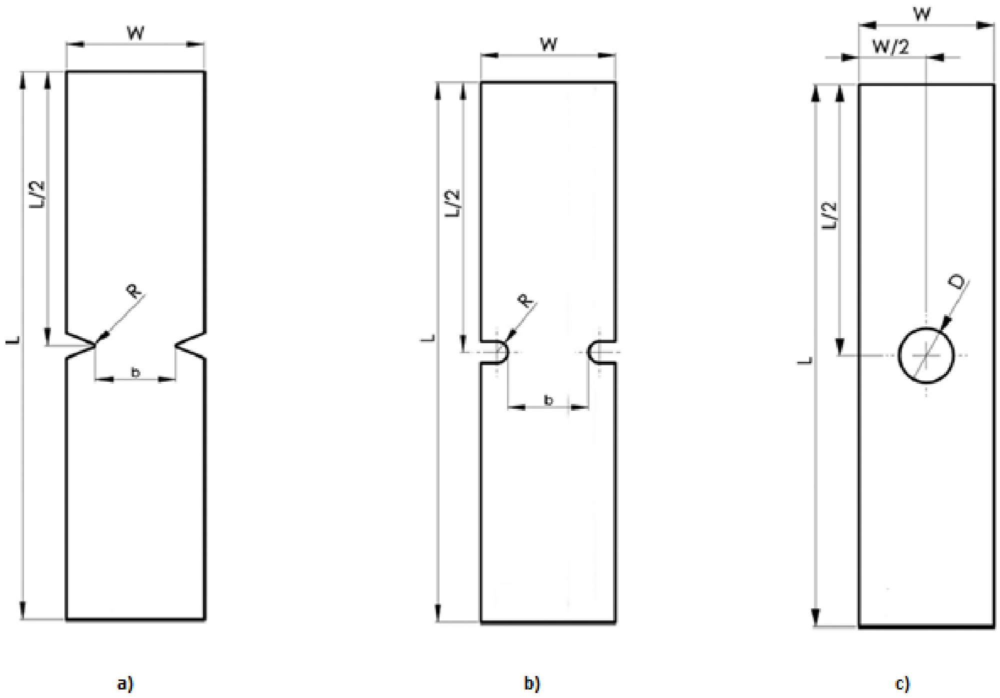


***Fig. 2.*** *Rounded V notch geometry a), U notch geometry b) and holed geometry c).*

**Plate with Rounded V notch**

The geometry is show in the Fig. 2a while the dimensions and the fracture loads are exhibit in the Table 1.

| **Geometrical parameters [mm]** | | | | **Average maximum load [N] for each density** | | | |
|---|---|---|---|---|---|---|---|
| l | W | b | R | 100 | 145 | 300 | 708 |
| 100 | 25 | 15 | 0.25 | *146.39* | *185.92* | *353.74* | *1811.43* |

**Table 1.** *Geometrical parameters and experimental fracture loads.*

The opening angle 2α is equal to 45° so:

$$q = \frac{2\pi - 2\alpha}{2\pi} = 1.75$$

$$r_0 = \frac{q-1}{q}\rho = 0.107 \text{ mm}$$

So the distance between origin of the polar system from the notch tip is 0.107 mm, placed in the same direction of the bisector line of the notch tip.

### Plate with U notch

The geometry is showed in Fig. 2b. The dimensions are:

| Geometrical parameters [mm] | | | | Average maximum load [N] for each density | | | |
|---|---|---|---|---|---|---|---|
| l | W | b | R | 100 | 145 | 300 | 708 |
| 100 | 25 | 15 | 2 | 189.45 | 262.4 | 397.0 | 2109.96 |

***Table 2.*** *Geometrical parameters and experimental fracture loads.*

The opening angle 2α is equal to 0 so:

$$q = \frac{2\pi - 2\alpha}{\pi} = 2$$

$$r_0 = \frac{q-1}{q}\rho = 1.0 \text{ mm}$$

So the distance between the origin of the polar system from the notch tip is 1.0 mm, placed in the same direction of the bisector line of the notch tip.

### Holed plate

The geometry are reported in Fig. 2c; the dimensions are:

| Geometrical parameters [mm] | | | | Average maximum load [N] for each density | | | |
|---|---|---|---|---|---|---|---|
| l | W | b | D | 100 | 145 | 300 | 708 |
| 100 | 25 | - | 10 | 187.89 | 267.31 | 521.5 | 1960.31 |

***Table 3.*** *Geometrical parameters and experimental fracture loads.*

For Necuron 651 it has been made test on holed plate with different hole's diameters. In Table 4 are exhibit all the parameters.

The hole are treated as a U notch, so q remains unchanged and $r_0$ changes with the diameter.

| **Geometrical parameters [mm]** | | | | **Average maximum load [N] for Necuron 651** |
|---|---|---|---|---|
| l | W | b | D | |
| 100 | 25 | - | 10 | *1960.31* |
| 100 | 25 | - | 8 | *2197.27* |
| 100 | 25 | - | 7 | *2290.76* |
| 100 | 25 | - | 6 | *2491.03* |
| 100 | 25 | - | 5 | *2544.66* |
| 100 | 25 | - | 3.5 | *2944.64* |
| 100 | 25 | - | 2.5 | *2961.78* |
| 100 | 25 | - | 1 | *3309.19* |

***Table 4.*** *Geometrical parameters and experimental fracture loads.*

## 4.2.Definition of the SED parameters through $\sigma_t$

The used formulas are the equation (1) and (2); the eq. (2), when the opening angle is equal to 0, the notch stress intensity factor $K_1^V$ can be substituted by the fracture $K_{Ic}$. When the opening angle is equal to 0, it's possible to use the following equivalent formulas:

$$Rc = \frac{(1+v)(5-8v)}{4\pi}\left(\frac{K_{Ic}}{\sigma_t}\right)^2 \qquad [6]$$

$$Rc = \frac{(5-3v)}{4\pi}\left(\frac{K_{Ic}}{\sigma_t}\right)^2 \qquad [7]$$

Where (6) is referred to plane strain condition while (7) is referred to plane stress condition. In all the tests made, the materials show a very brittle behaviour so it has been made the assumption that the material's behaviour can be represented through the plane strain condition. For this reason, it will be used eq. (6) to determine the parameter $R_c$. In Table 5 are reported all the data necessary to define the parameters.

| Density [Kg/m³] | E [MPa] | Kic [MPa*m^0.5] | ν | $\sigma_t$ [MPa] |
|---|---|---|---|---|
| **100** | 30 | 0.087 | 0.285 | 3.19 |
| **145** | 67 | 0.131 | 0.285 | 4.39 |
| **300** | 281 | 0.372 | 0.302 | 7.13 |
| **708** | 1250 | 1.376 | 0.343 | 28.31 |

***Table 5.*** *Properties of the materials*

**Necuron 100**

The stress at the notch tip is equal to 3.19 MPa, so:

$$W_c = 0.169\ [MJ/m^3]$$

$$R_c = 0.2\ [mm]$$

**Necuron 160**

The stress at the notch tip is equal to 4.39 MPa, so:

$$W_c = 0.143\ [MJ/m^3]$$

$$R_c = 0.24\ [mm]$$

**Necuron 300**

For Necuron 300 it has been calculated two different $\sigma_t$ , in two different cases: the first taking in account about all the loads and the second the stress is calculated excluding the higher loads.

In the first case, $\sigma_t$ is equal to 7.13 MPa, so:

$$W_c = 0.09\ [MJ/m^3]$$

$$R_c = 0.73\ [mm]$$

In the second case, $\sigma_t$ is equal to 6.06 MPa, so:

$$W_c = 0.065\ [MJ/m^3]$$

$$R_c = 1.0\ [mm]$$

**Necuron 651**

As for Necuron 300, in this case it has been calculated two $\sigma_t$ .

In the first case, $\sigma_t$ is equal to 28.31 MPa, so:

$$W_c = 0.32\ [MJ/m^3]$$

$$R_c = 0.56\ [mm]$$

While excluding the higher loads, $\sigma_t$ is equal to 26.79 MPa, so:

$$W_c = 0.285\ [MJ/m^3]$$

$$R_c = 0.62\ \ [mm]$$

With these parameters is possible to apply the SED method and to calculate all the parameters to create the Ansys model.

Knowing the $R_c$ is possible to define the radius of the control volume $R_2$ for each geometry, showed in Table 6, 7, 8, 9 (through the parenthesis is indicated the value of $R_2$ in the case that the higher loads are excluded).

| Density [Kg/m$^3$] | $R_c$ [mm] | $r_0$ [mm] | $R_2$ [mm] |
|---|---|---|---|
| **100** | *0.2* | *0.107* | *0.307* |
| **145** | *0.24* | *0.107* | *0.347* |
| **300** | *0.73 (1.0)* | *0.107* | *0.837 (1.107)* |
| **708** | *0.56 (0.62)* | *0.107* | *0.667 (0.727)* |

***Table 6.*** *Radius control Volume rounded V notch geometry.*

| Density [Kg/m$^3$] | $R_c$ [mm] | $r_0$ [mm] | $R_2$ [mm] |
|---|---|---|---|
| **100** | *0.2* | *1.0* | *1.2* |
| **145** | *0.24* | *1.0* | *1.24* |
| **300** | *0.73 (1.0)* | *1.0* | *1.73 (2.0)* |
| **708** | *0.56 (0.62)* | *1.0* | *1.56 (1.62)* |

***Table 7.*** *Radius control Volume U notch geometry.*

| Density [Kg/m$^3$] | $R_c$ [mm] | $r_0$ [mm] | $R_2$ [mm] |
|---|---|---|---|
| **100** | *0.2* | *2.5* | *2.7* |
| **145** | *0.24* | *2.5* | *2.74* |
| **300** | *0.73 (1.0)* | *2.5* | *3.23 (3.5)* |
| **708** | *0.56 (0.62)* | *2.5* | *3.06 (3.12)* |

***Table 8.*** *Radius control Volume holed plate geometry.*

## 4.3.Finite element analysis

For the finite element analysis it has been used Ansys Multiphysics 14.5 software. The analysis is linear elastic and all the geometries are modelled in 2 D . All the geometries present two axis of symmetry so it's possible to model only a quarter of each geometry. For a 2 D model it has been choose the plane element ***PLANE 184***, with 8 nodes. For each geometry has been modelled the control volume through parameters defined in the previous paragraphs.

One of the main advantage of the SED method is that the mesh doesn't play a fundamental role, so the mesh doesn't change the results. Anyway the mesh is more refined inside the control volume. As it said precedent, all the analysis are made under ***plane stress conditions***.

All the loads are applied as a pressure on lines because this configuration's load it's more similar to the reality. To define the pressure is necessary to divide the load for the area of the specimens, that is defined as thickness multiplied the width.

In Fig. 3a and 3b is possible to see the control volume that has radius $R_2$ while in Fig. 3c and 3d is reported the distribution of the first principal tension around the notch tip.

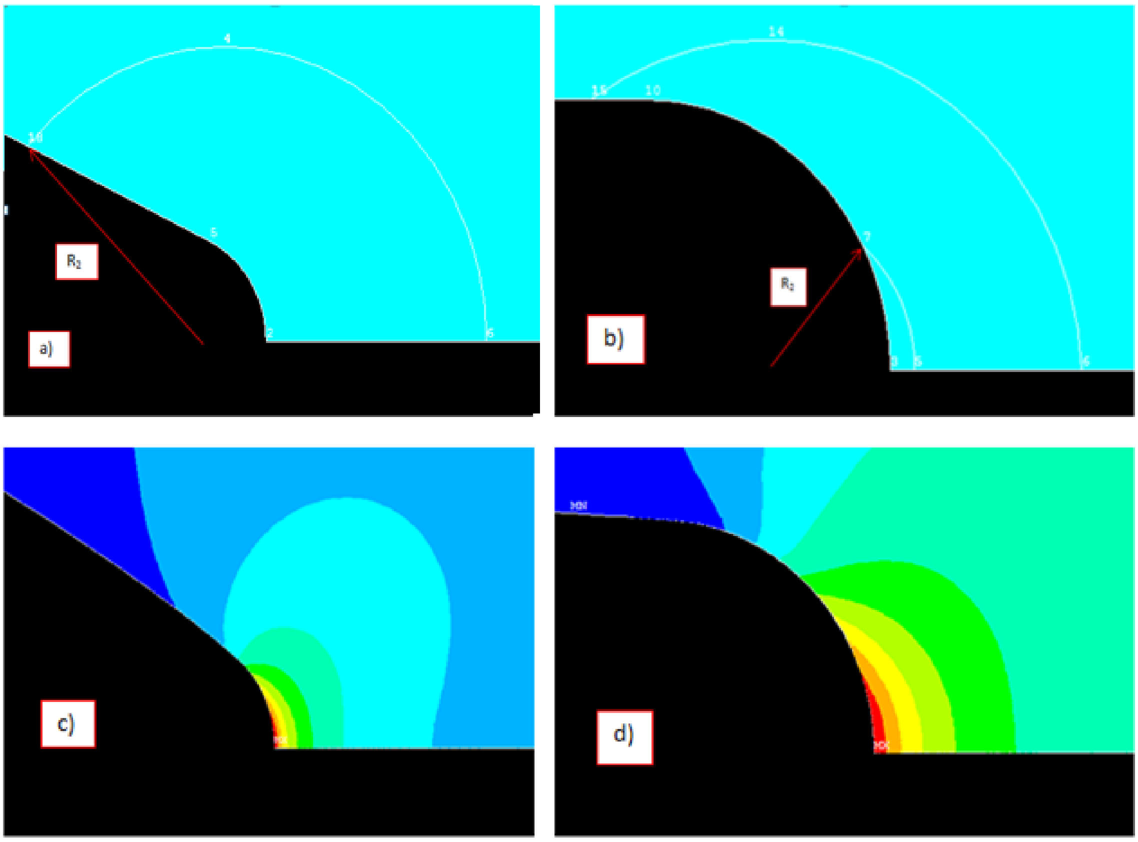


***Fig. 3.*** *The control volume and his radius $R_2$ for rounded V notch a) and U notch b), distribution of the principal tension around the notch tip for rounded V notch c) and for U notch d).*

For each control volume is calculated the strain energy: dividing the strain energy for the volume is possible to define the strain energy density. Ansys allows to calculate these two parameters separately and after an operation of division is possible to determine the density of the strain energy.

All the commands are not reported only to make lighter the reading.

Following are reported the predicted loads defined through the simulations with Ansys.

**Necuron 100**

In Table 9 is showed the predicted loads for all the geometries made in Necuron 100.

| Geometry | $W_c$ [MJ/m$^3$] | $R_c$ [mm] | $F_{experimental}$ [N] | $F_{predicted}$ [N] |
|---|---|---|---|---|
| **V notch** | 0.169 | 0.2 | 146.39 | *147* |
| **U notch** | 0.169 | 0.2 | 189.45 | *210* |
| **D=10** | 0.169 | 0.2 | 187.89 | *228* |

***Table 9.*** *Predicted loads for Necuron 100.*

**Necuron 160**

| Geometry | $W_c$ [MJ/m$^3$] | $R_c$ [mm] | $F_{experimental}$ [N] | $F_{predicted}$ [N] |
|---|---|---|---|---|
| **V notch** | 0.143 | 0.24 | 185.92 | *218* |
| **U notch** | 0.143 | 0.24 | 262.4 | *300* |
| **D=10** | 0.143 | 0.24 | 267 | *321* |

***Table 10.*** *Predicted loads for Necuron 160.*

**Necuron 300**

For Necuron 300 it has calculated the predicted load in the two cases explained in the precedent paragraph.

| Geometry | $W_c$ [MJ/m^3] | $R_c$ [mm] | $F_{experimental}$ [N] | $F_{predicted}$ [N] |
|---|---|---|---|---|
| **V notch** | 0.09 | 0.73 | 353.74 | *550* |
| **U notch** | 0.09 | 0.73 | 397.7 | *610* |
| **D=10** | 0.09 | 0.73 | 521.5 | *612* |

***Table 11.1*** *Predicted load for Necuron 300, case that taking in account the higher stress $\sigma_t$.*

| Geometry | $W_c$ [MJ/m$^3$] | $R_c$ [mm] | $F_{experimental}$ [N] | $F_{predicted}$ [N] |
|---|---|---|---|---|
| **V notch** | 0.065 | 1 | 353.74 | *570* |
| **U notch** | 0.065 | 1 | 397.71 | *600* |
| **D=10** | 0.065 | 1 | 521.5 | *567* |

***Table 11.2*** *Predicted load for Necuron 300, case that taking in account the lower stress $\sigma_t$.*

**Necuron 651**

| Geometry | $W_c$ [MJ/m$^3$] | $R_c$ [mm] | $F_{experimental}$ [N] | $F_{predicted}$ [N] |
|---|---|---|---|---|
| **V notch** | 0.32 | 0.56 | 1811.43 | *2250* |
| **U notch** | 0.32 | 0.56 | 2109.96 | *2400* |
| **D=10** | 0.32 | 0.56 | 1960.31 | *2375* |

***Table 12.1*** *Predicted load for Necuron 651, case that taking in account the higher stress $\sigma_t$.*

| Geometry | $W_c$ [MJ/m$^3$] | $R_c$ [mm] | $F_{experimental}$ [N] | $F_{predicted}$ [N] |
|---|---|---|---|---|
| **V notch** | 0.285 | 0.62 | 1811.43 | *2160* |
| **U notch** | 0.285 | 0.62 | 2109.96 | *2300* |
| **D=10** | 0.285 | 0.62 | 1960.31 | *2300* |

***Table 12.2*** *Predicted load for Necuron 651, case that taking in account the lower stress $\sigma_t$.*

In the following table are showed the holed plates with different diameters.

| Diameter [mm] | $W_c$ [MJ/m$^3$] | $R_c$ [mm] | $F_{experimental}$ [N] | $F_{predicted}$ [N] |
|---|---|---|---|---|
| **10** | 0.32 | 0.56 | 1960.31 | *2350* |
| **8** | 0.32 | 0.56 | 2197.27 | *2650* |
| **7** | 0.32 | 0.56 | 2290.76 | *2800* |
| **6** | 0.32 | 0.56 | 2491.03 | *2970* |
| **5** | 0.32 | 0.56 | 2544.66 | *3200* |
| **3.5** | 0.32 | 0.56 | 2944.64 | *3700* |
| **2.5** | 0.32 | 0.56 | 2961.78 | *4210* |
| **1** | 0.32 | 0.56 | 3309.19 | *5100* |

***Table 13.1*** *Predicted load for holed plates, in the case that taking in account the higher stress $\sigma_t$.*

| Diameter [mm] | $W_c$ [MJ/m$^3$] | $R_c$ [mm] | $F_{experimental}$ [N] | $F_{predicted}$ [N] |
|---|---|---|---|---|
| **10** | 0.285 | 0.62 | 1960.31 | *2300* |
| **8** | 0.285 | 0.62 | 2197.27 | *2600* |
| **7** | 0.285 | 0.62 | 2290.76 | *2740* |
| **6** | 0.285 | 0.62 | 2491.03 | *2870* |
| **5** | 0.285 | 0.62 | 2544.66 | *3070* |
| **3.5** | 0.285 | 0.62 | 2944.64 | *3700* |
| **2.5** | 0.285 | 0.62 | 2961.78 | *4150* |
| **1** | 0.285 | 0.62 | 3309.19 | *5000* |

***Table 13.2*** *Predicted load for holed plates, in the case that taking in account the lower stress* $\sigma_t$.

Following are showed the dispersion between the experimental load and the predicted load; the dispersion is evaluated through the eq. (8). In this case Error means dispersion of the data.

$$Error = \left|\frac{F_{experimental} - F_{predicted}}{F_{experimental}}\right| * 100 \qquad [8]$$

| Geometry | Error [%] |
|---|---|
| **Necuron 100** | |
| **Rounded V notch** | *0.42* |
| **U notch** | *10.85* |
| **Holed plate, D=10** | *21.35* |
| **Necuron 160** | |
| **Rounded V notch** | *17.25* |
| **U notch** | *14.33* |
| **Holed plate, D=10** | *20.22* |
| **Necuron 300** | |
| **Rounded V notch** | *61.14* |
| **U notch** | *34.02* |
| **Holed plate, D=10** | *8.72* |
| **Necuron 651** | |
| **Rounded V notch** | *19.24* |
| **U notch** | *9.01* |
| **Holed plate, D=10** | *17.33* |
| **Holed plate, D=8** | *18.33* |
| **Holed plate, D=7** | *19.61* |
| **Holed plate, D=6** | *15.21* |
| **Holed plate, D=5** | *20.64* |
| **Holed plate, D=3.5** | *25.65* |
| **Holed plate, D=2.5** | *40.12* |
| **Holed plate, D=1** | *51.09* |

***Table 14.*** *Dispersion for the analysed specimens.*

It's possible to notice that the dispersions between the experimental load and the predicted load are less than 20 % and in engineering field represents a good approximation.

For Necuron 300, only for the holed plate the error is less than 15 % while for the other geometries the errors are more than 30 %. In Table 14 are exhibit the errors for Necuron 300 and Necuron 651 in the case that the higher loads are excluded; this because these cases fit better the results.

Necuron 300 has always presented, in all the tests, scattered results and is the only density that presents a wide range about the length of the cells. For this reason it has tried to define a new $R_c$ .

In the Fig. 6. is plotted the parameters $R_c$ versus the density, where it' possible to define a linear relation between the $R_c$ and the density, through a linear interpolation of the data.

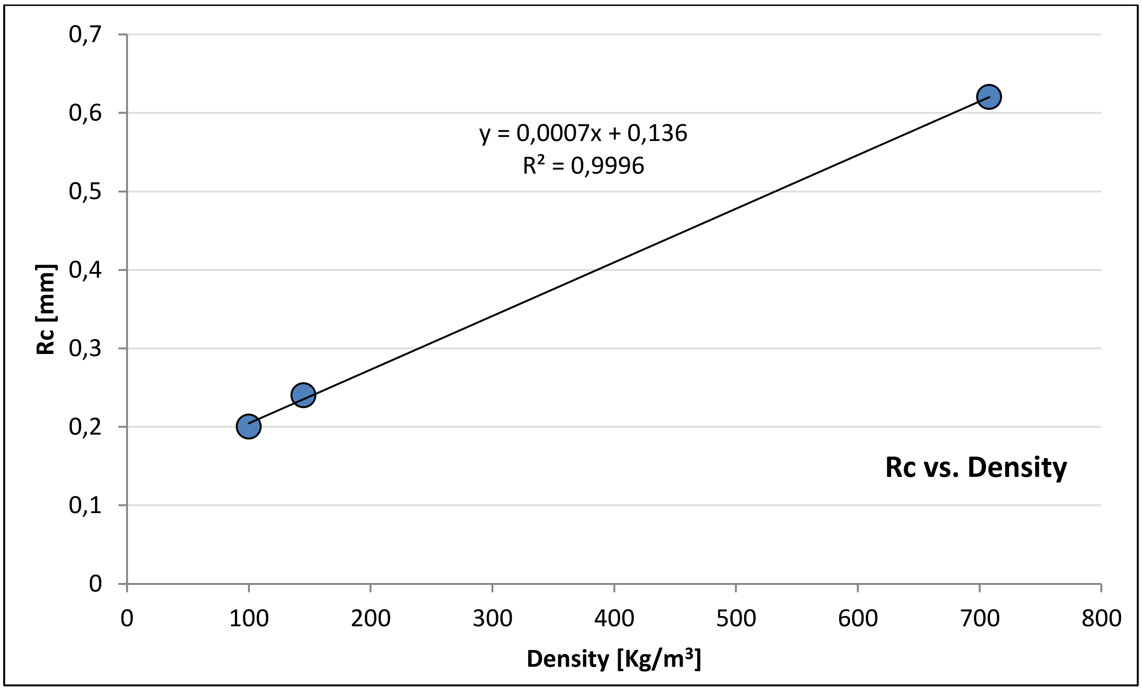


***Fig. 4.*** *Linear interpolation between $R_c$ versus density.*

The linear interpolation is equal to (9):

$$R_c = 0.0007*[Density] + 0.136$$

When the density is equal to 300 the $R_c$ is equal to 0.35 mm.

Using this $R_c$ , with the same critical value of strain energy density, the errors are exhibit in Table 15.

| Geometry | Error [%] |
|---|---|
| Rounded V notch | *4.60* |
| U notch | *12.82* |
| Holed plate, D=10 | *7.96* |

***Table 15.*** *Errors for Necuron 300 using $R_c$ equal to 0.35 mm.*

Using this $R_c$ the predicted loads is very close to the experimental loads, in facts the errors are less than 13 %.

## 4.4.Results

In this paragraph are plotted in graphs the dispersion of the predicted loads in comparison with the experimental loads; the dispersion is evaluated as the ratio between the predicted force and the experimental force.

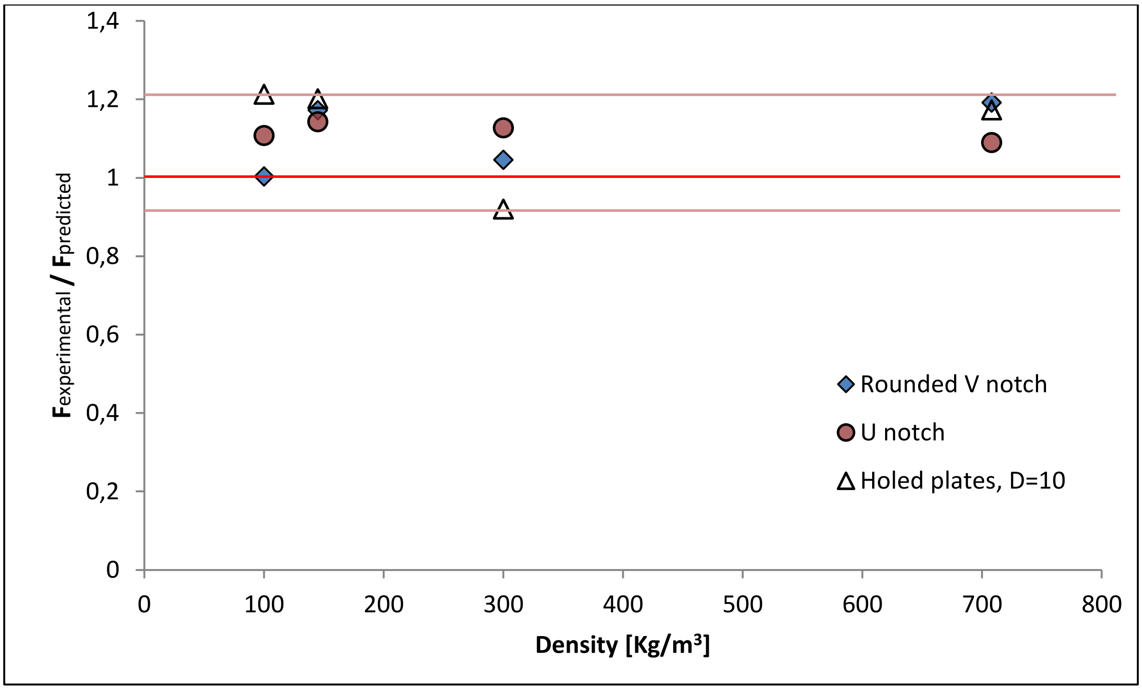


***Graph 1.*** *Dispersion of the results, evaluated through the fracture load, for rounded V notch, U notch and holed plates.*

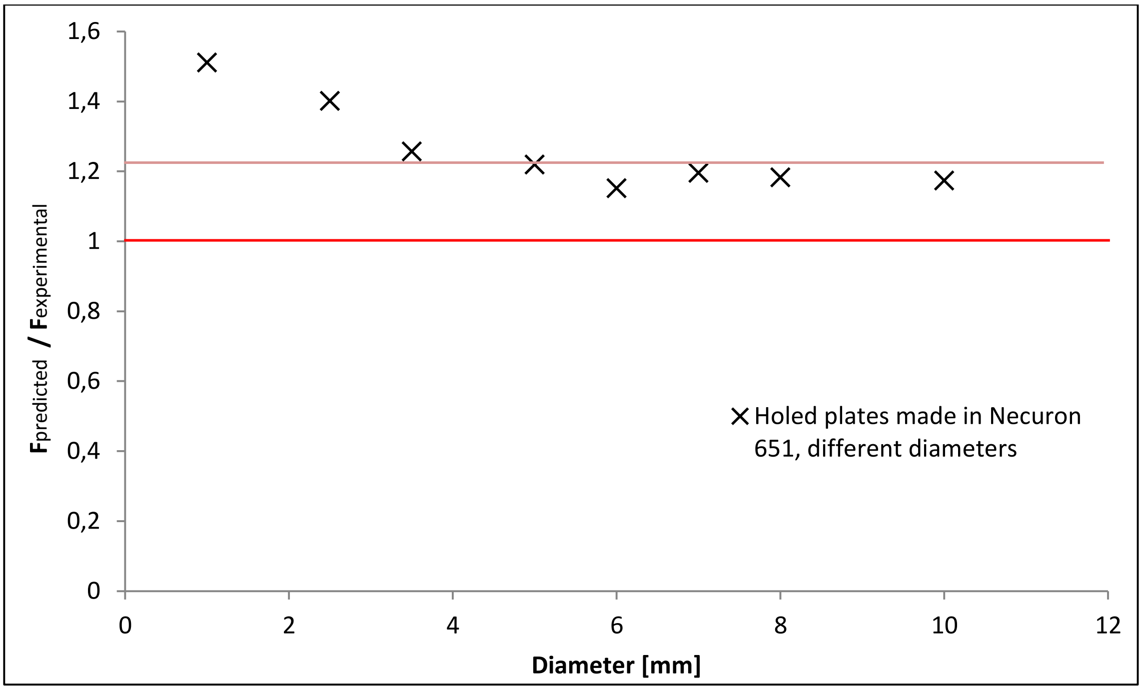


***Graph 2.*** *Dispersion of the results, evaluated through the fracture load, for holed plates with different diameters, made in Necuron 651.*

In literature, for the SED method , the dispersion of the data usually are evaluated on the value of the average strain energy density W found in the specimens compared with critical energy density value through the eq. (9).

$$Dispersion = \sqrt{\frac{\overline{W}}{W_C}} \quad [9]$$

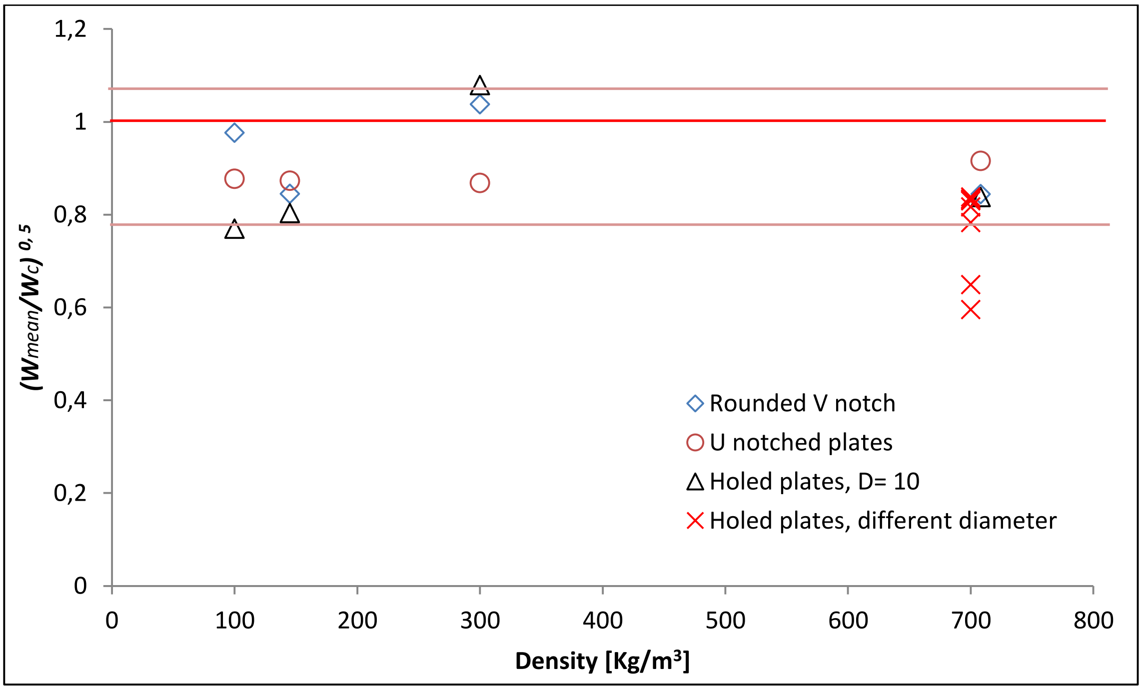


***Graph 3.*** *Dispersion of the results, evaluated through the strain energy density value.*

Excluding the holed plates with the lower diameters ( diameter equal to 2.5 and 1 mm) the scatter band is contained between  + 10 % and – 22 %. It's possible to say that the major dispersion is represented by the holed plates; in fact if has been exclude the holed plates, the scatter band is contained between +10 % and – 15 %. For the holed plates is very important to underline that, in literature, is an assumption to treat as a U notch so it's not proved that the holed geometry has the same control volume centre of the U notch geometry. These approximation seems working because the dispersion is very small: usually, in engineering field, an acceptable scatter band is included between 10 % and 20 %. For the holed plates could be possible to change the centre of the control volume but only with these experimental data is not possible to say if these new centres are good for every holed components or are valid only for these ones. Also, it has to take in account that all the analysis are made under plane strain conditions and this is a common assumption.

# CHAPTER 5: Verify SED method on cracked specimens

In chapter 4 there are defined the SED parameters (that are $R_C$ and $W_C$) that are used to predict the theoretical fracture loads on notched specimens. The following step is to apply the SED method in a cracked specimens, made with different densities, under different load conditions. In the notched specimens taking in account at the beginning, were all under pure load of pure mode I. The specimens, that will be investigate, are the ASCB specimens (Asymmetric Semi Circular Bend) that are showed in Fig. 1.

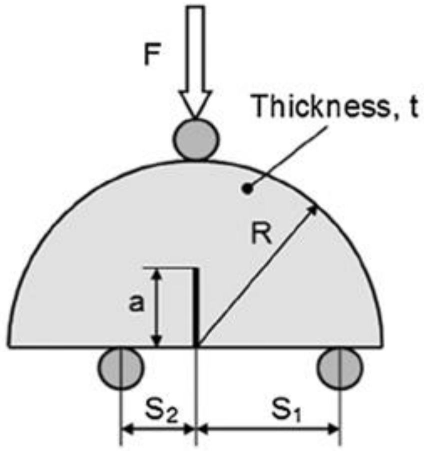


***Fig. 1.*** *Geometry of the ASCB specimen (on the left) and the specimen positioned in the machine (on the right).*

Through these specimens had been possible to define the fracture toughness of the material, in pure mode I and pure mode II. For ASCB is easy to test in different loads configuration, in fact only changing the distance of the support ( $S_2$) changes the configuration of the load.

This ASCB has radius *R* which contains an edge crack of length *a* oriented normal to the specimen edge, loaded with a three point fixture, was proved to give a wide range of mixed modes from pure mode I ($S_2$=$S_1$) to pure mode II ($S_2 \neq S_1$), only by changing the position of one support.

It's necessary to say that usually in literature for mode II and for the mixed mode, it has been used the $R_c$ and $W_c$ derived from pure mode I; this is a common assumption and is still an open problem.

In the crack case, the control volume is centred at the crack tip and the control volume is not subjected to a rotation when the configuration load change from mode I to mode II, as seen in Fig. 2.

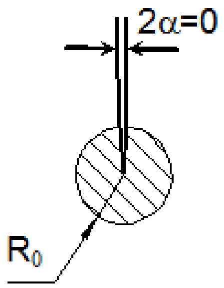


***Fig. 2.*** *Control volume in the crack case.*

In Fig. 2. $R_0$ corresponds to the $R_c$ .

An important parameter is $M_e$ (mixed parameter or multiaxial parameter) that quantify the mode that are acting on the specimens. This parameter is define through eq. (1).

$$M_e = \frac{2}{\pi} \tan^{-1} \frac{|K_I|}{|K_{II}|} \qquad [1]$$

When $M_e$ is equal to 1, the load configuration is pure mode I, when is equal to 0 the load configuration is pure mode II and when the value is situated between 0 and 1 the load configuration is the mixed mode.

For the crack case, an useful expression of the energy density is represented by eq. (2).

$$W = \frac{e1}{E} \frac{KIc^2}{Rc^{2(1-\lambda 1)}} + \frac{e2}{E} \frac{KIIc^2}{Rc^{2(1-\lambda 1)}} \qquad [2]$$

For the ASCB geometry it has determined a formula to know the stress intensity factor in each case, from pure mode I to pure mode II; so for each load configuration is possible to determine the energy in control volume that has radius equal to $R_c$.

The approach is the same followed in the previous chapter, so:

- Definition of the investigated geometry and experimental results.
- Construction of the model with Ansys.
- Calculation of the predicted loads only for mode I and comparison with the experimental results.

The following step is to apply the SED method for the case of mixed mode and pure mode II. The procedure followed in this step it has treated successively.

The specimen analysed is the ASCB (Asymmetric semi-circular bend) of 5 different densities:

1. Necuron 1020: density 1218 kg/m$^3$
2. Necuron 651: density 708 kg/m$^3$
3. Necuron 301 :density 300 kg/m$^3$

4. Necuron 160: density 145 kg/m$^3$

5. Necuron 100: density 100 kg/m$^3$

## 5.1.Geometry and experimental results

The geometry is presented in Fig. 1. In the following tables are exhibit the experimental results (Table 1,2,3,4,5).

In this case: $R$=40, $a$=20 mm, $t$=10 mm, $S_1$=30 mm, $S_2$ =30 mm for pure mode I and 2.66 mm for pure mode II (between these two values there is the mixed mode).

| $S_1$ [mm] | $S_2$ [mm] | $F_{max}$ [N] | $K_I$ [MPa*m$^{0,5}$] | $K_{II}$ [MPa*m$^{0,5}$] | $M_e$ |
|---|---|---|---|---|---|
| 30 | 30 | *1586.7* | *2.860* | *0.000* | *1* |
| 30 | 12 | *2857.5* | *2.500* | *0.687* | *0.83* |
| 30 | 8 | *4056.7* | *2.207* | *1.351* | *0.651* |
| 30 | 6 | *4530.0* | *1.622* | *1.765* | *0.472* |
| 30 | 4 | *4458.0* | *0.677* | *2.022* | *0.206* |
| 30 | 2.66 | *4839.7* | *0.015* | *2.424* | *0.004* |

***Table 1.*** *Experimental data for Necuron 1020.*

| $S_1$ [mm] | $S_2$ [mm] | $F_{max}$ [N] | $K_I$ [MPa*m$^{0,5}$] | $K_{II}$ [MPa*m$^{0,5}$] | $M_e$ |
|---|---|---|---|---|---|
| 30 | 30 | *704.3* | *1.253* | *0.000* | *1* |
| 30 | 12 | *1340.0* | *1.183* | *0.322* | *0.83* |
| 30 | 8 | *1622.5* | *0.899* | *0.542* | *0.651* |
| 30 | 6 | *1910.0* | *0.670* | *0.747* | *0.472* |
| 30 | 4 | *2133.3* | *0.333* | *0.966* | *0.206* |
| 30 | 2.66 | *2130.0* | *0.011* | *1.073* | *0.004* |

***Table 2.*** *Experimental data for Necuron 651.*

| $S_1$ [mm] | $S_2$ [mm] | $F_{max}$ [N] | $K_I$ [MPa*m$^{0,5}$] | $K_{II}$ [MPa*m$^{0,5}$] | $M_e$ |
|---|---|---|---|---|---|
| 30 | 30 | 190 | *0.372* | *0* | 1 |
| 30 | 12 | 397.25 | *0.363* | *0.098* | 0.83 |
| 30 | 8 | 535.5 | *0.307* | *0.185* | 0.651 |
| 30 | 6 | 645 | *0.243* | *0.262* | 0.472 |
| 30 | 4 | 601.75 | *0.0973* | *0.284* | 0.206 |
| 30 | 2.66 | 712.3 | *0.004* | *0.374* | 0.004 |

***Table 3.*** *Experimental data for Necuron 300.*

| $S_1$ [mm] | $S_2$ [mm] | $F_{max}$ [N] | $K_I$ [MPa*m$^{0,5}$] | $K_{II}$ [MPa*m$^{0,5}$] | $M_e$ |
|---|---|---|---|---|---|
| 30 | 30 | *67.8* | *0.131* | *0* | 1 |
| 30 | 12 | *133.5* | *0.122* | *0.033* | 0.83 |
| 30 | 8 | *152.25* | *0.087* | *0.052* | 0.651 |
| 30 | 6 | *158.0* | *0.059* | *0.064* | 0.472 |
| 30 | 4 | *151.25* | *0.0244* | *0.071* | 0.206 |
| 30 | 2.66 | *148.67* | *0.001* | *0.078* | 0.004 |

***Table 4.*** *Experimental data for Necuron 160.*

| $S_1$ [mm] | $S_2$ [mm] | $F_{max}$ [N] | $K_I$ [MPa*m$^{0,5}$] | $K_{II}$ [MPa*m$^{0,5}$] | $M_e$ |
|---|---|---|---|---|---|
| 30 | 30 | *43.8* | *0.087* | *0* | 1 |
| 30 | 12 | *88.55* | *0.08* | *0.021* | 0.83 |
| 30 | 8 | *91.47* | *0.052* | *0.031* | 0.651 |
| 30 | 6 | *102.55* | *0.038* | *0.041* | 0.472 |
| 30 | 4 | *97.3* | *0.015* | *0.045* | 0.206 |
| 30 | 2.66 | *92.4* | *0.001* | *0.049* | 0.004 |

***Table 5.*** *Experimental data for Necuron 100.*

Following are reported some images about the experimental test on ASCB specimens; Fig. 3. Shows the crack's path with the changing of the support's distance.


***Fig. 3.*** *Crack paths for different position of $S_2$ support; a) $S_2$ = 30 mm (pure mode I), b)$S_2$ =12 mm, c) $S_2$ =2.66 mm (pure mode II).*

### 5.2.Finite element analysis

The finite element model has been generated through Ansys, a 2 D linear-elastic model has been created. There are not symmetry axes so it has to create the entire geometry. As for the precedent specimens, all the analysis are made under plane strain conditions. It's used an element plane to define the model, ***PLANE 184*** with 8 nodes Around the crack tip is defined a circular area with radius equal to $R_C$, and this area represents the control volume, Fig. 4 and 5.

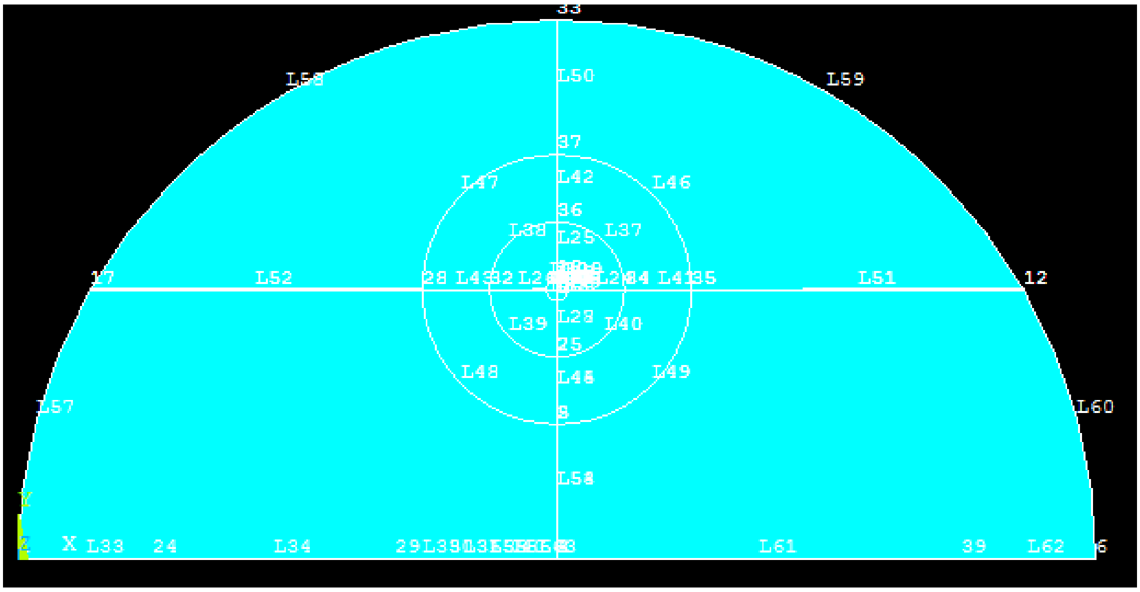


***Fig. 4.*** *Geometry modelled and control volume with centre in the crack tip.*

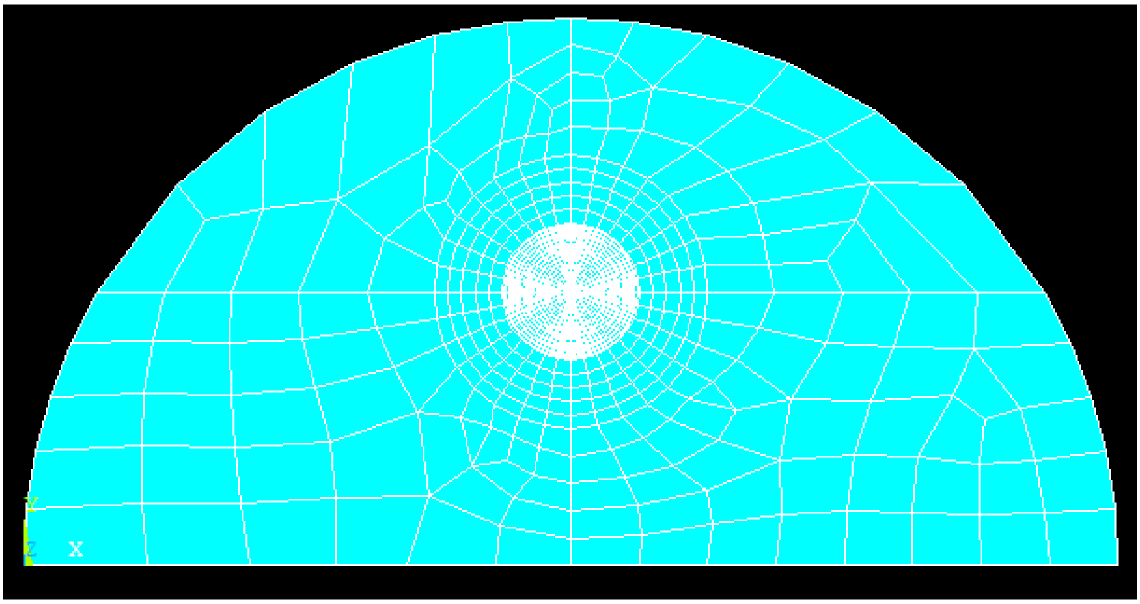


***Fig. 5.*** *Refined mesh in the control volume.*

During the test the model is not perfectly stable in the support but it has the possibility to do small translation so one support ($S_1$) has fixed all the degree of freedom while the other ($S_2$) has fixed only the vertical translation ($U_Y$).

To model the control volume, it has used the $R_c$ determined in the previous chapters; for ASCB specimens are available the experimental data for Necuron 1020. For Necuron 1020 is not determined the stress $\sigma_t$ through experimental test but the characteristics curve of the material is very similar to a characteristics curve of a ideally brittle material. So it has been the assumption that the material is ideally brittle and it's possible to use the ultimate tensile strength to determine the SED parameters.

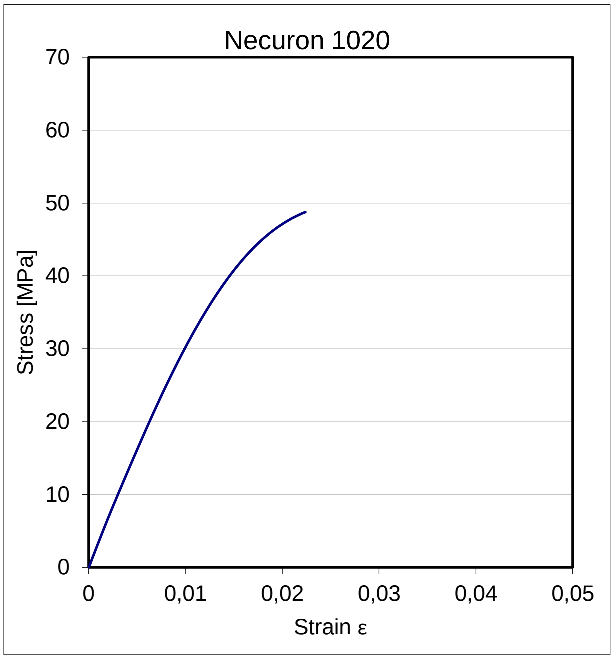


***Fig. 6.*** *Characteristics curve for Necuron 1020.*

The $\sigma_{uts}$ is equal to 49.75 MPa, so the material parameters are:

$$Wc = \frac{\sigma u^2}{2E} = 0.137\ MJ/m^3$$

$$Rc = \frac{(1+v)(5-8v)}{4\pi}\left(\frac{K_{Ic}}{\sigma_{uts}}\right)^2 = 0.80\ \text{mm}$$

### 5.2.1Results for pure mode I

As for the notched specimens, for the cracked case it has determined the predicted loads that can reach the critical value $W_c$ in the control volume; in Table 6 are showed the predicted loads for ASCB specimens under pure mode I.

| Density | $F_{experimental}$ | $F_{predicted}$ | $R_c$ |
|---|---|---|---|

| [Kg/m³] | [N] | [N] | [mm] |
|---|---|---|---|
| **100** | 43.8 | *42* | 0.2 |
| **145** | 67.8 | *65* | 0.24 |
| **300** | 190 | *200* | 1.0 |
| **708** | 704.3 | *670* | 0.62 |
| **1218** | 1586.7 | *1550* | 0.8 |

***Table 6.*** *Experimental loads for ASCB specimens in pure mode I.*

For Necuron 300 it has used the $R_c$ defined through the interpolation; using the $R_c$ equal to 1 mm the predicted load is equal to 200 N. Following are reported dispersion of the predicted loads in comparison with the experimental load.

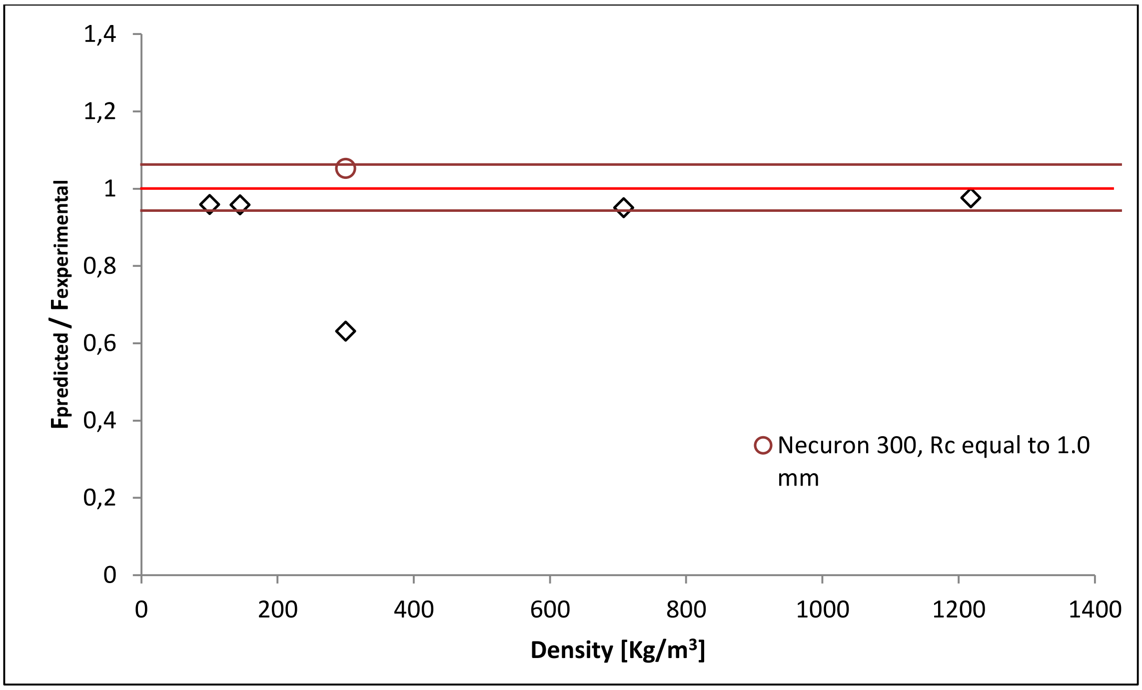


***Graph 1.*** *Dispersion of the data with Rc=1 mm for Necuron 300.*

The scatter band is contained between + 6 % and – 7 %; in pure mode I, the parameters $R_c$ and $W_c$ used works, in fact the predicted loads are very near to the experimental loads. If it has used $R_c$ equal to 0.35 mm for Necuron 300, the predicted fracture load has a dispersion more than 35 %, so for the cracked specimens it's not reasonable to use the interpolated $R_c$ .

From the beginning it's clear that Necuron 300 presents a different behaviour, is a "special" density. For the following analysis, for Necuron 300, it will be used the $R_c$ equal to 1.0 mm.

### 5.3. Prediction of fracture loads under mode II and mixed mode I+II

Usually, in the literature, it has made the assumption that in mixed mode and in pure mode II the parameters remain constant and doesn't change. So the first approach is to determine the predicted loads using the parameters for mode I; for Necuron 300 it has used $R_c$ equal to 1.0 mm. Following are exhibit the obtained results.

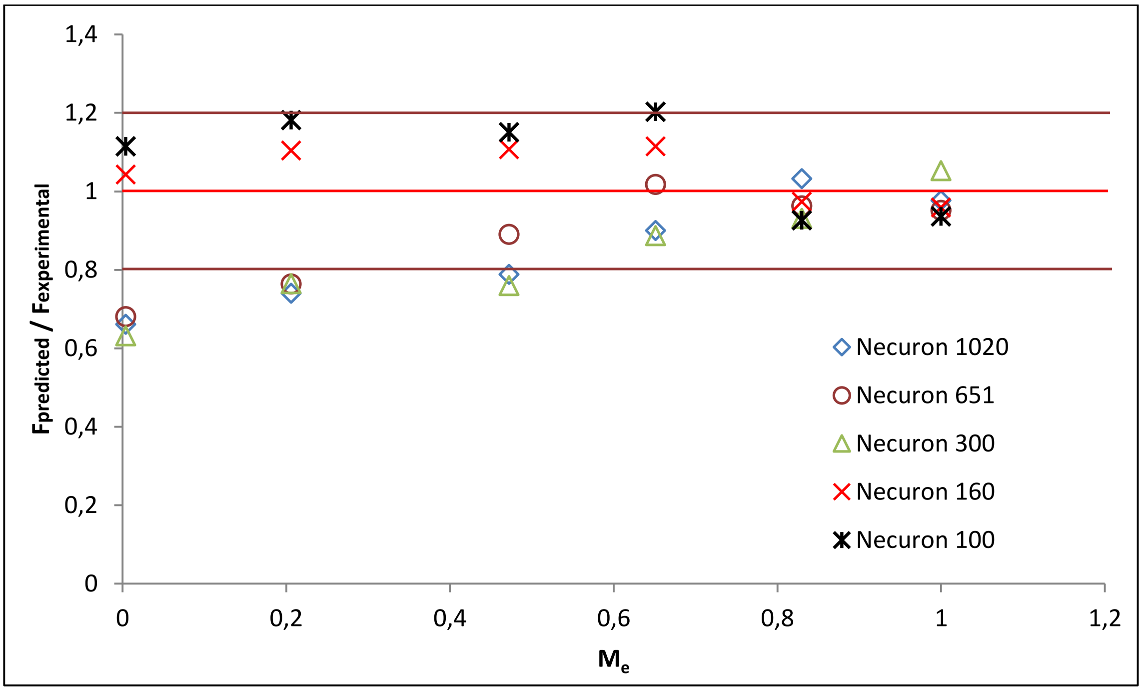


***Graph 2.*** *Dispersion of the data using Wc and Rc from pure mode I.*

From the graph is possible to see that for highest densities the dispersion are more or less near the 30 % while for the lowest densities the dispersion results contained between – 10 % and + 20%.

It has noticed that for the highest densities the $W_c$ calculate in pure mode II is higher than mode I, and this is what usually happen to the materials, but for the lowest densities ( Necuron 160 and 100) the theoretical energy density in pure mode II is lower in comparison with the energy density in the case of pure mode I. For the lower densities the porosity change the behaviour of the materials so is possible that the energy required to reach the failure in mode II is less than the energy in mode I.

When $M_e$ is near to 0 (to pure mode II), the predicted loads for the highest densities is far from the experimental fracture loads. Following are showed an approach that permit to decrease the scatter band.

### 5.3.1.Personal approach for mixed mode and mode II

In the paper of R. Negru, L. Marsavina, "*Application of TCD for brittle fracture of notched PUR materials*", the authors determined different inherent stresses and characteristic length for mixed mode and pure mode II. In this case, the stresses defined through the experimental tests referred only for mode I: for mode II is not easy to define a geometry that can permit to quantify the stresses in mode II. In all the analysis it has been notice that the value of the energy density changes from mode I to mode II; so it has tried to take in account of this one starting from eq. (2).

Eq. (2) represents the expression of the energy density in the case of a crack: knowing $R_c$ is possible to calculate the energy density. The hypothesis made is that the control volume remains the same while changes the strain energy density critical value: this means that $R_c$ is constant.

Knowing $R_c$ and the stress intensity factor $K_{Ic}$ is possible to determine the new value of the strain energy density. In Table 7. is showed the values of the strain energy density dependent from $M_e$ .

| | $M_e$ | | | | | | |
|---|---|---|---|---|---|---|---|
| **Density [Kg/m³]** | **1** | **0.83** | **0.651** | **0.472** | **0.206** | **0.004** | **$W_c$ [MJ/m³]** |
| **1020** | *0.37* | *0.334* | *0.44* | *0.503* | *0.528* | *0.73* | |
| **651** | *0.285* | *0.287* | *0.268* | *0.323* | *0.429* | *0.5* | |
| **300** | *0.065* | *0.074* | *0.086* | *0.111* | *0.102* | *0.169* | |
| **160** | *0.143* | *0.151* | *0.123* | *0.117* | *0.112* | *0.129* | |
| **100** | *0.169* | *0.173* | *0.117* | *0.129* | *0.12* | *0.137* | |

***Table 7.*** *Values of the critical strain energy density vary Me.*

Following are showed the dispersion of the data using these new values of critical strain energy density.

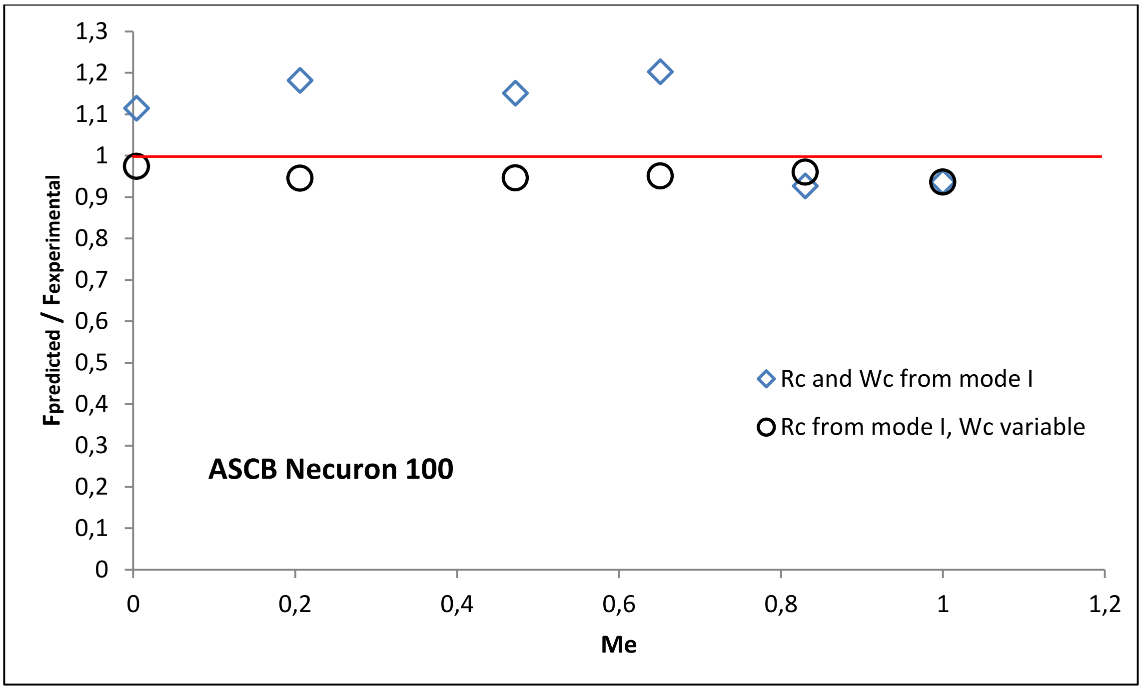


***Graph 3.*** *Dispersion of the data for Necuron 100.*

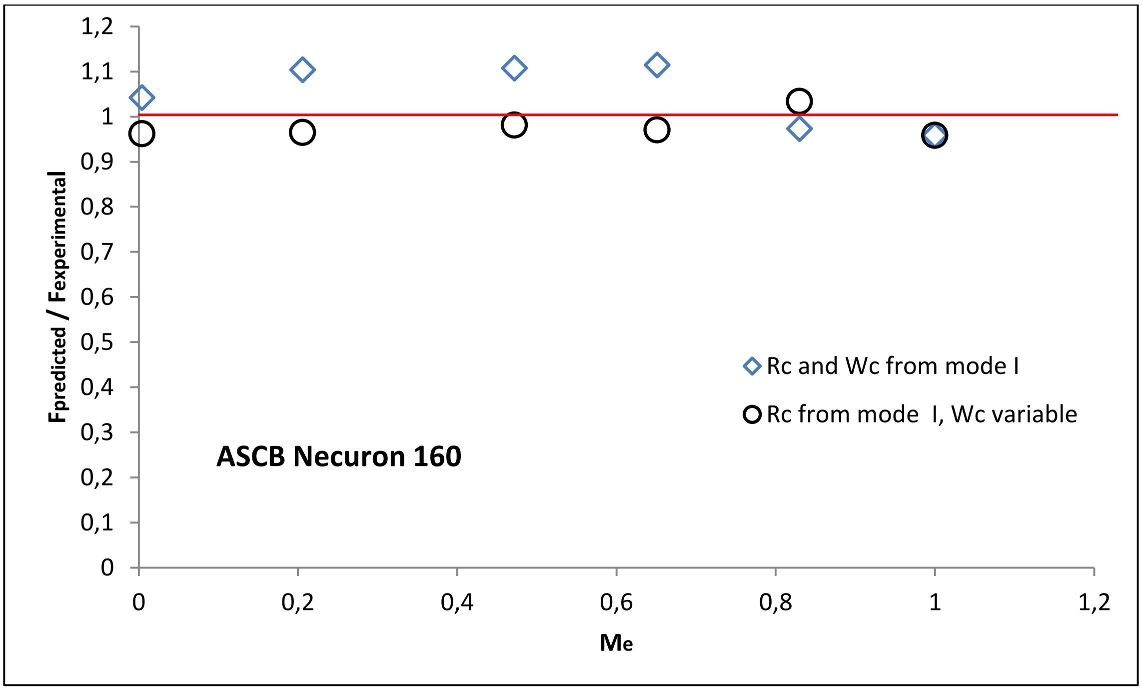


***Graph 4.*** *Dispersion of the data for Necuron 160.*

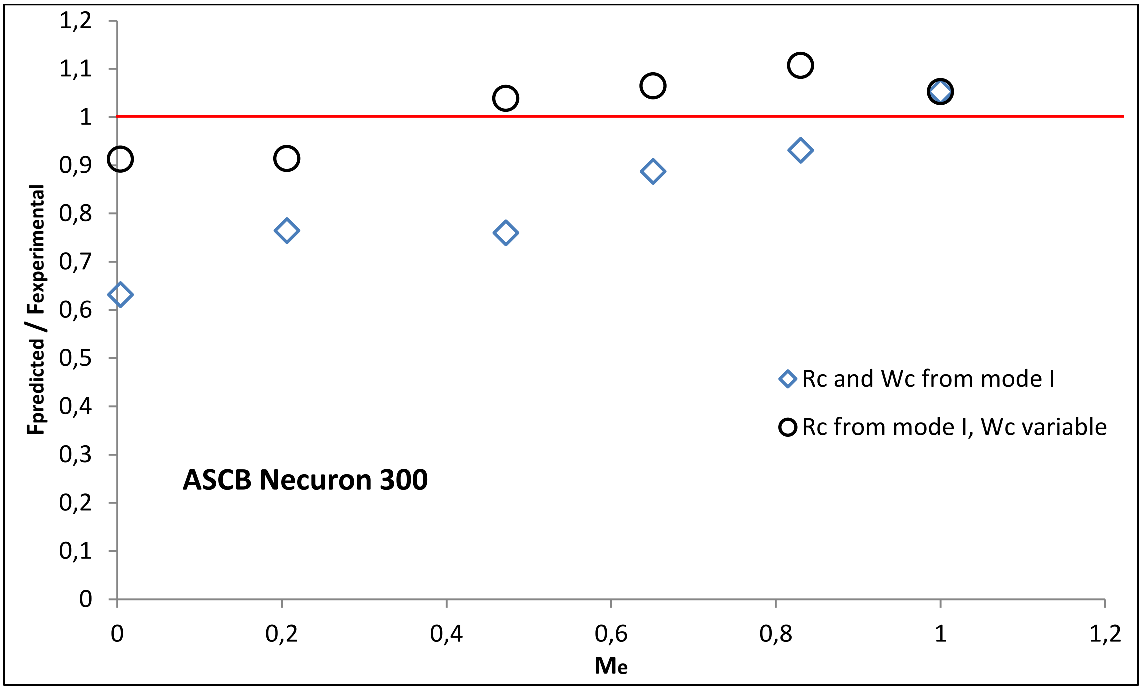


***Graph 5.*** *Dispersion of the data for Necuron 300.*

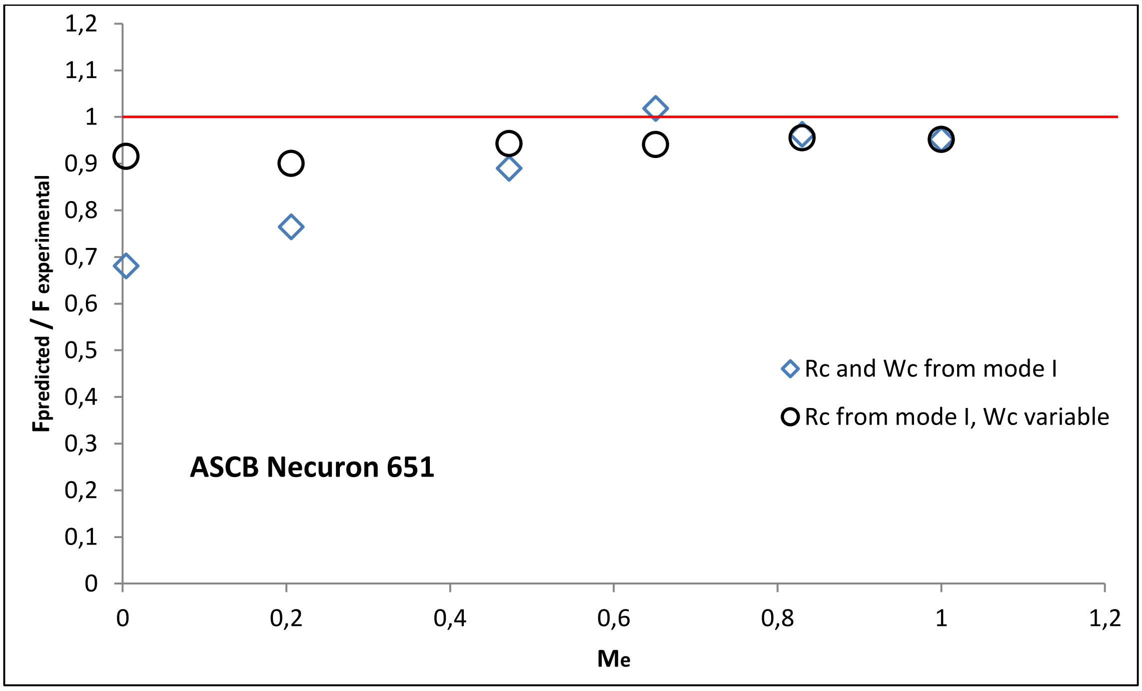


***Graph 6.*** *Dispersion of the data for Necuron 651.*

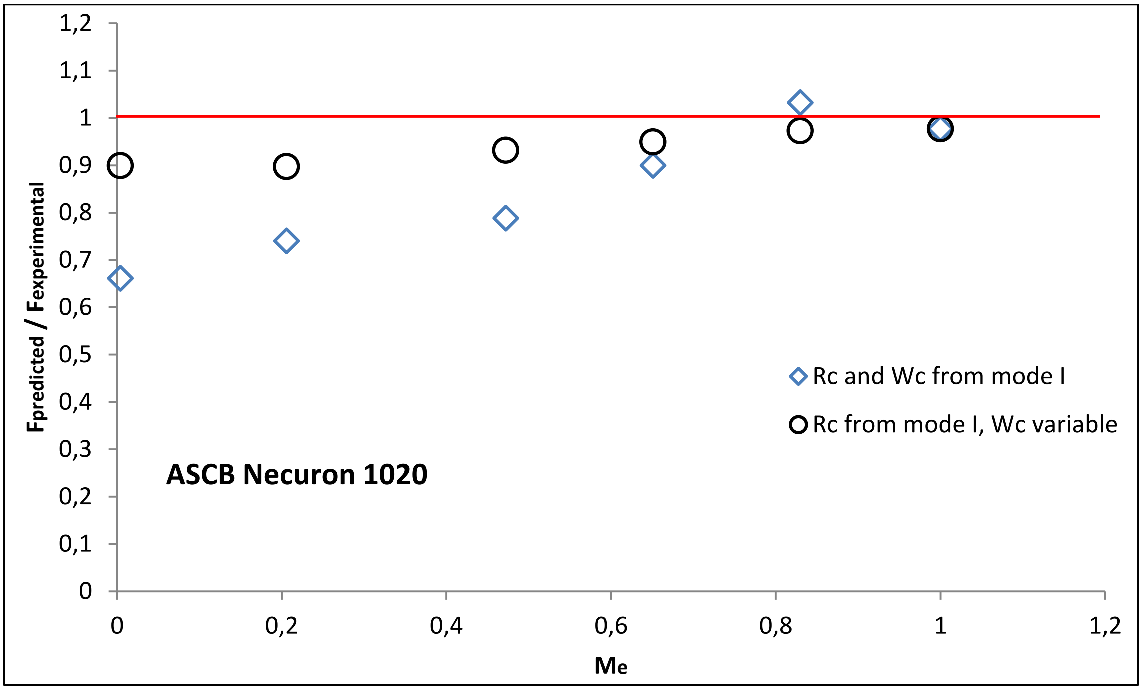


***Graph 7.*** *Dispersion of the data for Necuron 1020.*

## 5.4.Results

Graph 3,4,5,6,7 show the dispersion in the case that $R_c$ and $W_c$ are constant and the case that $R_c$ is constant and $W_c$ is variable. Is possible to see that the dispersion in the case that $W_c$ changes is very low and the scatter band is contained between + 10 % and -10 %. The following graph represents the range of the scatter band; the dispersion is evaluated through the strain energy density, as usually has made in literature (Graph 8).

As it seen, the scatter band is contained between + 10 % and – 10 %, a good engineering prediction.

The idea that the control volume remains constant and the critical energy density changes, gives a good results; it's possible to notice from eq. (2) that W depends from control radius $R_c$ and the stress intensity factor. The control radius derives from pure mode I and it's constant while the stress intensity factor could be defined through an experimental expressions, show in chapter 2.

It's important to underline that the hypothesis about the constance of the control volume is a personal assumption. The best way to proceed is to test a notched specimen with bland curvature radius under pure mode II and define the stress at the notch tip; through this one is possible to calculate a new parameters ($R_c$ and $W_c$ ) in pure mode II.

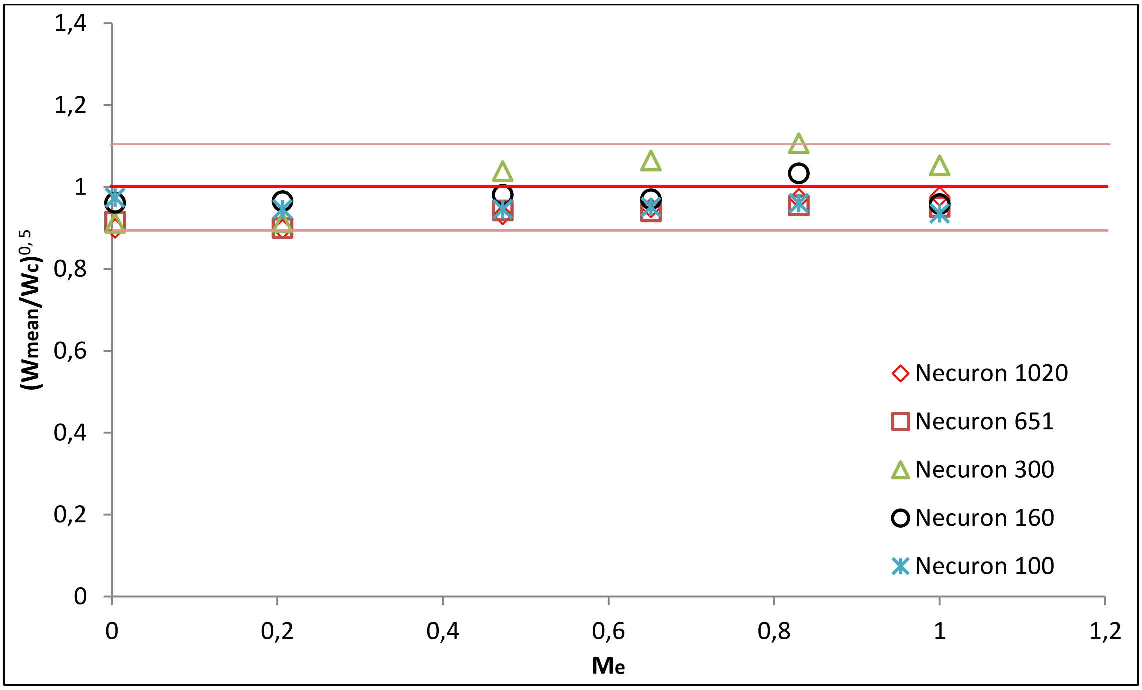


***Graph 8.*** *Dispersion of the data for all densities, from pure mode I case to pure mode II case.*

# CHAPTER 6: Holed specimens under compression loads

The main goal in this chapter is to analyse a holed specimen under compression load: the difference in comparison with the other cases is  that these specimens shows a plasticity zone near the notch tips, but these plasticity zones are not where the cracks born and grow, as it seen in Fig. 1.

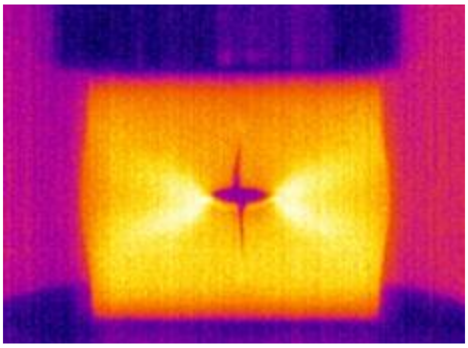

***Fig. 1.*** *Thermographic image of the holed specimen: the lighter zone represent the plasticity zone.*

The main purpose is to apply the SED method and see if its works or not, and to discover if the presence of the plasticity could influence the results or not.
The first step is to apply the SED method through a linear-elastic analysis; before to see the followed procedure, is important to show the tested geometries and the experimental obtained results.

## 6.1.Experimental tips

Polyurethane (PUR) materials of three different densities (100, 145 and 300 kg/m$^3$) manufactured by Necumer GmbH, Germany under commercial designation Necuron (100, 160 and 301) were investigated. Microscopic investigations of these materials show a closed cell structure.
Square specimens (*W* = 80 mm) having a thickness *b* of 25 mm with central hole of different diameters (*D* = 16, 28 and 40 mm), were used, figure 2. One face of the specimens was sprayed with matt black paint in order to have a constant emissivity for thermographic measurements.
The experimental tests were performed using a universal testing machine LBG 100 kN on displacement control (v=2 mm/min) and at room temperature, figure 3.

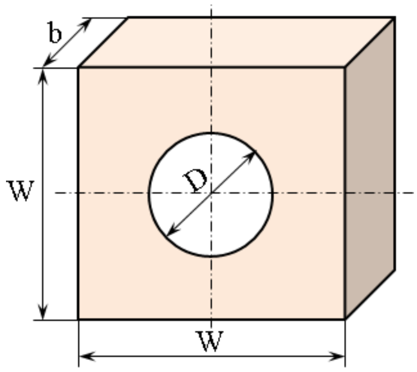


***Fig. 2.*** *Geometry of the holed specimen.*

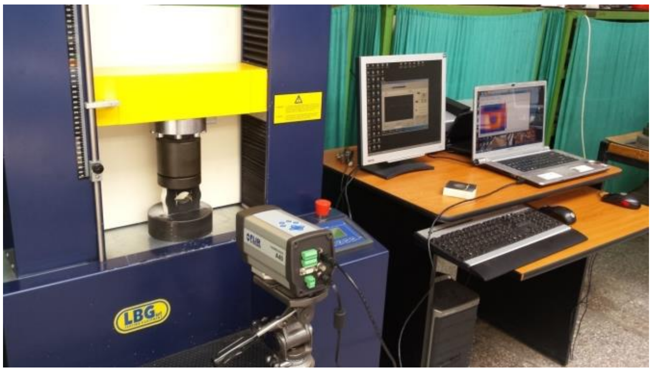

***Fig. 3.*** *Experimental set-up.*

In Table 1 are showed the geometries analysed.

| Density [Kg/m$^3$] | W [mm] | b [mm] | D [mm] |
|---|---|---|---|
| **100** | *80* | *25* | *16, 28 ,40* |
| **145** | *80* | *25* | *16, 28, 40* |
| **300** | *80* | *25* | *16, 28, 40* |

***Table 1.*** *Dimensions of the holed specimens investigated.*

Typical load - displacement curves for the three foam densities are shown in figure 4.a for 16 mm hole diameter. An increase of supported load with increase of density was observed. A drop of load occurs after the plateau stress is reached, at this point the ultimate tensile stress is reached on the hole upper and bottom edges, where tensile occurs and a crack initiates. The load carrying capacity of holed foams decreases with increasing the hole diameter, figure 4.b plotting results for foam of 100 kg/m$^3$ density.

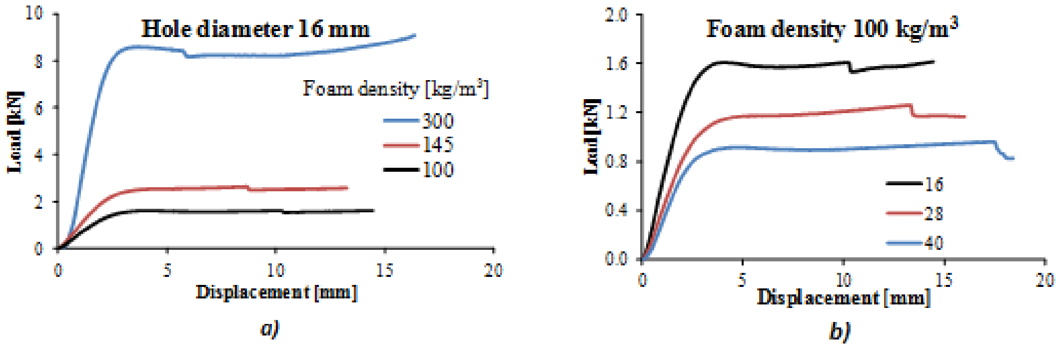


***Fig. 4.*** *Influence of the density (a) and influence of the hole diameter (b).*

Figure 5 presents the ratio between the maximum net stress of notched specimen $\sigma_{max}$ and the ultimate tensile strength of the foam $\sigma_{UTS}$ versus ratio between hole diameter D and specimen width W. For all three investigated foams a notch insensitive response in compression was observed, which could be explained by the ability of foams to crush at a constant plateau stress $\sigma_{plateau}$.

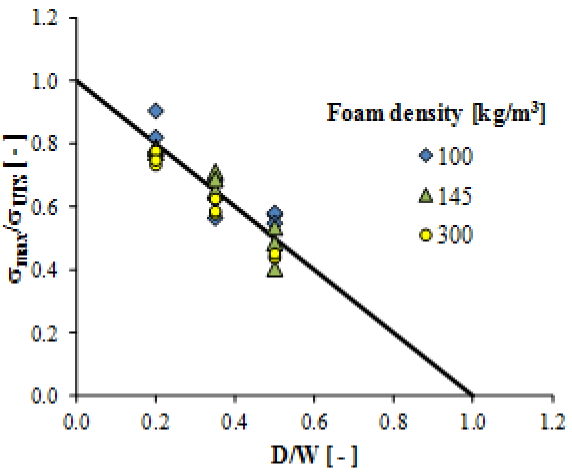


***Figure 5.*** *The effect of hole diameter on the compressive strength of PUR foams blocks with central holes.*

Thermography was used in order to identify the damage mechanism. A FLIR A40M infrared camera was used to measure emitted infrared radiation from the specimen which increases with plastic deformations occurred in the foam specimens due to loading. For example in Fig. 6. are presented different stages of temperature distribution, corresponding to different load stages (displacements 0, 4.2, 8.5, 10.5 and 11.7 mm), from the compression test of foam density of 145 kg/m$^3$, with a central hole of 16 mm. After a short linear elastic part, the temperature starts to increase in the vicinity of the hole due to plastic deformations (figure 6. b, c), than a crack initiates and propagates from the top and bottom surfaces of the hole (Fig. 6. d, e). The increase of temperature could be also seen plotting the temperature variations together with load-displacement curve, figure 7.

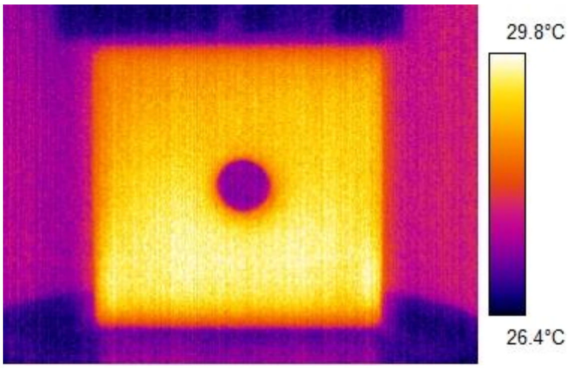

a) Initial stage - deformation 0 mm

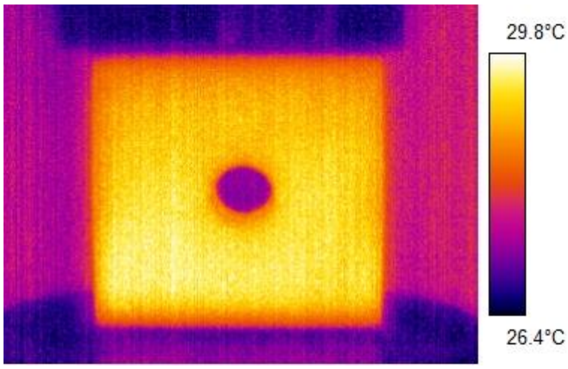

b) Deformation 4.2 mm

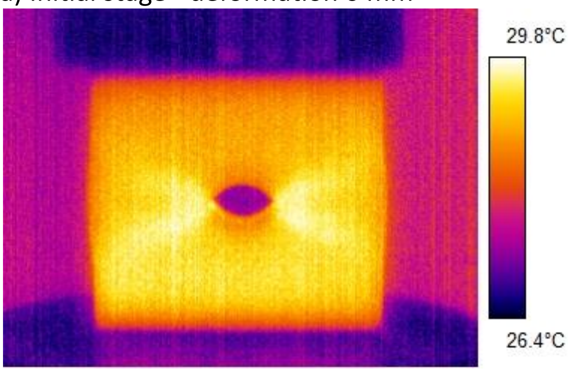

c) Deformation 8.5 mm

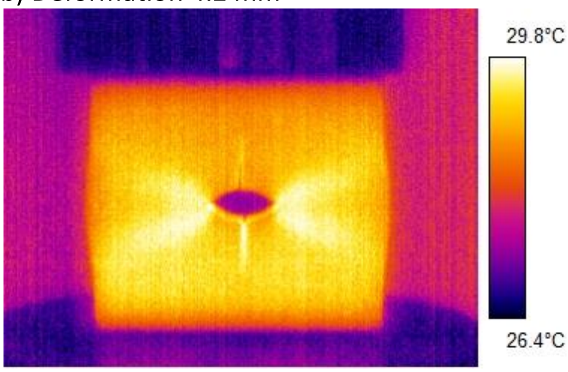

d) Deformation 10.5 mm

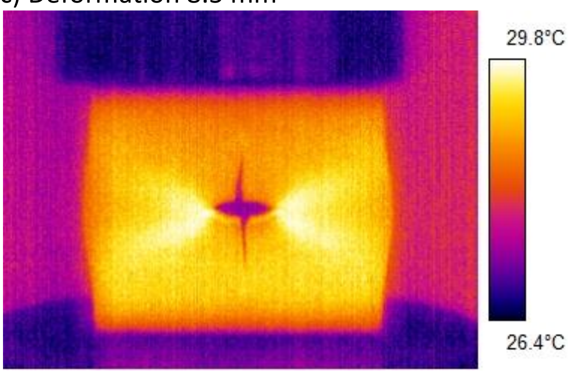

e) Deformation 11.7 mm

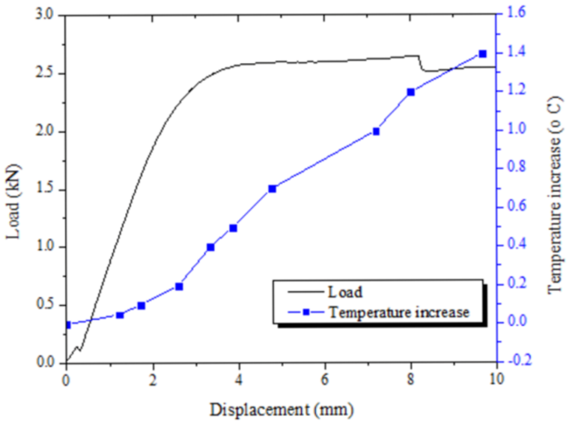


***Fig. 6.*** *Temperature distributions at different load stages from compression testing of 145 kg/m³ foam with a hole of 16 mm.*

***Fig. 7.*** *Load - displacement curve for foam density block of 145 kg/m³ with hole with 16 mm diameter and the temperature increase.*

From the measurements the angle of maximum temperature (Fig. 8), which corresponds to bands of deformation of cellular structure of the foams and the maximum temperature increase on these directions (Fig. 9) were determined. It could be observed that angle of the bands of deformation increases with increasing hole diameter, but is not influenced by the foam density. In contrary the maximum temperature increases with increasing density from 0.8ºC for 100 kg/m$^3$ density to 1.6ºC for 300 kg/m$^3$ density.

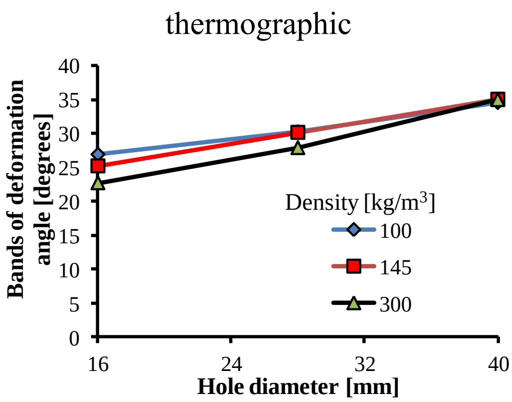


*Fig.8. Bands of deformation angles.*

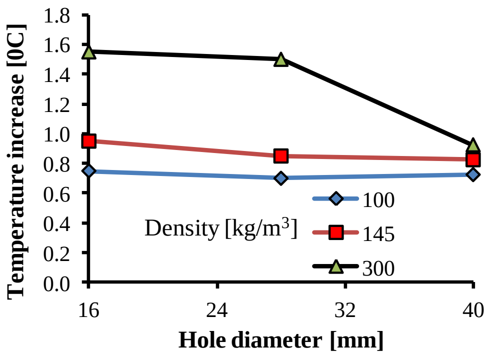


***Fig. 9.*** *Maximum temperature increase on the band of deformation direction.*

## 6.2.Numerical investigations

As it possible to see in the previous paragraph, the plasticity zone is not where the crack born and seems that where the crack born the material has a linear elastic behaviour. For this reason the first step is to try to apply the SED using a 2 D model through a linear elastic analysis, without taking in account the plasticity.

Under this case, it has been used a 2 D model generated with a plane element ( *PLANE 184 8 nodes* ); the specimens present two axis of symmetry so it's possible to model a quarter of the geometry. The analysis were linear elastic. As for the previous analysis the simulations are made under plane strain conditions.

The parameters used are the following:

| | | |
|---|---|---|
| **Density [Kg/m$^3$]** | **$W_c$ [Kg/m^3]** | **$R_c$ [mm]** |
| **100** | *0.169* | *0.2* |
| **145** | *0.143* | *0.24* |
| **300** | *0.065* | *0.35* |

***Table 2.*** *SED parameters used.*

The parameter $r_0$ depends from the geometry:

| Diameter [mm] | $r_0$ [mm] |
|---|---|
| **16** | *4* |
| **28** | *7* |
| **40** | *10* |

***Table 3.*** *Parameter $r_0$ for each geometry.*

Following are showed the obtained results:

| D [mm] | $R_c$ [mm] | $W_c$ [Kg/m$^3$] | $F_{experimental}$ [N] | $F_{predicted}$ [N] | Error [%] | $R_{contr\_volume}$ [mm] |
|---|---|---|---|---|---|---|
| **16** | 0.2 | 0.169 | 1610 | *5500* | *241* | 4.2 |
| **28** | 0.2 | 0.169 | 1370 | *3300* | *140* | 7.2 |
| **40** | 0.2 | 0.169 | 970 | *1750* | *80* | 10.2 |

***Table 4.*** *Predicted loads and respective dispersion for Necuron 100.*

| D [mm] | $R_c$ [mm] | $W_c$ [Kg/m$^3$] | $F_{experimental}$ [N] | $F_{predicted}$ [N] | Error [%] | $R_{contr\_volume}$ [mm] |
|---|---|---|---|---|---|---|
| **16** | 0.24 | 0.143 | 2580 | *5800* | *124* | 4.24 |
| **28** | 0.24 | 0.143 | 2260 | *4500* | *99* | 7.24 |
| **40** | 0.24 | 0.026 | 1466 | *2500* | *70* | 10.24 |

***Table 5.*** *Predicted loads and respective dispersion for Necuron 160.*

| D [mm] | $R_c$ [mm] | $W_c$ [Kg/m$^3$] | $F_{experimental}$ [N] | $F_{predicted}$ [N] | Error [%] | $R_{contr\_volume}$ [mm] |
|---|---|---|---|---|---|---|
| **16** | 1 | 0.065 | 9088 | *5500* | *39* | 5 |
| **28** | 1 | 0.065 | 6844 | *7800* | *13* | 8 |
| **40** | 1 | 0.065 | 5142 | *3850* | *25* | 11 |

***Table 6.*** *Predicted loads and respective dispersion for Necuron 300.*

From Table 4,5 the errors for Necuron 100 and 160 are more than 70 % while for Necuron 300 (Table 6) the errors are more than 25 % for the highest and for the smallest diameter while for the middle diameter the error is less than 15 %.

From these tables is possible to see that the predicted loads are very far from the experimental loads.

These results derive from a linear elastic analysis and it's known that the specimen presents a plasticity zone. For this reason the idea is to see if the plasticity influences the results.

To see this, it's necessary to do a non-linear analysis, an analysis where the relation between stress and strain is not linear.

The characteristic curve of the material is different in the case of compression load and in the case of tensile load. The specimens present a zone under tensile load ( the notch tip of the hole where the crack born and propagates) and zone under compression load so in the finite element model it's necessary to implement two characteristic curves; to do this it has to know the part of the specimen under compression load and tensile load.
The characteristic curves of the materials in compression, for the elastic tract, is very similar to the characteristics curves of the materials under tensile load: for this reason, in a first moment, the approximation made is to implement only the compression curve and to see if the results are influenced or not. If the results changes a lot using a non-linear analysis, it's necessary to differentiate the part of the material under compression load and the part of the material under tensile load.

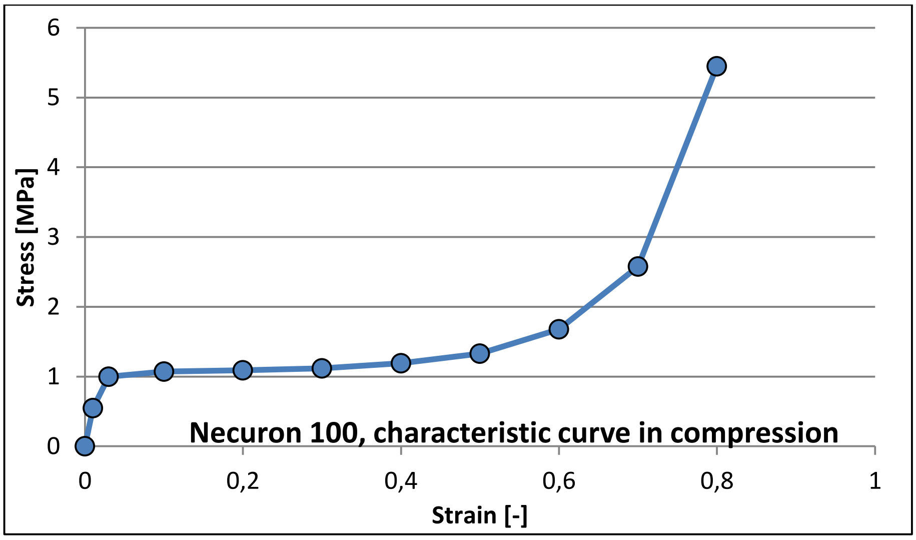


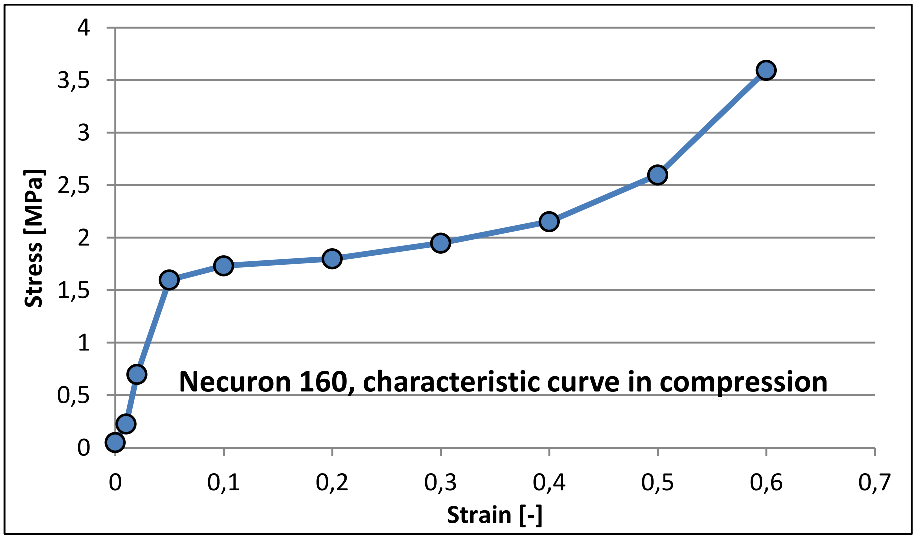

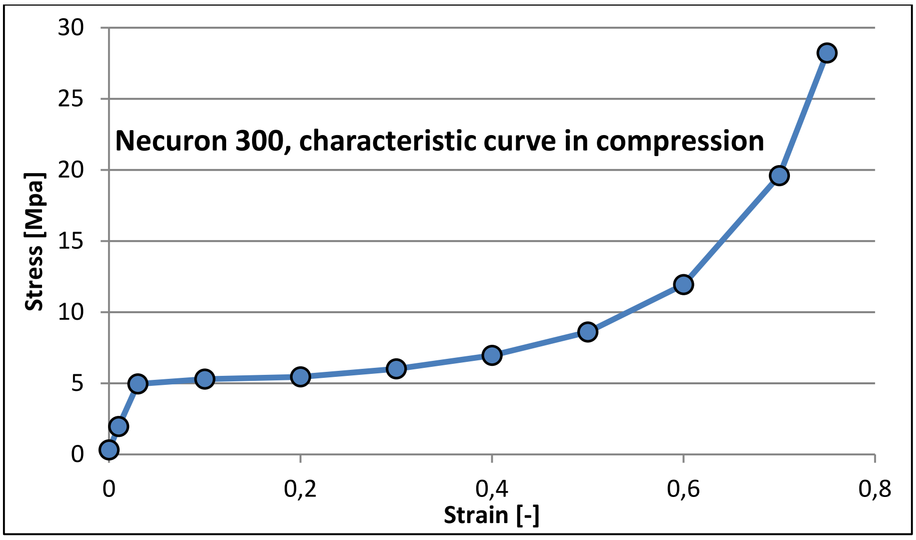


In the graphs are exhibit the characteristic curve under compression load for Necuron 100,160 and 300; the line represents the continue curve while the circle spots represent the points used to implement the characteristic curve in the software. It's possible to see that the first tract of the curves is very similar to the characteristic curve in tensile and the "yeld stress" is not so far from each other.

For all the non-linear analysis, it has used Ansys Workbench software, a different version of Ansys Multiphysics. Usually the characteristic curve of a polymer is represented through a Mooney Rivlin curve; the Mooney Rivlin is used to describe the hyper elastic behaviour of the material and it's used for elastomeric materials. The Mooney Rivlin model is defined through unless three parameters and is not easy to define these parameters (is defined through the energy of the material and deviatoric tensor) and request a characterization of the material. Workbench permits to define every characteristic curve through points and after gets the material behaviour for every stress-strain condition through an interpolation of these points. In particular, the model utilized is the isotropic linear hardening model. The specimens (80x80x25 mm) with holes (diameter 16, 28, 40 mm) used in the experiments were modelled in Ansys Workbench 15.0 software. 3D 20 node quadratic solid elements were used, with a refined mesh near the hole (Fig. 9).

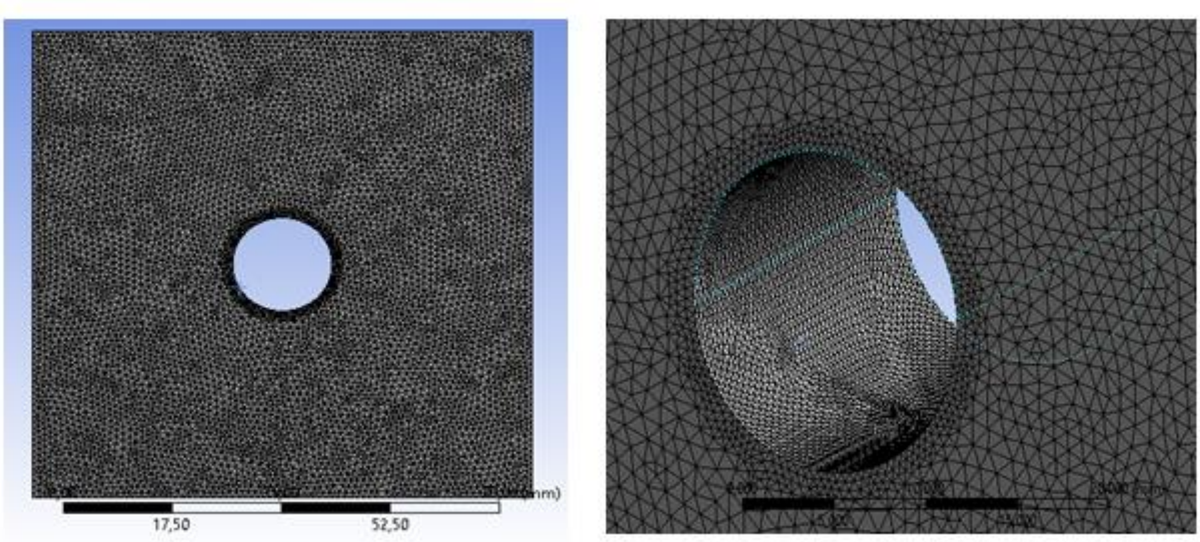

a) b)

*Fig. 9. Defined mesh of the model a) and the refined mesh near the hole b).*

A convergence study was carried out resulting the present mesh topology. The boundary conditions represent the experimental setup: 0 displacements of vertical direction were imposed at the bottom side of the specimen, while 15 mm displacements were applied on the top side. For each specimen has been applied the displacement when the failure occurs (Fig. 10).

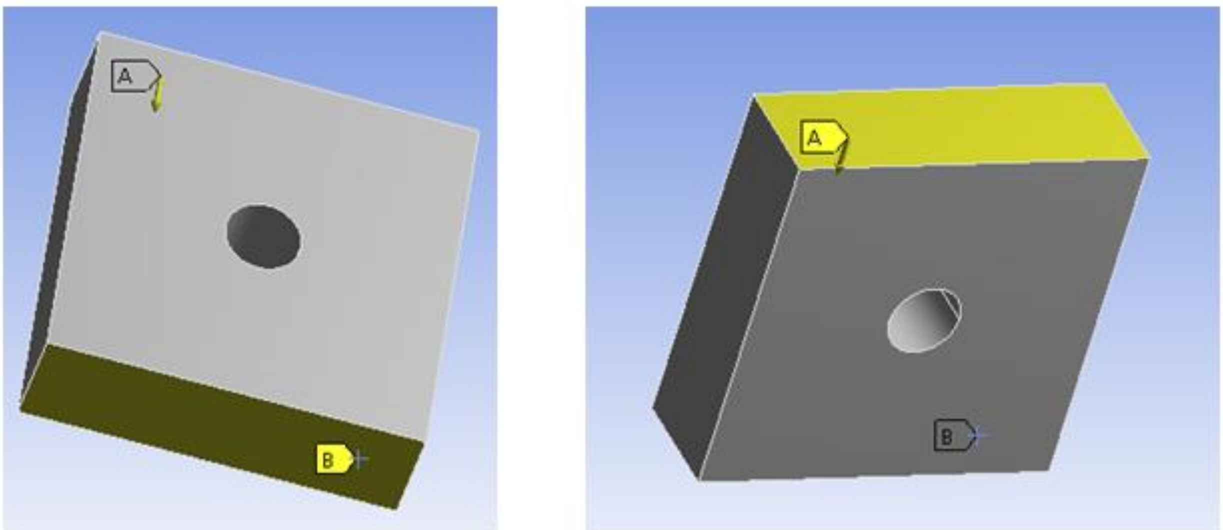


a) b)

***Fig. 10.*** *The boundary conditions: a) the 0 displacements on the bottom of the specimen, b) the failure displacement applied to the top of the geometry.*

In Fig. 11 is showed the equivalent plastic strain obtained with Ansys and compared with the thermographic image (specimen made in Necuron 100, D=16 mm). It's possible to see that the plastic strain zone is very near to the reality. Where the crack born there's no apparently plasticity. It has been modelled the control volume and it has noticed that there is a plasticization zone in this one, so at the first moment is logical to say that is not possible to apply the SED method. It's important to underline that this plasticity is very small in fact the value is very small in comparison with the maximum value of equivalent plastic strain (Fig. 12, Fig. 13). Also it has to take in account that it has used the compression stress-strain characteristic curve.

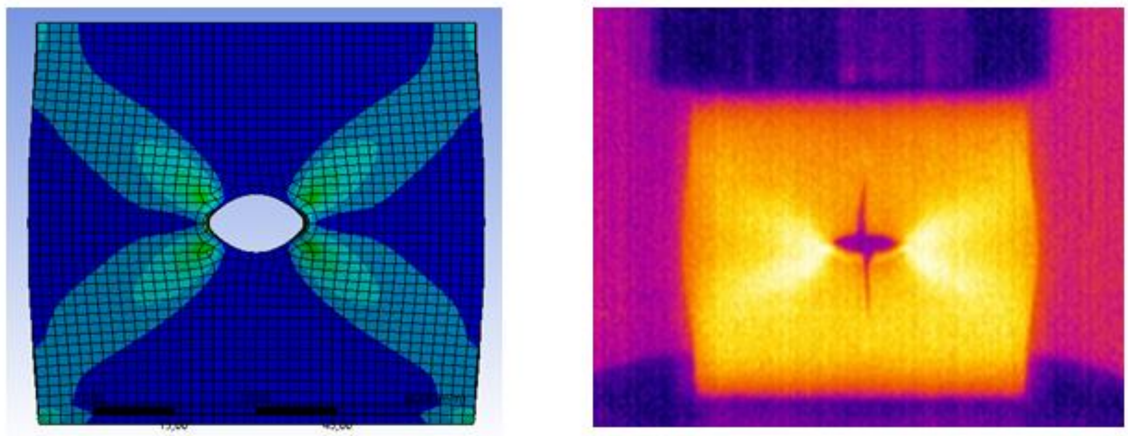

*a)* *b)*

***Fig. 11.*** *Comparison of equivalent plastic strain region between numerical model a) and experimental specimen b).*

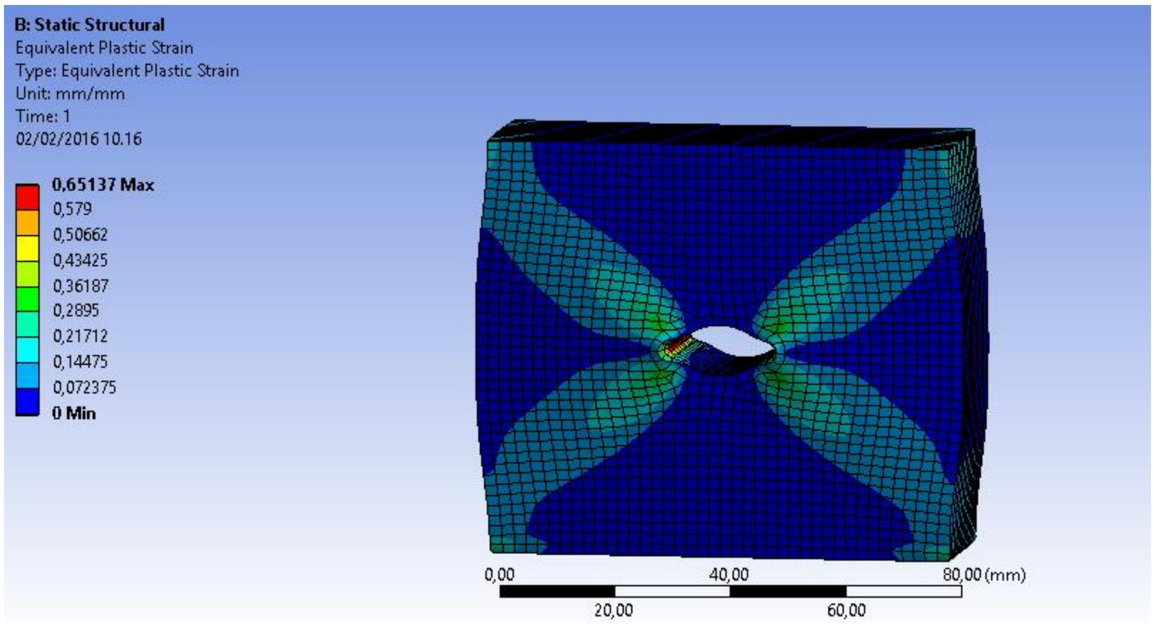


***Fig. 12.*** *Equivalent plastic strain and maximum value (Necuron 100, D=16 mm).*

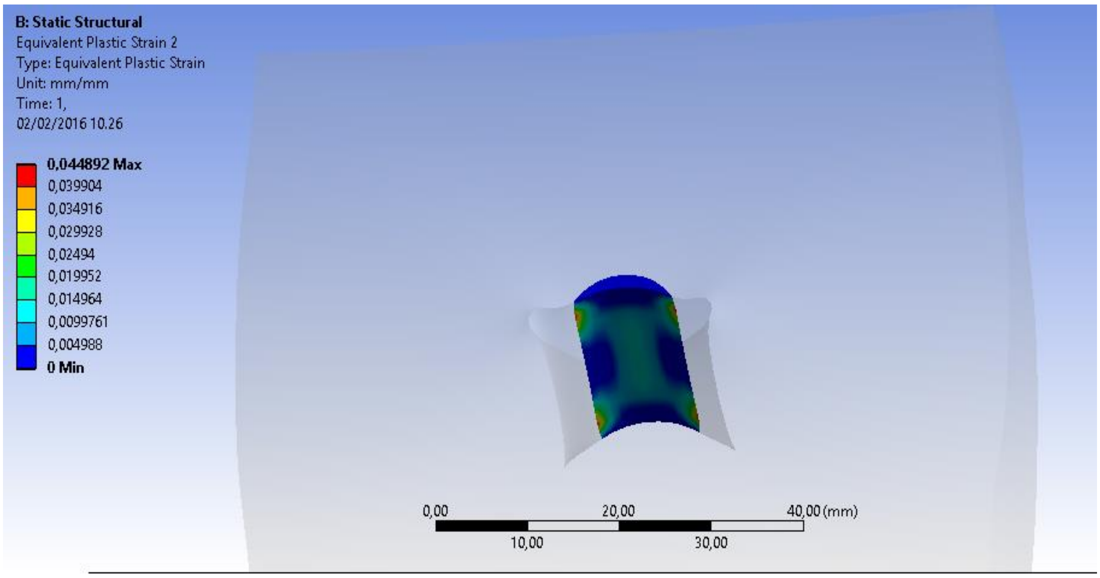


***Fig. 13.*** *Equivalent plastic strain in the control volume (Necuron 100, D=16 mm) and maximum value of this one.*

The plastic strain value in the control volume is very small so it has tried to apply the SED method and the respective fracture load for each specimen.

To be sure that the numerical model is in accord with the experimental data, it has compared the experimental load-displacement curve of the machine with the numerical curve. Following are showed the graphs that compared the numerical curve with the experimental curve; in this case are reported the comparison for Necuron 100.

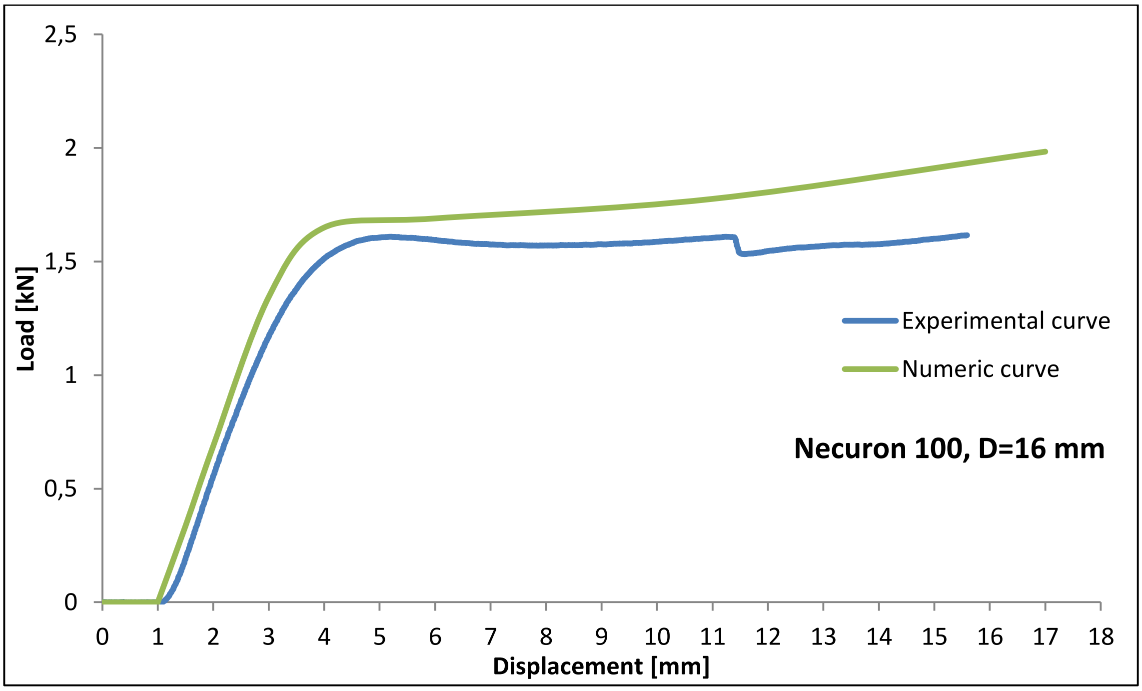

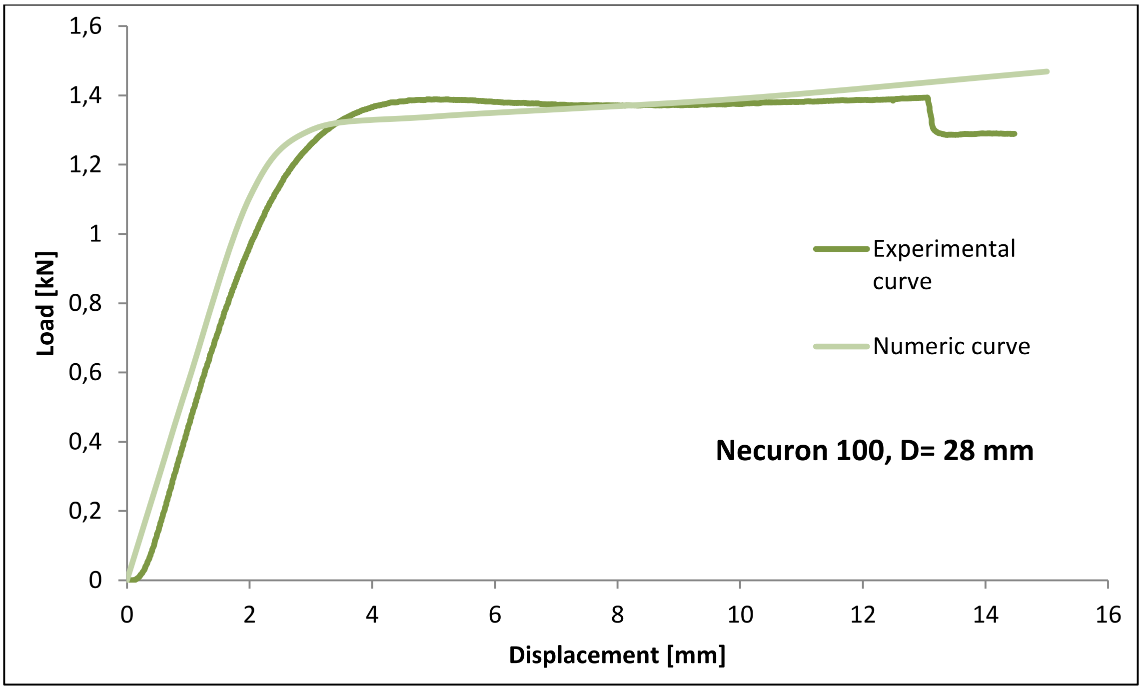


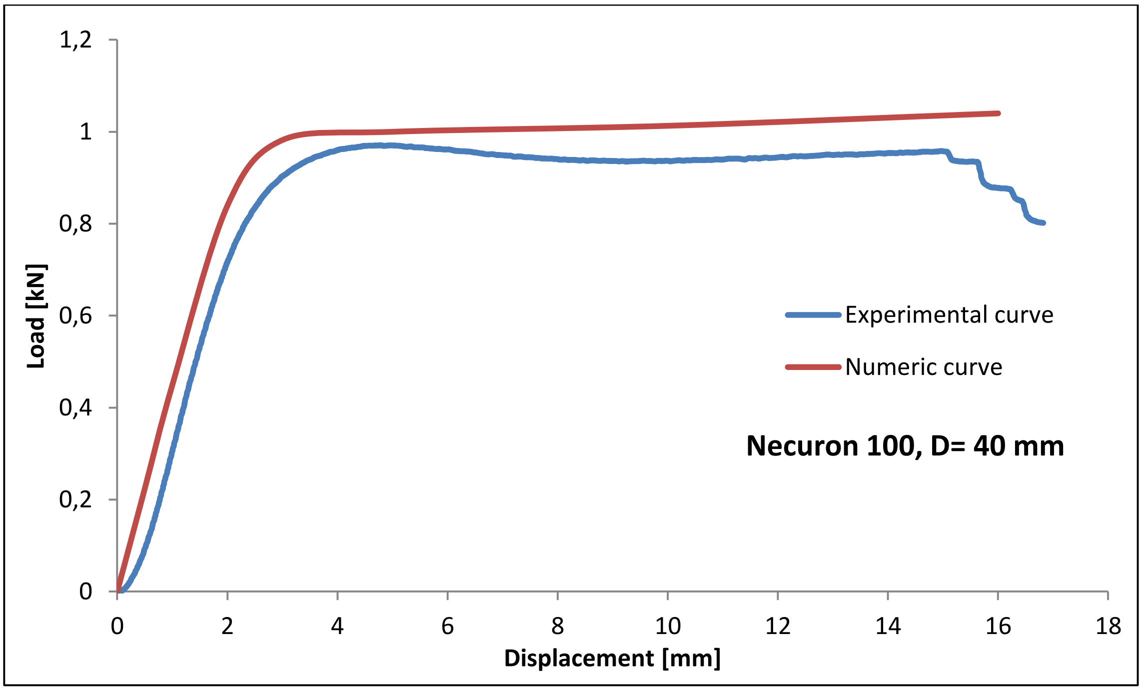


The same approximation are determined for the other densities.

The experimental curve are very near to the experimental curve so the SED method will be applied.

## 6.3.Comments

The obtained results defined with a non-linear analysis is very near from the results obtained with a linear elastic analysis. This confirms that the plasticity doesn't influence the results so a linear elastic analysis is equivalent to a non-linear analysis, regarding these cases.

Probably the SED method can't be applied because in compression the specimen has not a quasi-ideally brittle behaviour; in fact, taking in example the specimen made in Necuron 100 with D= 16 mm, the crack born when the displacement is equal to 10 mm and the failure of the specimen is reached when the displacement is equal to 16 mm while for the other specimens investigated in the previous chapter, the displacement when the crack born is more or less the same of the displacement when the failure occurs.

It's necessary to say that these analysis are the first approach with these experimental tests, so it's important to underline that for a sure results it needs further studies. In this chapter is presented an entry level approach and study of this problem.

# Conclusions

The main purpose of this essay is to apply the SED method using the stress failure $\sigma_t$ defined through experimental tests, on U notched specimen with bland curvature radius, for PUR foams made by different densities. The stress failure determined through these tests are very closed to the stress failure defined in a precedent studies [7], as it possible to see in Table 1.

| Density of PUR foams | 100 | 145 | 300 | 708 |
|---|---|---|---|---|
| $\sigma_{failure}$ as inherent stress [MPa] | *2.17* | *3.12* | *5.56* | *23.14* |
| $\sigma_{failure}$ as $\sigma_t$ [MPa] | *3.19* | *4.39* | *6.06* | *26.79* |

***Table 1.*** *Comparison between experimental stress failure and stress failure determined for TCD method.*

For the lower density the difference is near about 30 % while for the highest densities the difference is less than 15 %. The precedent studies determined the stress failure as the inherent stress, in a different way: two different approaches give results very near.

For Necuron 1020, the characteristic stress strain curve is very similar to a stress strain characteristic curve of a ideally brittle material so it has been made the assumption that $\sigma_t$ is equivalent to the ultimate tensile strength.

The SED parameters ,as the control radius $R_c$ and the value of the critical energy density, defined through the $\sigma_t$ are reported in Table 2.

| Density [Kg/m$^3$] | $R_c$ [mm] | $W_c$ [MJ/m$^3$] |
|---|---|---|
| **100** | 0.2 | 0.169 |
| **145** | 0.24 | 0.143 |
| **300** | 1 | 0.065 |
| **708** | 0.62 | 0.285 |
| **1218** | 0.8 | 0.37 |

***Table 2.*** *SED parameters defined through $\sigma_t$.*

The strain energy density approach is applied to different notched components made by different densities. The dispersion of the obtained results in comparison with experimental results are reported in Graph 1 (the dispersion is evaluated through the strain energy density, as usually has made in literature, the expression of the dispersion is reported on the y axis).

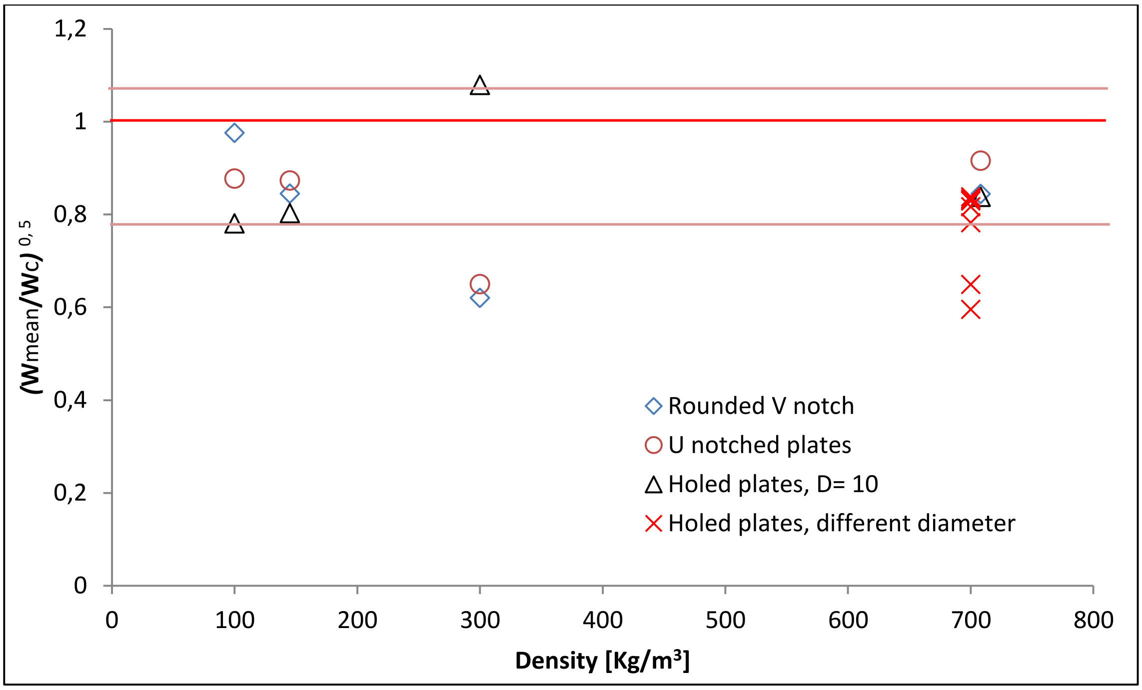


***Graph 1.*** *Dispersion of the results under mode I for rounded V notch, U notched plates, holed plates (D=10) and holed plates with different diameter.*

Excluding the holed plates with the lowest diameters ( diameter equal to 2.5 and 1 mm) the scatter band is contained between + 10 % and – 22 %. It's possible to say that the major dispersion is represented by the holed plates; if has been exclude the holed plates, the scatter band is contained between +10 % and – 15 %. For the holed plates is very important to underline that, in literature, is an assumption to treat as a U notch so it's not proved that the holed geometry has the same control volume centre of the U notch geometry. These approximation seems working because the dispersion is very small: usually, in engineering field, an acceptable scatter band is included between 10 % and 20 %. For the holed plates could be possible to change the centre of the control volume but only with these experimental data is not possible to say if these new centres are good for every holed components or are valid only for these ones. Also, it has to take in account that all the analysis are made under plane strain conditions and this is a common assumption.

For the holed plates with the lowest diameters (made in Necuron 651) the SED gives not a good prediction, probably because the radius of the control volume is comparable with the hole's diameter.

The SED method has been applied to ASCB specimens, tested from pure mode I to pure mode II.

Usually, in the literature, it has made the assumption that in mixed mode and in pure mode II the parameters remain constant and doesn't change. Following are exhibit the results calculated using $R_c$ and $W_c$ in mode I, for mode II and mixed mode I+II ( Graph 2).

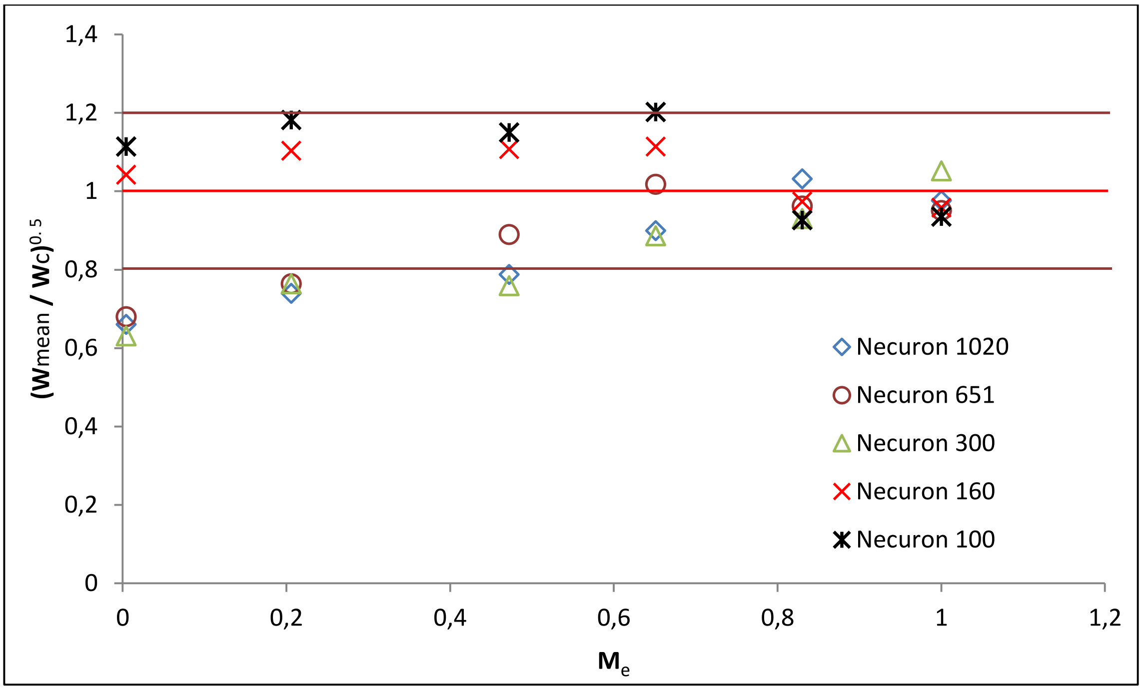


***Graph 2.*** *Dispersion of the predicted loads for ASCB specimens under mode I, mode II and mixed mode using SED parameters from pure mode I.*

It's possible to see that for pure mode II and for the mixed mode I+II, the dispersion is more than 25 %. So it has been defined a personal approach where the main assumption is that the control volume remains the same while changes the critical value for strain energy density: this means that $R_c$ is constant. Knowing $R_c$ and the stress intensity factor $K_{ic}$ is possible to determine the new value of the strain energy density. The new value of the critical energy density is calculable through the following expression:

$$W = \frac{e1}{E}\frac{KIc^2}{Rc^{2(1-\lambda1)}} + \frac{e2}{E}\frac{KIIc^2}{Rc^{2(1-\lambda1)}}$$

Using this approach the dispersion decrease drastically, in fact the scatter band is contained between + 10 % and -10 %, as it seen in Graph 3.

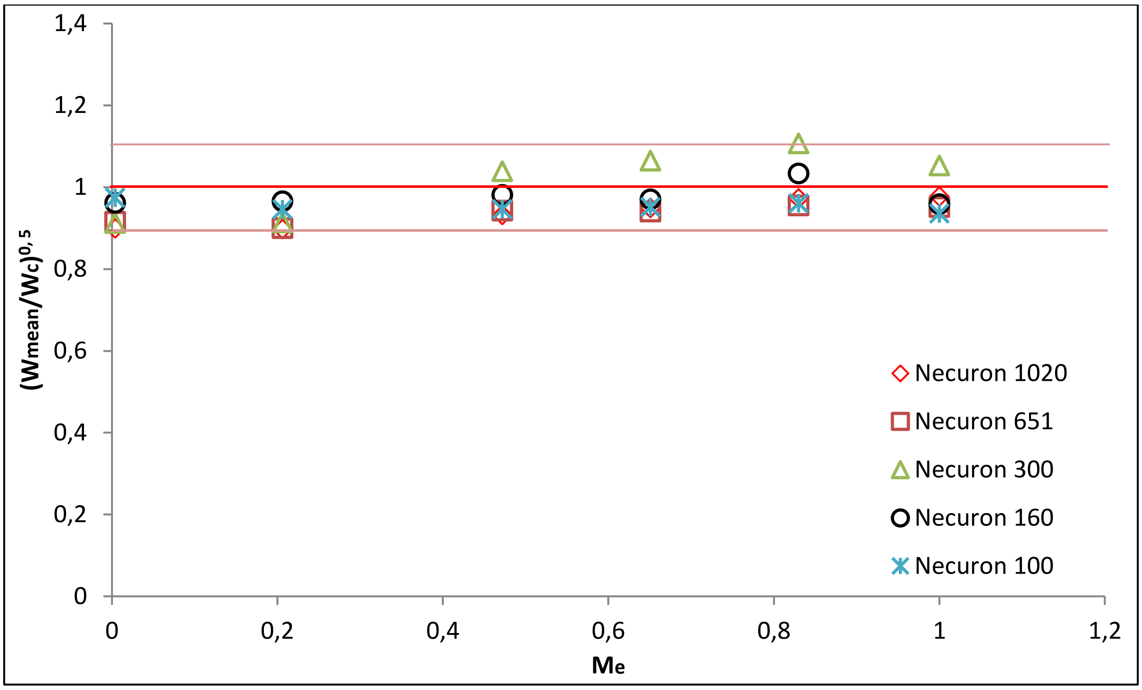


***Graph 3.*** *Dispersion of the predicted loads for ASCB specimens under mode I, mode II and mixed mode with varying the Wc.*

For Necuron 300 is possible to see that the predicted loads for the rounded V notch plate and for the U notched plate are far from the experimental loads. Plotting the parameter $R_c$ versus the density is possible to define a linear interpolation: through this relation (Graph 3) it has been defined a new $R_c$ for Necuron 300.

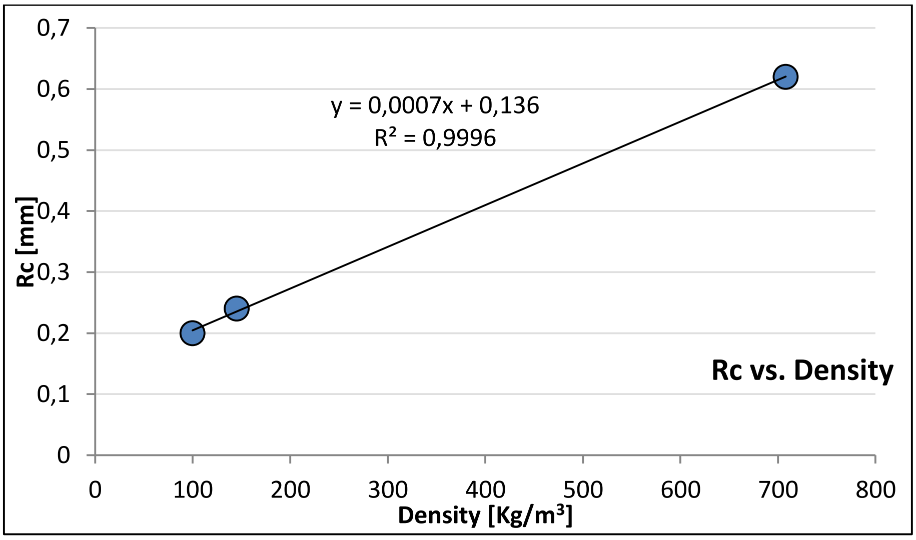


***Graph 3.*** *Linear relation between Rc parameter and density.*

Using this relation, for Necuron 300 $R_c$ is equal to 0.35 mm and the dispersion is less than 15% for all the specimens except the cracked specimens.

As it says previously, Necuron 300 in all the test made shows scatter results and this is possible to see for the predicted results. This kind of behaviour probably is explainable from the fact that, for Necuron 300, the dimensions of the porosities are very scattered and probably this is the reason because in all the tests, for all the geometries, the experimental loads are very scattered ( this trend it’s possible to see in the experimental tests made for the U notch plates with a bland curvature radius, where the fracture loads were scattered).

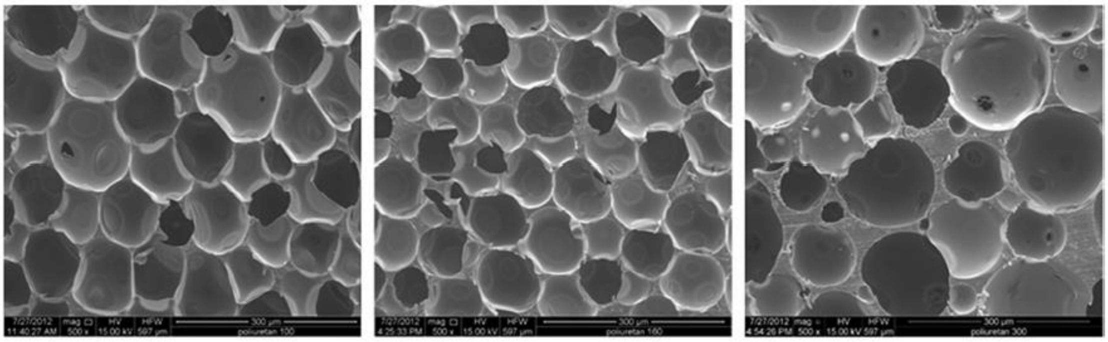

(a) 100 kg/m$^3$ (b) 145 kg/m$^3$ (c) 300 kg/m$^3$

***Fig. 1.*** *Image of the cell dimensions for different densities.*

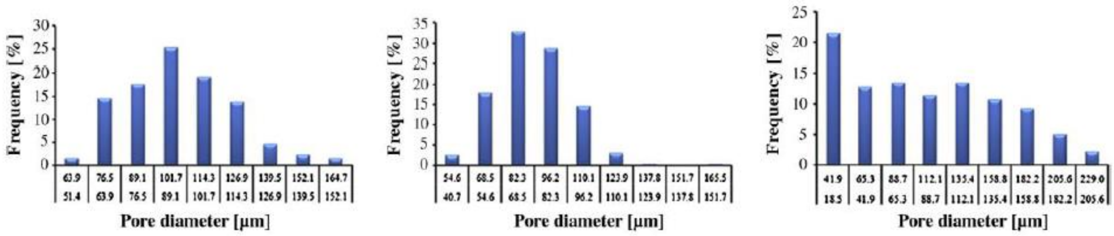


(a) Necuron 100 (b) Necuron 160 (c) Necuron 301

***Fig. 2.*** *Statistical analysis of the cell dimensions.*

In Fig. 1 and 2 is possible to notice the scattered dimensions of the cell for Necuron 300 while for the other densities the dimensions of the cell are very near to an average value.

From the results is possible to say that the SED method can be applied to these foams.

The approach used to define the failure stress $\sigma_t$ it’s different in comparison with previous studies but gives similar results; this confirms the idea that the parameters that validate the SED method for all the notched geometries are not so far from the determined parameters.

This approach is an entry level approach and it’s necessary to do more tests, for example using different geometry of the specimens with bland curvature radius (for example use symmetric specimen with semi-circular notches with bland radius) or test specimens with bland curvature radius under pure mode II.

With this essay has been demonstrate that is possible to define the parameters for SED method, and this one represents a good approach to predict the static failure. The behaviour of the notched components is not perfectly linear elastic, especially with the decreasing of the density, and all the investigations are made through a linear elastic analysis. A linear elastic analysis doesn’t represent perfectly the behaviour of the material but gives an easy tool to predict the failure; in fact the dispersion scatter band of the results is, in the majority of the cases, contained between ± 15 %, a good scatter band in engineering field. In this case the main goal is predict the failure and not predict how the crack born and propagates, so the assumption of a linear behaviour of the material is reasonable.

In the Appendix, at the bottom of this essay, it has been applied the TCD method, on the specimens analysed through the SED method, using the tension at the notch tip defined in the experimental tests. The TCD method is based on the same theory of the SED method so if one works the other have to works: here the two methods give a scatter band of dispersion contained between – 20 % and +20 %, an acceptable dispersion in engineering field.

Being the firsts studies conducted on SED method applied on these foams, it’s requested further studies and experimental tests.

# AKNOWLEDGMENTS

I wish to say thank you to all the people that have supported me during this research and during the writing of this essay.

I would say thank you to my Italian relator, professor Filippo Berto, for his availability to be my advisor and to support me in all the phases of my work; thank you to professor Liviu Marsavina, professor of Universitatea Politehnica Din Timisoara, he followed me in my research made in Timisoara (Romania) and he permitted me to do this project. These two professors allowed me to grow as a person and not only as a student, through the help that I have received, for the manners in which they have treated me and to believe in me since from the beginning.

I am grateful to my Family , Elio and Maria (parents), Paolo and Stefano (brothers), they inspire me to keep on pushing myself to the limit and all that I am (and that I have) I owe to them; thank you to my friends that supported me spiritually during my experience abroad and during my university career, they helped me to feel less the pressure . Finally I would say thank you to my Erasmus colleagues, a life's companions during a life's experience.

I dedicate this project to Professor Filippo Berto and Professor Liviu Marsavina.

# APPENDIX

In the third chapter, the stress at the notch tip have been compared with the inherent stress define of the TCD method. As it said in the comments of third chapter, the TCD method is based on the same theory of the SED method: for this reason it has been applied to the geometries analysed previously.

The Theory of Critical Distances (TCD) represents a group of methods – Point, Line, Area and Volume method – which postulates that static brittle fracture in notched components can be predicted using the data from the linear-elastic stress field in the area of the notch tip, through an appropriate effective stress $\sigma_{eff}$ .

The Point Method says that the failure occurs when the stress, at an certain distance from the notch tip and along the direction where the normal stress is maximum, reaches a critical value called inherent strength or $\sigma_0$ ; the distance from the notch tip is called critical distance or L/2, where L is called characteristics length. The inherent strength and the characteristic length are a material's parameters so they depend only from the material, the geometry doesn't influence this parameters.

If the behaviour of the material is ideally brittle, the inherent strength is equal to the stress failure $\sigma_{failure}$ .

Characteristic length L under static loading could be evaluated on the basis of linear elastic fracture mechanics:

$$L = \frac{1}{\pi}\left(\frac{K_{IC}}{\sigma_0}\right)^2 \qquad [1]$$

If the stress at the notch tip has been used to define the SED parameters, it has to use to define the TCD's parameters.

In Table 1 is reported the TCD parameters that are the characteristic length L and the inherent stress: the characteristic length is defined through eq. (1) while the inherent stress corresponding with $\sigma_t$ at the notch tip.

| Density [Kg/m$^3$] | 100 | 145 | 300 | 708 |
|---|---|---|---|---|
| Characteristic Length [mm] | 0.24 | 0.28 | 1.20 | 0.70 |
| Inherent stress [MPa] | 3.19 | 4.39 | 6.06 | 26.7 |

***Table 1.*** *TCD's parameters.*

For  what regards the finite element analysis, it has been used the model create for the SED method: the only modify is represented for the mesh that is more redefined near the notch tip. Following is showed the dispersion between the experimental and theoretical fracture loads using TCD method.

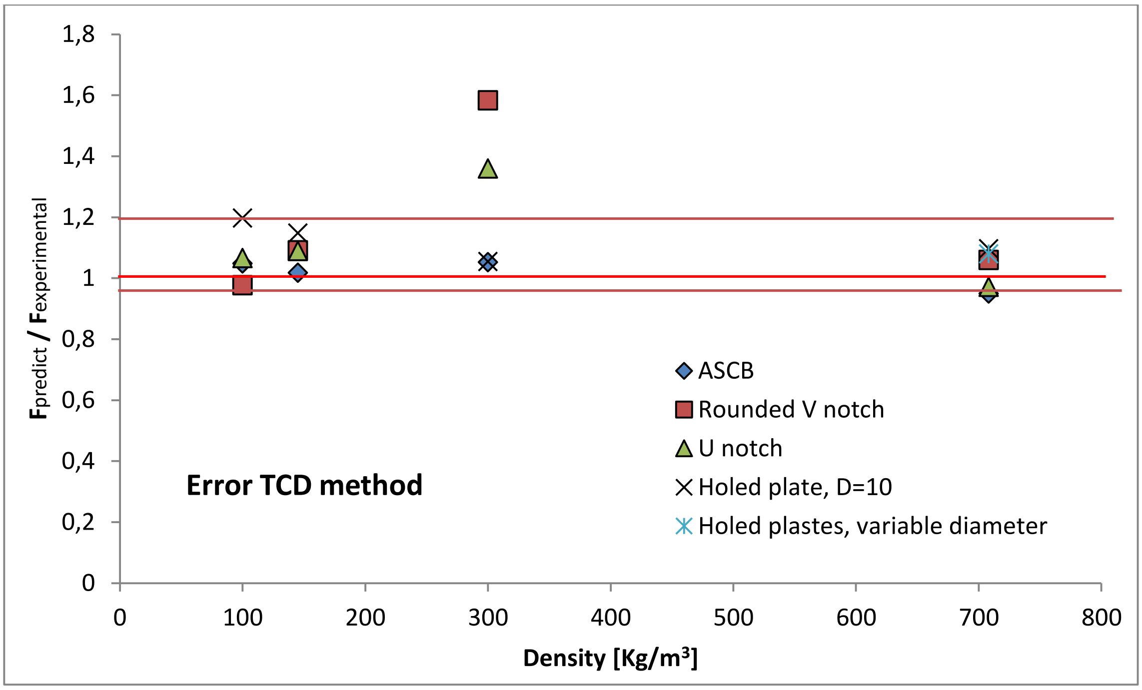


***Graph 1.****Dispersion of the obtained results through TCD method.*

As it said, Necuron 300 represents a “special” density, in fact for some geometries the predicted loads are very near from the experimental loads while for other geometries the predicted loads are very far from the experimental ones. If it has been excluded this special density, the scatter band is contained between – 4 % and + 20 %, a very good range of dispersion ,in engineering field.

Through these results, it’s possible to affirm that is possible to define a characteristic length and a inherent stress that permit to predict the static failure for notched components.

These results it’s the logic demonstration that it’s possible to use these kind of method to predict the failure for these foams, even if the behaviour of the unnotched material is not ideally brittle.

# BIBLIOGRAPHY

[1] - "*Developments of some explicit formulas useful to describe elastic stress fields ahead of notches in plates*" S.Filippi, P. Lazzarin, R. Tovo, Int. J. Solids Struct. 39 (2002)

[2] - "*Review of the volume based strain Energy density approach applied to V-notches and welded structure*", F. Berto, P. Lazzarin (2009)

[3] - "*Advanced methods of fatigue assessment*" D. Radajand, M. Vormwald (2013)

[4] - "*A finite-volume-energy based approach to predict the static and fatigue behaviour of components with sharp V-shaped norches*", P. Lazzarin, R. Zambardi (2001)

[5] - "*Plane elastostatic analysis of V-notched plates*" R. Gross, A. Mendelson, (1972)

[6] - "*Some expressions for the strain energy in a finite volume surrounding the root of blunt V-notches*" P. Lazzarin, F. Berto (2005)

[7] - "*Application of TCD for brittle fracture of notched PUR materials*" R. Negru, L. Marsavina, T. Voiconi, E. Linul, , H. Filipescu, G. Belgiu (2015)

[8] - "Fatigue strength of steel and aluminium welded joints based on generalised stress intensity factors and local strain energy values", Livieri,Lazzarin, (2005)

[9] - "*Mixed mode brittle fracture of sharp and blunt V-notches in polycrystalline graphite*" , M.R. Ayatollahi , F. Berto, P. Lazzarin

[10] - "Local strain energy to assess the static failure of U-notches in plates under mixed mode loading", F. J. Gómez , M. Elices , F. Berto, P. Lazzarin

[11] - " From Neuber's elementary volume to Kitagawa and Atzori's diagrams: an interpretation based on local energy", P. Lazzarin, F. Berto